ISSN 1727–6209

RESEARCH INSTITUTE FOR INTELLIGENT COMPUTER SYSTEMS
TERNOPIL NATIONAL ECONOMIC UNIVERSITY
IN COOPERATION WITH
V.M. GLUSHKOV INSTITUTE FOR CYBERNETICS,
NATIONAL ACADEMY OF SCIENCES, UKRAINE

International Journal of

Computing

Published since 2002

March 2014, Volume 13, Issue 1

Ternopil – 2014

International Journal of Computing

March 2014, Vol. 13, Issue 1

Research Institute for Intelligent Computer Systems, Ternopil National Economic University

Editorial Board

Address of the Editorial Board

Research Institute for Intelligent Computer Systems
Ternopil National Economic University
3, Peremoga Square
Ternopil, 46020, Ukraine

Phone: +380 (352) 47-5050 ext. 12234
Fax: +380 (352) 47-5053 (24 hours)
computing@computingonline.net
computer.journal@gmail.com
www.computingonline.net

ISSN 1727–6209

НДІ ІНТЕЛЕКТУАЛЬНИХ КОМП'ЮТЕРНИХ СИСТЕМ
ТЕРНОПІЛЬСЬКИЙ НАЦІОНАЛЬНИЙ ЕКОНОМІЧНИЙ УНІВЕРСИТЕТ
У СПІВПРАЦІ
З ІНСТИТУТОМ КІБЕРНЕТИКИ ІМ. В.М. ГЛУШКОВА,
НАЦІОНАЛЬНА АКАДЕМІЯ НАУК УКРАЇНИ

Міжнародний журнал

Комп'ютинг

Видається з 2002 року

Березень 2014, Том 13, Випуск 1

Постановою президії ВАК України № 1-05/3 від 14 квітня 2010 року міжнародний журнал "Комп'ютинг" віднесено до переліку наукових фахових видань України, в яких можуть публікуватися результати дисертаційних робіт на здобуття наукових ступенів доктора і кандидата технічних наук

Тернопіль – 2014

Міжнародний журнал Комп’ютинг

Березень 2014, том 13, випуск 1

НДІ інтелектуальних комп’ютерних систем, Тернопільський національний економічний університет

Зареєстрований Міністерством юстиції України. Свідоцтво про державну реєстрацію друкованого засобу масової інформації – серія КВ №17050-5820ПР від 15.07.2010.

Друкується за постановою вченої ради ТНЕУ, протокол № 3 від 12 лютого 2014 року

Редакційна колегія

Адреса редакції :
НДІ інтелектуальних комп’ютерних систем
Тернопільський національний економічний університет
площа Перемоги, 3
Тернопіль, 46020, Україна
Тел.: 0 (352) 47-50-50 внутр. 12234
Факс: 0 (352) 47-50-53
computing@computingonline.net
computer.journal@gmail.com
www.computingonline.net

CONTENTS

ЗМІСТ

СОДЕРЖАНИЕ

computing@computingonline.net
www.computingonline.net

ISSN 1727-6209
International Journal of Computing

PASSWORD PROTECTION: END USER SECURITY BEHAVIOR

Keisuke Kato [1], Vitaly Klyuev [2]

[1] Department of Computer Science and Engineering, University of Aizu, Fukushima, Japan, s1190085@u-aizu.ac.jp
[2] Department of Computer Science and Engineering, University of Aizu, Fukushima, Japanvkluev@u-aizu.ac.jp, http://www.u-aizu.ac.jp/~vkluev/

Abstract: Password authentication is one of essential services in our life for protecting data. In other words, we may loose a lot of money, sensitive data, etc., if passwords leak out. Thus, we have to understand clearly what is important for creating and/or changing passwords. Our goal is to analyze key issues for setting passwords. We surveyed 262 students of the University of Aizu, Japan. We discussed key security problems, main password protection issues and techniques, and misunderstandings about passwords by end users. Furthermore, we compared the obtained data with results provided by the National Institute of Standard Technology (NIST) and others. The results can help the users set stronger passwords.

Keywords: Security, Password Protection, User Study, Survey, Tendency.

1. INTRODUCTION

In the last decade, a growing number of Internet services made password authentication very important to protect our sensitive data. On the other hand, cracking attacks to steal user passwords increased rapidly. To make password protection stronger, techniques such as two-step verification [1] and two-factor authentication [2] were developed. However, a password is not the only way to authenticate users in the systems.

Book [3] discusses three key options for authentication. The first one is to retain physical control on the device such as a remote car door key. The second one is to use a password. The third option is to utilize something like a fingerprint or iris pattern. However, for the cost reason, most systems work only with passwords. Thus, we need to understand all possible details about passwords. To obtain good knowledge on password authentication, there are a lot of sources. To understand password security better, we consider the problem from three different directions:

- Will the user be able to remember the password?
- Will the user choose a password that is hard to crack or guess?
- Will the user reuse the password on other systems and/or applications?

In this paper, we seek better understanding of the tendencies that create and/or change passwords. We discuss key security problems, tendencies in password protection techniques, misunderstandings by the users, etc. We present the results of a survey of 262 University of Aizu undergraduate students. Based on the analysis of literature, we suggest some practical recommendations to set a strong password as a framework for our investigation. The suggestions and results of our investigations are useful for the end user to help in setting it.

This paper is based on study [4]. It is organized as follows. In Section 2, we briefly review the recent publications examining password protection issues. In Section 3, we propose a framework to set strong passwords. In section 4, we give detailed information about the survey and discuss basic issues to analyze user data. In Section 5, we analyze the tendencies in password protection, examine the results of the survey, and compare them with data from other sources. In Section 6, we highlight our significant findings.

2. RELATED WORK

For a cracker, the first step to crack a password is to encrypt the possible password candidates and to compare the result values with the values of the encrypted real password. There may be vulnerability in a system or crackers can find the vulnerability faster than specialists in security can do that. So, crackers may attack the vulnerability utilizing several ways. The one of the common ways to break the passwords is to scan the whole space of the character set used in passwords for a brute force attack. The one-way functions or algorithms such as

MD5, SHA etc. are very fast to run. For crackers, however, this is very important because they can use a brute force attack easily. Based on this, a time-effective approach is to think about the candidates that are to be the actual words, patterns, or combination of the characters, which are not difficult to remember [5].

Another common way used in practice is a dictionary attack. In the past, some systems that use an encrypted password file made it readable. Users may fetch this file and then try to break passwords offline by using a dictionary. Thus, a cracker encrypts the values in his dictionary and compares them with the records in the file. This activity is called a dictionary attack. Actually modern operating systems have fixed this problem. However, the dictionary attacks are still implemented. Study [6] discusses fast dictionary attack algorithms by using time-space tradeoff and actually their algorithm recovered 67.6 % of the passwords using a 2×10^9 search space.

There are several cracking tools available to crack or guess passwords. Two objects are the targets of cracking tools: passwords and the function for administrators to reactively check the passwords used in the system. The reactive checking may increase the system security by finding the easy to crack passwords and by warning the related uses to change their passwords to protect their accounts from being cracked by intruders [5]. *John the Ripper* and *Hashcat* [7, 8] are the tools to analyze and provide information on methods used by crackers.

Report [26] shows the statistical data on privacy issues. They are compared with results of investigations [27] by The Institute for Prospective Technology Studies (IPTS) that is one of seven scientific institute of the European Commission's Joint Research Centre. Data in Table 1 and 2 are excerpts from the aforementioned report.

Table 1 illustrates the different view of Japanese and EU citizens on the privacy issues. Data from Table 2 give answers to the question about the responsibility for leaking the private data on the Internet. Japanese users want another person or company to take responsibility. A view of EU users is different: the user itself should take it. Thus, Japanese users have different understanding of security issues compared to people from other countries.

Table 1. Positive answers to the question: Could you provide your private data online?

Data type	IPTS	Japanese user
Name	86 %	37 %
Address	65 %	19 %
Own Photo	58 %	7 %
Bank Information	30 %	4 %

Table 2. Who should take a responsibility for leaking private data?

Answer	IPTS	Japan
The user should take a responsibility	32 %	38 %
The company that has the private data should take a responsibility	27 %	40 %

3. PRACTICAL SUGGESTIONS

Analysis of literature on security issues and users misunderstandings [11, 16–19] allows us to state the following conclusions:

- A long password is not always equal to the strong password. When someone sets the passwords, s/he should avoid usage of a language grammatical structure, which helps memorize passwords [11].
- A password consisting only of numerical characters or only alphabetical characters such as only upper-case or only lower-case is very dangerous. It will be easily cracked or guessed. The users should use numerical and alphabetical characters to set passwords [17, 19].
- To be hard to guess or crack password, the user should use many types of characters as possible. Because the password strength would be stronger if the password's entropy was bigger.
- In order to memorize passwords, it recommend that users use a password management tools such as *LastPath, 1Password, KeePass, Password Dragon*, etc. [18]
- To use a password management tools, you can reduce a burden of creating and changing password. Because the tools can generate random password automatically and the user should memorize only master password.
- Users should avoid the use of passwords such as *"password"*, *"abc123"* and personal data such as name, birthday, address, telephone number, etc. directly. Unfortunately many users set such passwords and crackers are familiar these oversights.
- A password that is usable as an abbreviation from a phrase of sentence is useful for end users to memorize.
- The user should not tell any person their passwords and should not share it with any person.

These suggestions, we consider as a framework for investigations.

Taking into account the differences in user behavior mentioned in Section 2, we analyze these issues considering the students of University of Aizu.

4. QUESTIONNAIRE

In this study, the main method to detect key details in creation and changing passwords is to survey the students of University of Aizu who use the Internet in everyday life. We start with an overview of the questionnaire used in this study. A survey on password protection issues was conducted in April 2013 at the University of Aizu. The participations are 163 2nd year undergraduate students and 99 3rd year undergraduate students majoring in Computer Science. Every participant is a native Japanese and age is between nineteen and twenty-two years old. The questionnaire is in Japanese, the mother language of participants. The questionnaire in the paper-based format was distributed among students. It consists of 15 questions. A goal of this survey was to get the information on password usage by users who are unprofessional in security.

Table 3. Classification of questions in questionnaire.

Elements of a password	Q1. How many characters does your password have? Q10. How many lower-case letters are in your current password? Q11. How many upper-case letters are in your current password? Q12. How many digits are in your current password? Q14. How many different passwords do you have?
Strategy of a password setting	Q2. When you create new or change your password, do you write down it on the paper? Q3. Do you use the same password for different accounts? Q5. Which strategy is more applicable to select your passwords? Q6. Do your passwords have some components such as your name or birthday?
Recognition of a strong password	Q8. How often do you change your password on accounts except the university account? Q13. Do you think your password is strong? Q15. Which of following three passwords is stronger password?

We have to get evidence on reliability of our data. To do that, we focus on two things that are the number of questions in the questionnaire and the rate of respondents who did not answer the questions. In questionnaire, every participant can choose *"I prefer not to answer"* for each question except for the last one. Study [9] analyzed 100,000 respondents and found that if a respondent begins answering a survey, the sharpest increase in drop-off rate occurs with each additional question up to fifteen questions and if the respondent is willing to answer fifteen questions, the drop-off rates for each incremental question, up to thirty-five questions, is lower than for the first fifteen questions added to a survey. And the respondent drop-off rate that consists of fifteen questions is between 4 % and 6 %. In our survey, we counted the rate of respondents who chose *"I prefer not to answer"* and/or did not answer more than twelve questions (80 % of the total number of questionnaire questions). 4 % (11 students out of 262 students) answered in such a way. It means our data are similar to the Survey Monkey's survey [9]. Thus, our data are reliable.

The questionnaire covers a wide range of problems in password security. The questions can be separated into three main groups: "Elements of a password", "Strategy of setting a password" and "Recognition of a strong password" (See Table 3).

In the group of *Elements of a Password*, we asked about elements of user passwords such as password length, type of characters in the password, etc. In the group of *Strategy of Setting a Password*, we tried to understand what strategies of creating and/or changing passwords are utilized by users. However, we could not find a strategy and predict it from this questionnaire. However, in the group of *Recognition of a Strong Password*, we tried to uncover the user's understanding of the strong password and we got one issue from these answers about it.

5. MAIN PASSWORD PROTECTION ISSUES

We hope that end users can set strong passwords in the future. However, now the Internet community is facing many problems. One of the most prevalent misunderstandings is a security issue. In this section, we focus on this problem. We discuss which information is true and which is not.

We illustrate the results of discussions by using survey data and data from others sources [5, 10–13, 20–24].

5.1. DIFFICULTIES WITH A PASSWORD STRUCTURE

As we mentioned in Section 3, there are some recommendations about password structure because it is very important and this is one of point that a lot of end users misunderstand and feel difficulty.

The results of our survey show that 8 % of respondents (22 students) said that their passwords are strong and 16 % of respondents (42 students) said that their passwords are weak. Fig. 1 shows the results that separate groups based on student's opinion about their own password. The mean of password length for a strong group is 10.1, for a weak group is 8.3 and for a normal group is 9.1. Thus, their opinion about password strength is objective.

Another interesting outcome is as follows: 43 % (114) of students use the same password for different accounts such as Google account, Facebook account, etc. The average number of accounts used with the same password is 5.4. Study [22] found that the ordinary user has 25 password-protected accounts on average. So, most participants of the survey use the same password for different accounts. Study [13] shows that about 30 % of users use the same password four or more times. Thus, we need a strategy to set a strong password by every end user.

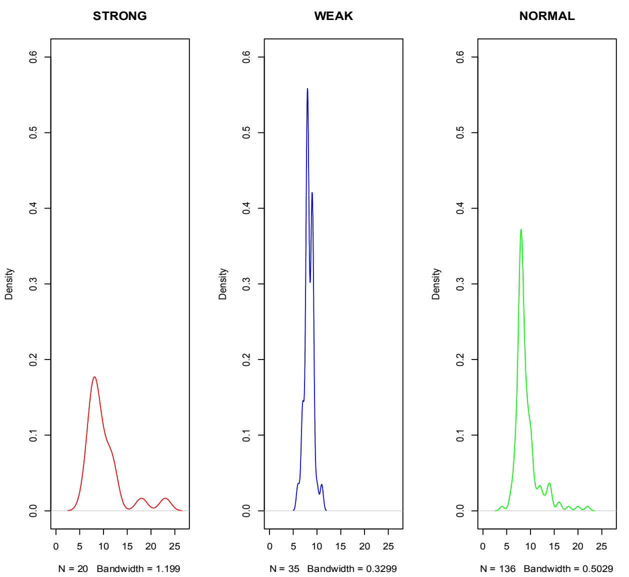

Fig. 1 – Password strength and password length.

We tried to understand strategies to set new passwords from the data of our survey but we could not detect any common patterns. We analyzed the following selections for this issue.

- Password based on the first letter of each word in a phrase.
- Password based on a phone number.
- Password based on an address.
- Password based on a birthday.
- Password based on a word or name with numbers or symbols added to the beginning or end of the term. (A symbol is a character which does not belong to the letters on digits)
- Password based on a word or name with numbers and symbols substituting some of the letters.
- Password based on a word in a language other than English.
- Abbreviation consisting of the first characters of the phrase/sentence.
- Others

36 % (96) of students selected "Others" and 16 % of students selected *"I prefer not to answer"*.

The length of the passwords is very important issue in the password protection. From our observation, we found that many users have one big misunderstanding related to this parameter. It is about long passwords. Actually, many users believe that long passwords are equal to strong passwords but this is not true. Why the long password is not equal to the strong password? All users must memorize the long passwords. However it is very difficult for them to memorize the string like this "qVwN2s6K@Ka". Thus, they create the long password that is very easy to memorize and then many users use a grammatical structure such as "Ihave3cats" for the passwords [11]. This password may be long but applying the dictionary attack, it can be easily guessed. As a result, the possibility to crack or guess increases from 6 % to 20.5 % [11].

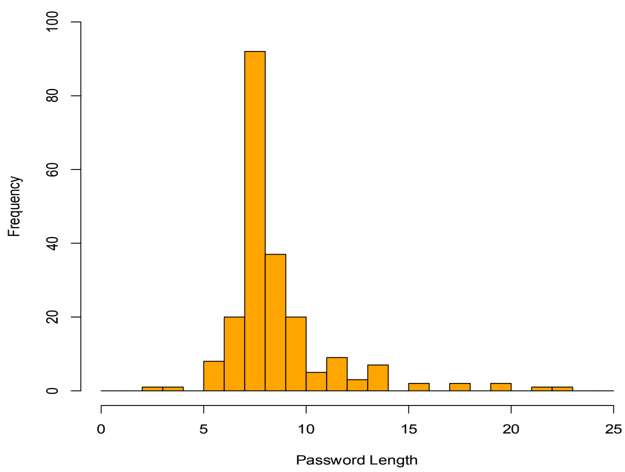

Fig. 2 – Password length.

We carefully analyzed resulting sheets. Fig. 2 shows the password length distribution. The mean of password length is 9.1 characters. Fig. 3 and Table 4 show the difference in distribution between second year and third year students. For the 2nd year students, the standard deviation is 2.4 but for the third year students, the standard deviation is 3.0. Fig. 4 shows the difference in density in password length between the 2nd year and 3rd year students. The graph of the density for the 3rdyear students is shaper compared to that for 2ndyear students. It means that third year students have more variations in password length compared to the second year students.

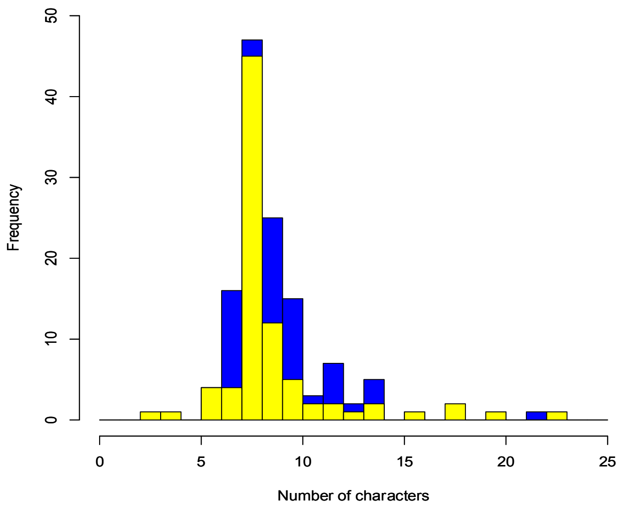

Fig. 3 – Difference between 2nd year and 3rd year students.

Table 4. Difference in standard deviation (SD) between 2nd year and 3rd year students.

Question Summary	σ (2nd year)	σ (3rd year)
Password Length	2.409025	3.071228
Number of lower-case letters?	2.832335	3.421342
Number of upper-case letters?	1.646054	2.66999
Number of numerical letters?	1.667903	3.61654

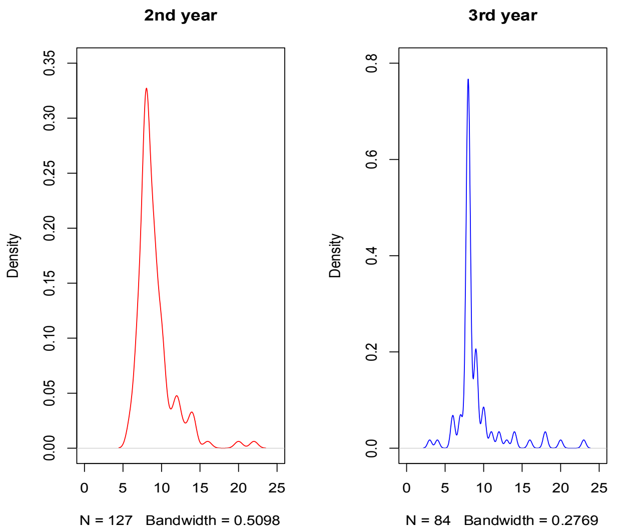

Fig. 4 – Density of password length.

Study [5] shows the relationship between the password length and strength of passwords. The portion of the strong passwords (passwords which were not cracked) with the length of 7 characters has a proportion of 96 % among the whole passwords. Such a high percentage is not observed for the passwords with the length less than 7. According to these results, number 7 is the critical threshold value of the password length and the passwords including less than 7 characters may be considered as weak passwords. Another data related to the character length of the passwords is that the passwords with the exact length of 8 characters have a rate of 45 % among the all passwords. This last observation implies that the users have a high tendency to choose passwords consisting of 8 characters.

Study [11] suggests not to use Part-of-Speech tagging system strategies such as "Determiner Adjective Noun" to set a password because it is easy to crack passwords by utilizing common cracking approaches characterized in Section 2.

5.2. DIFFICULTIES WITH MEMORIZING PASSWORDS

The password problem may be summed up as *"Choose a password that is difficult to remember and don't write down it on paper"* [3]. Book [3] discusses problems related to memorizing passwords under four main headings.

1) Naive Password Choice: One possible explanation is that many people try to use the same password everywhere.

2) User Abilities and Training: The best compromise will often be a password checking program that rejects clearly bad user choices, plus a training program to get your compliant users to choose mnemonic passwords. Password checking can be done using a program such as *crack to filter user choices* [14].

3) Design Errors: There are many sources in the Internet to check whether the password is weak or strong. One of them is a password meter [25]. Study [21] found the impact of password meters. At the registration at the online services, the suggestion from password meters is too late. However, at creating a new password, it might have affects.

4) Operational Failures: The user is not only one who is wrong with password selections. Nowadays, there are many web applications utilizing databases that use well-known default master passwords and websites listing the defaults for everything in sight. These passwords will be cracked soon because the default password use well-known patterns and crackers know this fact.

5.3. DIFFICULTIES TO CREATE AND CHANGE PASSWORDS

In this section, we show details about the nature of characters in the passwords. According to the results of our survey, the mean of lower-case characters in the password is 5.1 characters, the upper-case characters is 1.3 characters and the numerical characters is 2.8 characters. These data are similar to data discussed in [10, 12]. Thus, these data are not unique for our university. The main result is as follows. About 50 % of characters in the passwords are in lower-case.

Study [5] reveals another issue in passwords creation. The users also prefer to include upper-case characters in the passwords. One important issue from these data is that passwords containing at least one punctuation character such as ”,!, &, <, >,etc are not used often but the probability to crack them is very low. The outcome from this is: Users may use more often punctuation characters to set strong passwords. From our survey, we observe that 6 % of students use these characters in the passwords.

Fig. 5 illustrates the situation with changing passwords. It shows the distribution of data obtained over periods of time. The value of 0 means that the participant of the survey does not change the password at all. Numbers on the horizontal axis mean the periods in days to change the password. This result is very surprising because about 43 % (115) of students have never changed the password at the resources such as Gmail, Facebook, etc. since they set the password for the first time. Actually, at our university, every student must change the university account password within 90 days since the password has been set. Only 17 % (28) of the second year students have changed the password within this period of time on external services. However we are not planning to force students to change their password because according to [15] changing passwords may improve security but on the other hand, it may increase everyone’s frustration. We should note that crackers might be waiting for the change of the password to crack it. Thus, changing the password should be considered very careful.

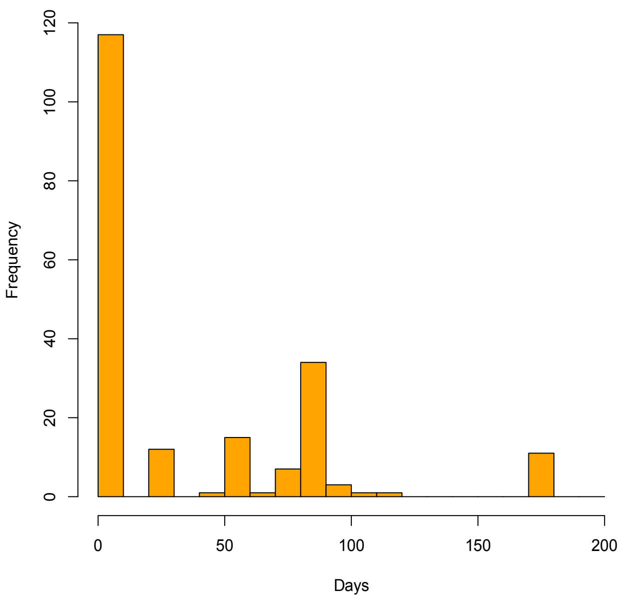

Fig. 5 - Period of time to change the password.

Table 5 shows the rate of participants answering questions touching their privacy. The privacy issue is very sensitive for the mentality of the students answering the survey. Every question in the questionnaire has the selection *“I prefer not to answer”* for participants who don’t want to answer the question.

We found an important outcome from our observation: The percentage of the students answered the questions related to privacy (questions from the third column of Table 5) is high and the percentage of the students answered questions not related to privacy (Table 6) is low.

Nowadays, there are very useful tools for end user to create, change, memorize, and manage passwords, called password management tools mentioned in Section 3. Actually some companies and specialists in security have utilized these tools to manage their passwords. And end users who are not specialist in security can also utilize it easily.

Table 5. Answers to the private questions.

Questions	**Students who answered**	**Students who preferred not to answer**
What is the length of your password?	80 % (211 students)	19 % (50 students)
Which strategy is more applicable to set passwords	88 % (168 students)	10 % (26 students)
How often do you change your password?	79 % (208 students)	18 % (48 students)
How many lower-case letters does your password contain?	62 % (163 students)	31 % (83 students)
How many upper-case letters does your password contain?	63 % (165 students)	30 % (81 students)
How many numerical letters does your password contain?	62 % (163 students)	31 % (82 students)

Table 6. Participants selected the option *“I prefer not to answer”*.

Questions	**Percent Answering**
Do you think your password is strong?	5 % (13 students)
Do you write down password?	7 % (19 students)
Do you use the same password for different accounts?	8 % (22 students)
Which strategy is more applicable to set passwords	10 % (26 students)
Do you use any strategy to create password?	16 % (44 students)
How often do you change your password?	18 % (48 students)

5.4. PASSWORD STRENGTH

In password security, Shannon entropy [23] is a measure of difficulty guessing a password. A password with a large value of entropy requires a larger number of attempts to guess it, making entropy useful as a measure of password strength [24]. To estimate the amount of entropy in passwords of different length, we need a number of characters, the value of each character and the total value of entropy. However, we do not have these data. We use the NIST guidelines [20]. According to it, these are 2 bits per letter for the entropy. To estimate entropy more accurately, we selected the students who answered the questions that are important for elements of passwords. Here are these questions.

- Q1: How many characters does your password have?
- Q10: How many lower-case letters are in your current password?
- Q11: How many upper-case letters are in your current password?
- Q12: How many numerical characters are in your current password?

Table 7. Mean and standard deviation to estimate entropy.

	Mean	SD
Upper-case	1.328671	2.14534
Lower-case	5.125874	3.153061
Numbers	2.916084	2.704968

We ignored the students who use symbol (punctuation) characters in passwords because we do not know what symbol was used. Only 6 % of users use symbols. The remaining number of student is 143. Table 7 shows the data used for estimating entropy. Our estimated entropy is 27.0 bits. In comparison with results of study [10], the mean of password length is 9.1 and 10.5. However, the entropy is 27.00 bits and 31.01 bits. We see the following reasons for this. There are different trends for password elements. The students of University of Aizu do not use the symbol character; whereas, Carnegie Mellon University students participating in study [10] use many types of character in passwords. The value of entropy for passwords in our study is relatively lower compared to the results of study [10]. According to the NIST guidelines [20], 27 bits entropy are in the passwords consisting of a sequence of 7 characters. Users chose these sequences using dictionaries and composition rules. In our study, the mean of password length is 9.2 for 143 aforementioned students. On the other hand, our entropy fits the sequences consisting of 7 characters. The reason for that is as follows. Our participants do not use symbol characters. Thus, we found that even if a password is long, it does not mean that it is strong because the password strength depends on password length and types of characters.

Comparing our finding with [10, 20], we may conclude that password length is similar in all studies but the value of entropy is very different because the students of University of Aizu do not use symbol characters in pass→words.

5.5. PASSWORD RECOGNITION

The final question in the questionnaire is on the participant understanding of strong passwords. We asked students to select the strongest password among the following:

a) the password that consists of some English phrases or words and it is as long as possible. (ex: thisisstrongpassword)
b) the password that includes numerical, upper-case, lower-case and special characters and it is short. (less than 8 characters)
c) the password that is created as an abbreviation from a phrase of the sentence. (ex : I want to be a great Software Engineer → IwtbgaSE)

26 students selected variant *a*, 182 students selected variant *b* and 35 students selected variant *c*. In Section 5.1, we revealed that the long password is not always a strong password and variant *a* is one such example. It can be easily guessed using grammar tools. Variant *c* is well known way for setting passwords and this is easy for the end user to memorize. However, crackers also know this way for setting and actually they work on how to break passwords created in this manner. So, variant *c* is not weak but not very strong. Variant *b* is actually a strong password. However, for memorizing the passwords, variant *b* is not good for end users.

From this survey, we studied that the end users can distinguish strong passwords. On the other hand, they do not have good strategies to set a strong password by themselves. Actually, in data collected from second year students, 9 % of students selected variant *a*, 71 % of students selected variant *b*, and 10 % of students selected variant *c*. Among the third year students, 11 % of students selected variant *a*, 65 % of students selected variant *b*, 18 % of students selected variant *c*. Thus, understanding the strong passwords is at the same level for second and third year students.

6. CONCLUSION

This study investigates the practical issues related to setting a strong password to use computers, online applications and services. We proposed the framework for practical suggestions to set a strong password and the questionnaire within this framework. We discussed security issues related to password protection difficulties, misunderstandings in the password protection, difficulties to memorize the passwords, and strategies to change passwords.

Our analysis is based on the survey of 262 University of Aizu students and obtained results are compared with data from different sources. We analyzed key problems for setting a strong password based on separated question groups.

We found that the students of University of Aizu majoring in Computer Science do not pay attention to the practical issues on password protection. They are quite realistic when evaluating the strength of their own passwords. They behave similar to the users from other countries when selecting the length of the password and the password structure. They behave differently when choosing types of character for passwords and passwords strength. They do not clearly understand that the strong password is. This is a one of the reasons why they do not accept the demand to change the password on the regular basis while using Internet services outside the university. 3rd year students are more experienced in computer and Internet applications. They have more variations in password length compared to the 2^{nd} year students.

To improve the situation in password protection, our results from the survey and practical recommendations can help the user set a stronger password.

How to create a strong password? The answer to this question is still an open problem.

7. REFERENCES

[1] Google 2-step verification, http://www.google.com/landing/2step/

[2] Introducing Login Approvals on Facebook, https://www.facebook.com/note.php?note_id=10150172618258920

[3] R. Anderson, *Security Engineering: A Guide to Building Depend- able Distributed System, Second Edition*, Wiley Publishing, 2008.

[4] Keisuke Kato, Vitaly Klyuev, Strong passwords: practical issues, *Proceedings of the 7th IEEE International Conference on Intelligent Data Acquisition and Advanced Computing Systems: Technology and Applications (IDAACS'2013),* Berlin, Germany (September 12-14, 2013), pp. 608-613.

[5] I. Korkmaz and M. E. Dalkilic, The weak and the strong password preferences: a case study on Turkish users, *Proceedings of the 3rd International Conference on Security of Information and Networks SIN'10*, pp. 56-61, 2010.

[6] A. Narayanan and V. Shmatikov, Fast dictionary attacks on password using time-space tradeoff, *Proceedings of the 12th ACM Conference on Computer and Communications Security CCS'05*, 2005, pp. 364–372.

[7] John the ripper, http://www.openwall.com/john/

[8] Hashcat, http://hashcat.net/oclhashcat-plus/

[9] Does adding one more question impact survey completion rate? https://www.surveymonkey.com/blog/en/blog/2010/12/08/survey_questions_and_completion_rates

[10] R. Shay, P. G. Kelley, S. Komanduri, P. G. Leon, M. L. Mazurek, L. Bauer, N. Christin, and L. F. Cranor, Encountering stronger password requirements: user attitudes and behaviors, *Proceedings of the 6th Symposium on Usable Privacy and Security*, 2010.

[11] Ashwini Rao, Birendra Jha, and Gananand Kini, Effect of grammar on security of long passwords", *Proceedings of the 3rd ACM Conference on Data and Application Security and Privacy CODASPY'13*, 2013, pp. 317–324.

[12] M. Dell'Amico, P. Michiardi, and Yves Roudier, Password Strength: An Empirical Analysis, *Proceedings of the IEEE International Conference on Computer Communications*, 2010, pp. 1–9.

[13] D. Hart, Attitudes and practices of students towards password security, *Journal of Computing Sciences in Colleges*, (23) 5 (2008), pp. 169–174.

[14] F. Bergadano, B. Crispo and G. Ruffo, Proactive password checking with decision trees, *Proceedings of the 4th ACM Conference on Computer and Communications Security*, 1997, pp. 67–77.

[15] P. Y. Logan and A. Clarkson, So long, and no thanks for the externalities: the rational rejection of security advice by users", *Proceedings of the New Security Paradigms Workshop NSPW'09*, 2009, pp. 133–144.

[16] C. Herley, Teaching students to hack: curriculum issues in information security, *Proceedings of the 36th Technical Symposium on Computer Science Education SIGCSE'05*, 2005, pp. 157–161.

[17] The maximum time required to analyze password by characters and/or the number of characters in use, http://www.ipa.go.jp/security/english/virus/press/200809/E PR200809.html/

[18] How I'd hack your weak passwords, http://lifehacker.com/5505400/how-id-hack-your-weak-passwords

[19] Password recovery speeds, http://www.lockdown.co.uk/?pg=combi&s=articles

[20] W. E. Burr, D. F. Dodson, and W. T. Polk. *Electronic Authentication Guideline*, Technical report, National Institute of Standards and Technology, 2006.
[21] Serge Egelman, Andreas Sotirakopoulos, Ildar Muslukhov, Konstantin Beznosov, and Cormac Herley, Does my password go up to eleven? The impact of password meters on password selection, *Proceedings of the SIGCHI Conference on Human Factors in Computing Systems CHI'13*, pp. 2379-2388.
[22] D. Florencio, and C. Herley. A large-scale study of web password habits, *Proceedings of the 16th International Conference on the World Wide Web,* ACM Press (New York, NY, USA, 2007), 657–666.
[23] C. E. Shannon, A mathematical theory of communication, *ACM SIGMOBILE Mobile Computing and Communications Review*, (5) 1 (1948).
[24] J. L. Massey, Guessing and entropy, *Proceedings of the IEEE International Symposium on Information Theory*, 1994, 204.
[25] http://www.passwordmeter.com
[26] Recognition and acceptance of security and privacy for eID, Technical Report: (The original title is in Japanese, Copyright © IPA, Japan), http://www.ipa.go.jp/security/economics/report/eid201008.html
[27] Young people and emerging digital services an exploratory survey on motivations, perceptions and acceptance of risks, http://ftp.jrc.es/EURdoc/JRC50089.pdf

Keisuke Kato *is a Bachelor student in the Department of Computer Science and Engineering at the University of Aizu, Japan. His areas of research interest are security Information and Big Data analysis.*

Vitaly Klyuev *received a Ph.D. degree in Physics and Mathematics from St. Petersburg State University (Russia) in 1983. He is presently a senior associate professor at the University of Aizu, Japan. His research domain includes information retrieval, software engineering and analysis of computer algorithms. He has more than 80 publications in referred journals and conference proceedings, three co-authored and eight co-edited books. Dr. Klyuev is a member of editorial board of several academic journals and a program committee member of more than 20 conferences sponsored by ACM, FTRA, IEEE, ISCA, IARIA, and WSEAS.*

computing@computingonline.net
www.computingonline.net

ISSN 1727-6209
International Journal of Computing

ONLINE DISTRIBUTED SOURCE LOCALIZATION FROM EEG/MEG DATA

Christof Pieloth [1)], Thomas R. Knösche [2)], Burkhard Maess [2)], Mirco Fuchs [1,2)]

[1)] Laboratory for Biosignal Processing, Leipzig University of Applied Sciences, Germany, www.labp.htwk-leipzig.de

[2)] Max Planck Institute for Human Cognitive and Brain Sciences, Leipzig, Germany, www.cbs.mpg.de

Abstract: Electroencephalography (EEG) and Magnetoencephalography (MEG) provide insight into neuronal processes in the brain in a real-time scale. This renders these modalities particularly interesting for online analysis methods, e.g. to visualize brain activity in real-time. Brain activity can be modeled in terms of a source distribution found by solving the bioelectromagnetic inverse problem, e.g. using linear source reconstruction methods. Such methods are particularly suitable to be used on modern highly parallel processing systems, such as widely available graphic processing units (GPUs). We present a system that, according to its modular scheme, can be configured in a very flexible way using graphical building blocks. Different preprocessing algorithms together with a linear source reconstruction method can be used for online analysis. The algorithms use both CPU and GPU resources. We tested our system in a simulation and in a realistic experiment.

Keywords: EEG, MEG, Source Imaging, GPGPU.

1. INTRODUCTION

The functioning of the brain is linked to biochemical and biophysical processes between interacting neurons and neuronal populations. This interaction is strongly related to current flows. Synchronous activity in a neuronal population, i.e. a large number of neurons concurrently respond to an excitatory input, produces currents which are strong enough to be detected. This can be done either on the head surface by measuring potentials between attached electrodes using Electroencephalography (EEG), or by measuring the magnetic flux density using Magnetoencephalography (MEG). In contrast to imaging techniques, e.g. functional magnetic resonance imaging (fMRI) or positron emission tomography (PET), which are essentially related to metabolism, EEG/MEG provides insight into brain processes in a real-time scale. To exploit the advantage of high time resolution, techniques for online processing of such signals are particularly interesting.

An important discipline in EEG/MEG analysis is source localization, i.e. inferring the current density which might have produced the measured data. This, however, is an ill-posed problem. Different approaches to solve this so called bioelectromagnetic inverse problem have been presented in literature, see [1] for an overview of this topic. A very common method is distributed source reconstruction, where a spatial current distribution is estimated from the data. In this approach, a large number of equivalent current dipoles (ECD), each of which has a fixed orientation and location, densely cover the source space. Usually, this is the cortical sheet which is approximated using a triangulated surface. Given a model of the volume conductor, which describes the conductivity profile inside the head, a so called leadfield vector can be calculated for each source, which relates its activity to a spatial pattern at sensor level. Based on this linear forward model, this approach provides the possibility for linear inverse solutions such as the popular minimum norm solution [2, 3], which actually minimizes the L2-norm of weighted current strengths.

Linear problems such as the mentioned EEG/MEG source localization technique can easily be parallelized, which renders them particularly suitable for online processing using modern high performance computing hardware such as general purpose graphic processing units (GPGPUs). Today, such hardware can easily be utilized using NVIDIA's CUDA technology which, among others, provides a comfortable way to use graphic processing units for computationally demanding problems. However, the practical realization of a system capable for the online reconstruction of brain activity from electromagnetic signals requires much more than only the parallelization of some algorithm. First, a system concept including an efficient data structure used to share information between processing steps is strictly necessary. Second, the processing pipeline needs to be flexible enough to be adopted and parameterized during measurement. Third, additional algorithms need to be provided to sufficiently prepare EEG/MEG data in real-time for source reconstruction. Fourth, other information, e.g. at least a general forward model, needs to be provided in advance to do source reconstruction.

To exploit the fact that EEG/MEG data provides insight into fast neuronal processes, we developed a software framework which principally allows online processing and visualization of brain activity in a real-time scale. According to our best knowledge, this framework is conceptually different from other solutions which provide online processing capabilities, e.g.[4, 5, 6, 7], because we aim to provide source localization using a high density source space (more than 250.000 ECDs) from high channel EEG/MEG data. Without loss of generality, we focused on the analysis of evoked brain responses in the time domain, i.e. activity which occurs due to sensory, auditory or visual stimulation. Based on simulations we have shown previously that our solution holds real-time requirement which are important for online processing and visualization [8].

Here, we introduce important extensions of the software which are essentially needed for practical applications. This includes a physical link to a real measurement device and a solution for the preparation of a forward model on demand. These extension allowed us to explore our framework under practical considerations using a simple experimental paradigm.

The paper is structured as follows. First, we will discuss some issues related to the online analysis of EEG/MEG signals. Second, the general concept of our framework will be introduced. Moreover, we will give a short explanation on each of the implemented modules, i.e. algorithms. Third, we describe how the system's online capabilities were tested. Fourth, we will demonstrate a practical application of the software in a realistic environment. Finally, we will discuss and conclude our results.

2. CHALLENGES FOR ONLINE SOURCE RECONSTRUCTION

In contrast to offline processing, online localization of brain activity depends on two important prerequisites. First, EEG/MEG data needs to be preprocessed in real-time. Second, a forward model is already required during the measurement whose calculation, however, partially depends on information only available after measurement setup (see below).

Signal preprocessing requires computational performance which competes with source localization resources. However, the quality of source localization highly depends on well preprocessed data, in which noise and artifacts are widely reduced. Noise can be distinguished in technical noise of the measurement system and neuronal noise from other brain regions, e.g. task-unrelated brain activity. To account for noise, filter techniques and signal averaging can be applied. The latter is only possible for phase related activity, such as evoked responses. Artifacts are either caused by strong electromagnetic activity emerging from external brain regions, e.g. eye blinks, heartbeat and even nearby passing trains, or result from defective sensors. Artifacts need to be detected and removed from the data. Sometimes, a correction rather than a rejection is possible. Due to the different types and characteristics of artifacts this is particularly challenging. Some artifacts can easily be detected and removed online, e.g. using a threshold based approach. For others, a universal and reliable automated detection is computationally intensive and, therefore, difficult to be realized in online systems [9, 10].

The calculation of a forward model to be used in an online framework is difficult in several aspects. First, the calculation requires a head model and the exact sensor positions. The former includes a description of the source space and of the volume conductor. The use of an individual head model would be optimal, but involves the recording of other modalities, e.g. MRI data, before the EEG/MEG measurement. Often, this is not available. The use of a standard head model is a feasible alternative. Second, the calculation of the forward model, i.e. in our case the leadfield matrix[1], is computationally expensive and takes a long time, in particular when a source space with high spatial resolution is used. But since it depends on the sensor positions, it cannot be prepared in advance. The solution to this problem is different for EEG and MEG.

For EEG, the sensor positions depend on the placement of electrodes on the head. Therefore, it is

[1]The Leadfield matrix describes the forward solution, i.e. the impact from each source on each sensor. It is computed by physical modeling of the electromagnetic fields in the head tissue.

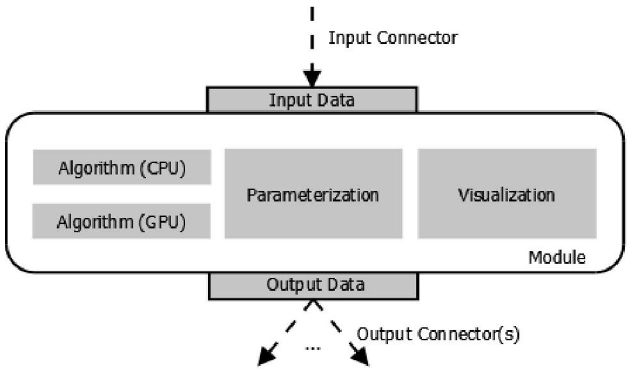

Fig. 1 - Abstract structure of a module in OpenWalnut. Gray shaded blocks represent functions that are provided by each module.

possible to place a dense grid of virtual sensors on the head surface and use them to calculate the leadfield matrix. When the true sensor positions are known, their leadfield can be derived from the virtual sensors, e.g. based on interpolation[11].

For MEG, the sensor positionsdepend on the relative position of the head in the measurement device. Thus, the forward model can be calculated under the assumption that the head is centered in the device. This can actually be achieved by applying head movement detection and correction algorithms to the recorded MEG data.

3. SOFTWARE CONCEPT AND ARCHITECTURE

The basic idea of our concept is to split the signal processing chain into separate functional units, i.e. modules that can be put together. Each module is realized in terms of a prototype that becomes part of a processing chain. The module parameters can be changed during measurement. This principle allows to set up and reuse modules easily, even several times during the same measurement. The module's intended functionality is reflected by a certain algorithm. Based on NVIDIA's CUDA technology, each module can separately use the graphic processing unit for high performance tasks. This allows an easy extension by new and efficient algorithms, which can either be executed on the CPU or on the GPU. Moreover, each module holds a separate visualization instance.

The possibility for a flexible organization of the signal processing chain requires a hybrid data structure consisting of static and dynamic areas which is shared among all modules at run time. This structure provides access to all data that might be used by any module. For example, the static part of this structure contains measurement parameters, e.g. EEG sensor positions, but also the shape of the source space. The dynamic part actually contains raw or transformed (filtered) sensor data, localized source time courses, or might be used differently. The modular concept allows signal branching, i.e. to set up signal chains using a tree structure. Such a configuration could be used to test different parameterizations of a certain algorithm or to realize different source localizations algorithms concurrently.

The implementation of our concept is based on *OpenWalnut*, a software for multi-modal brain visualization [12, 13]. This platform also follows a strict modular concept. The modules have so called input and output connectors to interact with other modules. These connectors can have any data type, only outputs and inputs that are directly connected need to share the same data structure. Whenever a module updates data at its output connector, connected modules are scheduled to allow seamless processing. Besides this useful architecture, OpenWalnut provides an intuitive mechanism to select modules and put them together by means of graphical building blocks.

According to our concept and the architecture of OpenWalnut, the structure of a module is summarized inFig. 1. It is worth to note that each module is responsible for the visualization of its results. On the one hand, this provides a very high flexibility and allows a relatively easy independent implementation because of non-existing dependencies or information from other modules. On the other hand, already a few sophisticated active visualizations instances can become computationally intractable and, besides that, drastically increase the complexity of the user front-end. Therefore visualization can be deactivated manually.

A brief overview of our data structure is depicted in Fig. 2. The main class for all modules is *EMMeasurement*, which allows to maintain any information which could be needed for EEG/MEG

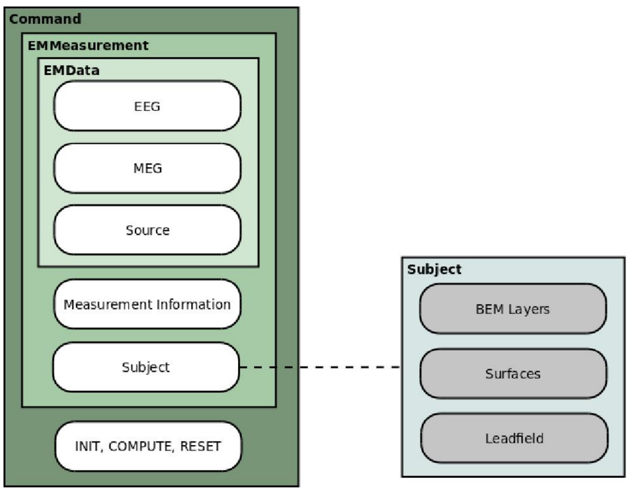

Fig. 2–Shared command and data structure. Modules can be connected based on the EMMeasurement class, which contains any sub-data that may be needed. EMData holds dynamic data, all other parts contain static information, e.g. individual surfaces.

online analysis. Within this class, other structures are nested, e.g. *EMData*, *Measurement Information* and *Subject*. While the *EMData* holds dynamic data, i.e. it contains raw and processed data, the other parts contain static data. Given this structure, the modules interact on the basis of commands. The *INIT* command forces a module to initialize all its required data structures. The *RESET* command forces a module to reset all data structures. *EMData* is computed by the module's algorithm on receiving the *COMPUTE* command. Note, the modular concept implies that data is processed in a block-wise manner.

4. MODULES AND ALGORITHMS

Based on this concept the open source toolbox *NA-Online*[2] was developed. It extends OpenWalnut by the following modules: *MNE Realtime Client*, *FIFF Reader/Writer*, *EMM Simulator*, *Alignment*, *Leadfield Interpolation*, *FIR Filter*, *Epoch Separation*, *Epoch Averaging* and *Source Reconstruction*. Their functions and purposes are introduced briefly:

(1) *MNE Realtime Client*: based on MNE software [14], it provides a physical link to a NeuromagVectorView System (Elekta, Helsinki, Finland).

(2) *FIFF Reader/Writer:*Reading and writing files using the FIFF format. It can read a previously recorded measurement or save a running measurement to disk.

(3) *EMM Simulator*:this module allows streaming of a recorded measurement for simulation purposes.

(4) *(Coordinate) Alignment*: co-registration between EEG/MEG device coordinate system and head model coordinate system, which is needed to calculate a leadfield matrix (see below) and for visualization.We implemented a semi-automatic coordinate transformation. The procedure depends on the manual labeling of three fiducial points (location of nasion, left ear, and right ear) on the skin surface in the head model before the measurement, and the digitization of these points with the EEG/MEG system. The subsequent transformation is based on iterative closet point algorithm [15].The coordinate transformation is done only once, after digitizing fiducials and electrode positions.

(5) *Leadfield Interpolation*: its purpose is to provide the EEG leadfield matrix for the digitized sensor positions before online processing. Before a measurement, a generic leadfield matrix is computed using the MNE toolbox [14] by placing virtual EEG electrodes on the skin surface in the head model. The virtual electrode positions are derived by randomly selectingapproximately 1.000 nodes from the triangulated head surface (usually consisting of more than 5.000 nodes). Note that the resulting leadfield matrix is already about 1 GB in size. During measurement setup, the true sensor positions are digitized. For each real electrode, we identify the four nearest virtual electrodes in the close vicinity. Then, linear interpolation scheme is applied. We preferred this naive linear approach over others, e.g. spline based interpolation [11], because it allows a fast and efficient computation. The leadfield information of each virtual sensor is weighted according the reciprocal value of its euclidean distance to the true electrode. Then, the leadfield at the true sensor position can be estimated by adding up the weighted leadfield vectors.

(6) *FIR Filter*: we implemented time domain filtering and provide lowpass, highpass, bandpass and bandstop characteristic. Filtering can either be done on CPU or on the GPU.

(7) *Epoch Separation*: Activity in the brain is evoked by presenting stimulus material. It is then particularly interesting to analyze this activity when a stimulus is applied. This module splits the continuous data stream according to stimulus presentation information into single epochs, i.e. data frames that range from a time point before to a point after stimulus onset. Only extracted epochs are passed to further modules.

(8) *Epoch Averaging*: Responses to an identical stimulus are expected to be phase related and very similar. This allows to apply averaging to increase the signal to noise ratio. This module implements total average and moving average. The former uses all epochs detected during a measurement to calculate an averaged evoked response. The latter only uses a certain number of the last epochs that were detected.

(9) *Source Reconstruction*: this module provides the concurrent linear reconstruction of distributed sources of all sampling points in an epoch, e.g. the average evoked response. We implemented the weighted minimum norm method [2, 3]. This algorithm requires information about the signal to noise ratio, which still has to be estimated manually. Source reconstruction is implemented for CPU and GPU. The module provides a view of the reconstructed source time courses and a 3D shape of the source space. By selecting a time point in the signal view, the corresponding spatial distribution pattern is mapped to the 3D surface. We ensured that the full resolution cortical surface can be used for the reconstruction (usually more than 200.000 sources). It is worth to note that the amount of both incoming and processed data, which has to be transferred between CPU and GPU, has a

[2]https://bitbucket.org/labp/na-online_ow-toolbox

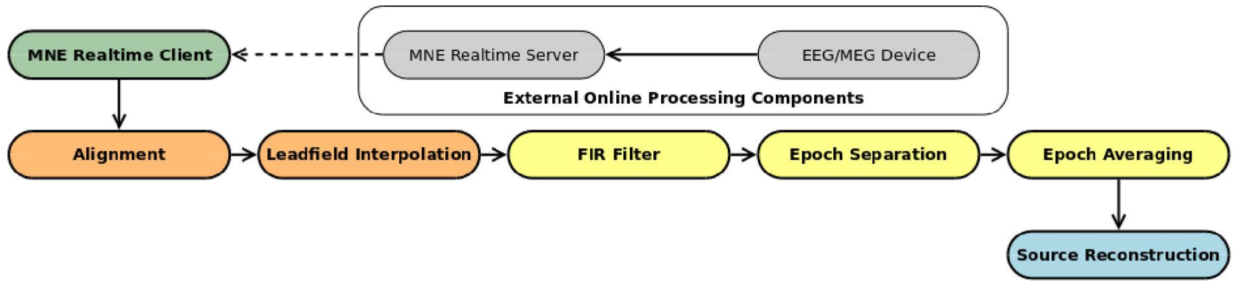

Fig. 3 – Signal processing chain used for experimental testing. The online pipeline of our software devides in data acquisition (green), which establishes a connection to an EEG/MEG device via TCP/IP, forward model preparation (orange), EEG/MEG data preprocessing (yellow) and analysis modules (blue).

tremendous impact on the total performance. If, for example, an epoch consists of 150 samples in float precision and 370 channels, the data size transferred from CPU to GPU is approximately 210 kByte. If activity is reconstructed to 250.000 sources, 143 MByte need to be transferred in the back direction.

5. SIMULATIONS AND EXPERIMENTAL TESTING

We tested our software in two steps: (1) we simulated an online measurement based on a previously recorded data set. (2) We performed real online analysis using a simple experimental paradigm. The purpose of these tests is to explore the real-time capabilities of the system and to demonstrate the signal flow. Due to the fact that a head movement correction is not yet implemented, we restricted the reconstruction to EEG data.

In the simulation, a FIFF file with 60 EEG channels (500 Hz sampling rate)and 1 trigger channel was streamed over a wireless LAN connection (54 Mbps) into our software system. The trigger channel encodes the occurrence of stimuli, here a total of 114 beep tones.The setup of the signal processing chain was according to Fig. 3with the parameterization as follows:

1) *MNE Realtime Client*: block size 1s
2) *Alignment*: 10 ICP iterations
3) *Leadfield Interpolation*: 1702 virtual sensors
4) *FIR Filter*: bandpass (1Hz-20Hz), order 200
5) *Epoch Separation*: [-100ms, +200ms]
6) *Epoch Averaging*: total average
7) *Source Reconstruction*: minimum norm method

A triangulated surface approximating the cortical sheet with one ECD at each node (cortical orientation constraint) represents the source space (244.662 sources). The volume conductor is based on a 3-layer BEM model (brain, skull, and skin surface). All surfaces were segmented from the subject's individual MRI data set using FreeSurfer[16].The positions of the virtual sensors were extracted from the head surface (skin) using the*EEG Sensor Generator*[3] tool. Finally, the generic leadfield matrix was computed using the MNE toolbox.

The general signal flow is as follows: The *MNE Realtime Client* module receives data from the streaming server, maps this into our data model (*Command*, *EMMeasurement*, *EMData*) and sets additional static data, e.g. BEM layers, source model and sensor positions. The readily prepared data block is transferred to the *Alignment* module, where the co-registration between EEG/MEG device and head model coordinate system is performed. Then, the leadfield columns at the true sensor positions are estimated in the *Leadfield Interpolation* module as described above. This results in a 60x244.662 sized leadfield matrix, which is stored in the data structure. The data blocks are passed to *FIR Filter*, where a filter routine is involved. In the subsequent*Epoch Separation* module, data segments with a length of 300ms are extracted according to stimulus information. Detected epochs are then passed to the *Epoch Averaging* module. Finally, the averaged evoked response is calculated and transferred to the *Source Reconstruction* module. Here, a source distribution is estimated at each sample point of the averaged signal (300ms), which basically involves a huge matrix-matrix

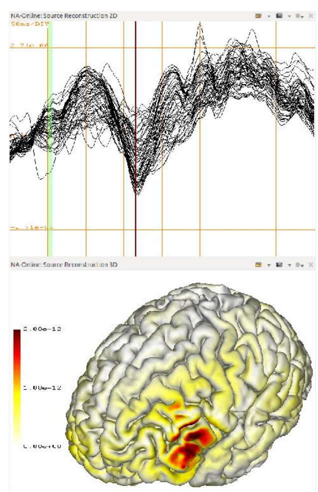

Fig. 4 - Source Reconstruction module in OpenWalnut. Top: Averaged epochs of all 60 EEG channels (overlapped). Bottom: 3D view, estimated source strength at selected time point mapped on individual cortical surface.

[3]https://bitbucket.org/labp/na-online_eeg_sensor_tools

multiplication. The calculation of the inverse operator (solution matrix based on minimum norm assumption) is done before the actual reconstruction. This is possible because it is largely independent of the data, only the signal to noise ratio has to be taken into account. The average time for this calculation was 2.2 seconds in our simulation. This means that the operator needs to be ready before a data block is subject of source localization. The source reconstruction module is invoked whenever a new epoch is detected.

Fig. 4 shows the result as it appears in OpenWalnut after all trials were averaged. The view can be rotated and different threshold values can be used to modify the color mapping. The mapping of a source distribution corresponds to a selectable time point in the signal view. The result evolves with each new epoch until the end of the measurement.

During tests we measured the processing time for each block in each module. This block processing time includes both the computational time for the algorithm and the time for visualization. The data transfer time between modules is not included in this measurement for two reasons: First, this time is difficult to estimate because the data transfer is not handled by modules but by the OpenWalnut kernel. Second, data transfer is based on the mapping and remapping of pointers and the time consumption should be negligible. It should be noted that the block size is automatically reduced at *Epoch Separation*, which is due to the selected epoch time interval.

The described signal chain was tested under two conditions: CPU-only processing and GPU-supported processing. While the former is only based on CPU execution, the latter involves GPU algorithms if modules support this. The tests were done on a high-performance workstation: Intel Xeon E5620 CPU with 2.4 GHz, 12 GB DDR3 RAM and a NVIDIA Tesla C2070 GPU.

The estimated processing times are summarized in Table 1. The times differ somewhat from earlier results [8],because, first, we now used double precision and, second, only EEG data is processed in the preprocessing stages. MEG data is excluded because source reconstruction was not yet possible at all. As can be seen, the processing time for *FIR Filter* and *Source Reconstruction* decreases if the GPU is used.*FIR Filter* scales better with increasing channel size, e.g. when processing EEG and MEG. The total processing time for the CPU-only case exceeds the block size by approximately70 percent, while the total time for GPU-supported processing is in the range of less than 25 percent of the block size. A total processing time less than the block size is necessary in order to process incoming data in time, i.e. to provide online capabilities. Given the setup presented here, this can only be achieved using the GPU.

Table 1. Averaged processing time for one block, all times in milliseconds.

	CPU-only	GPU-supported
Alignment	*77.20*	
Leadfield Interp.	*3188.0*	
FIR Filter	13.56	8.34
Epoch Separation	2.16	2.16
Epoch Averaging	0.87	0.87
Source Rec.	1,742.71	225.84
Total sum	**1,759.30**	**237.21**

In addition to the above test, we practically applied the software for the online localization of evoked brain activity in the primary motor cortex, which can be triggered based on electrical stimulation. The signal processing chain was similar to the simulation setup. As before, head model information of the individual subject was available (source space with 277.370 sources). We now used the real physical link to a NeuromagVectorView MEG system (306 MEG channels, 64 EEG channels). The online analysis was performed on a notebook: Intel Core i7-3630QM with 2.4 GHz, 8 GB DDR3 RAM and a NVIDIA GeForce GTX 660M. The reconstructed brain activity could clearly be localized to areas in the primary motor cortex. This test showed, that our implementation even performs well under real world conditions and on common end-user hardware.

6. CONCLUSION

We have shown that the current system can principally be used to reconstruct and visualize evoked brain activity based on distributed source localization during EEG/MEG measurements. Particular the usage of GPUs provides promising resources that can be utilized to improve the system further and to implement additional functions and algorithms.

Still, some issues need to be tackled before the presented system can finally be used in a real online processing framework in a seamless manner.

For example, we currently use a fixed value for the estimated signal-to-noise-ratio (SNR). This value is actually required to calculate the inverse operator, where it scales between the portion of data to be explained and modelling assumptions. Thus, this values should automatically be estimated. Moreover, the inverse operator should be updated whenever the SNR changes. In case of evoked responses, this actually happens with every new epoch. As shown in the simulation section, the calculation of the inverse operator exceeds the block size. One possible solution to this issue is to calculate a set of inverse operators in advance, where each covers a certain SNR range. Thus, recalculation would be replaced by the selection of a selection mechanism. We also currently do not account for the actual noise covariance. While solutions to this issue is straightforward, it was not required to verify the online processing capabilities of our software.

Another issue is the computation of the forward model, i.e. the leadfield matrix. We believe that our solution for EEG, which is based on leadfield interpolation, is a good compromise between computational time and accuracy. Comparisons between a leadfield matrix for a given sensor setup estimated from leadfield interpolation and using a normal forward calculation revealed only slight differences between both results. Due to the head movement in MEG devices, which can be expected in most scenarios, such an interpolation approach, e.g. as proposed in[11], is not possible for MEG data. Instead, the head position in the MEG device has to be taken into account. The method presented in [17] effectively allows to correct the data for the head position based on a simplified forward model and the minimum norm approach. The corrected data can then be used for the localization with a more complex forward model, e.g. again using the individual folded surface. It seems worthwhile to employ this approach for online processing. Before this can be done, the detection of the true head position in the MEG device is necessary which, thanks to dedicated tracking coils, is possible in an effective way [18]. These methods are currently being realized.

Other important issues are the access to further EEG/MEG systems, which we plan to achieve by integrating the *FieldTrip Buffer*[4], progress in the field of efficient artefact detection procedures, and further optimization of existing modules. For example, it is easily possible to drastically reduce the computational time for source reconstruction just be limiting the number of reconstructed time points, e.g. to only some automatically selected extrema of the signal or to a few user defined samples.

While we proofed our concept for online processing based on time domain analysis, future development will certainly include processing in the frequency domain. Possible fields of applications can be found in neurosciences, e.g. neurofeedback with the interesting possibility to measure information in the source domain.

It is worth to note that, like OpenWalnut, our toolbox is licensed under LGPL and therefore can easily be modified, improved or extended.

[4]http://fieldtrip.fcdonders.nl/development/realtime

6. ACKNOWLEDGEMENT

This work was supported by grants of the German Federal Ministry of Education and Research (17108X10) and the European Social Fund (100098255).

7. REFERENCES

[1] S. Baillet, J. C. Mosher and R. M. Leahy, Electromagnetic brain mapping, *IEEE Signal Processing Magazine*, Vol. 18, Issue 6, 2001, pp. 14-30.

[2] M. S. Hämäläinen and R. J. Ilmoniemi, *Interpreting Measured Magnetic Fields of the Brain: Estimates of Current Distributions*, Helsinki University of Technology, 1984.

[3] M. S. Hämäläinen and R. J. Ilmoniemi, Interpreting magnetic fields of the brain: minimum norm estimates, *Medical and Biological Engineering and Computing,* (32) 1 (1994), pp. 35-42.

[4] C. Dinh, J. Rühle, S. Bollmann, J. Haueisen and D. Güllmar, A GPU-accelerated performance optimized RAP-music algorithm for real-time source localization, Biomedical Engineering/ Biomedizinische Technik, DOI: 10.1515/bmt-2012-4260, September 2012.

[5] C. Dinh, M. Luessi, L. Sun, J. Haueisen and M. S. Hamalainen, MNE-X: MEG/EEG Real-time acquisition, real-time processing, and real-time source localization framework, *Biomedical Engineering / Biomedizinische Technik*, (58) (2013).

[6] Y. Renard, F. Lotte, G. Gibert, E. Maby, V. Delannoy, O. Bertrand and A. L'cuyer, OpenViBE: An open-source software platform to design, test and use brain-computer interfaces in real and virtual environments, *Presence Teleoperators Virtual Environments Presence Teleoperators and Virtual Environments,* (19) 1 (2010), pp. 35-53.

[7] Q. Noirhomme and R. I. Kitney, Single-trial EEG source reconstruction for brain–computer interface, *IEEE Transactions on Biomedical Engineering,* (55) 5 (2008), pp. 1592-1601.

[8] C. Pieloth, J. M. Pizarro, T. Knösche, B. Maess and M. Fuchs, An online system for neuroelectromagnetic source imaging, *Proceedings of the IEEE 7th International Conference on Intelligent Data Acquisition and Advanced Computing Systems (IDAACS'2013)*, Berlin, Germany, 12-14 September 2013, pp. 270-274.

[9] H. Nolan, R. Whelan and R. B. Reilly, FASTER: Fully automated statistical

thresholding for EEG artifact rejection, *Journal of Neuroscience Methods*, (192) 1 (2010), pp. 152-162.

[10] A. Delorme, T. Sejnowski and S. Makeig, Enhanced detection of artifacts in EEG data using higher-order statistics and independent component analysis, *NeuroImage*, (34) 4 (2007), pp. 1443-1449.

[11] B. Yvert, A. Crouzeix-Cheylus and J. Pernier, Fast realistic modeling in bioelectromagnetism using lead-field interpolation, *Human Brain Mapping,* (14) 1 (2001), pp. 48-63.

[12] S. Eichelbaum, M. Goldau, S. Philips, A. Reichenbach, R. Schurade and A. Wiebel, OpenWalnut: A new tool for multi-modal visualization of the human brain, *Proceedings of the EG VCBM*, 2010.

[13] S. Eichelbaum, M. Hlawitschka, A. Wiebel and G. Scheuermann, OpenWalnut – An open-source visualization system, *Proceedings of the 6th High-End Visualization Workshop*, 2010.

[14] A. Gramfort, M. Luessi, E. Larson, D. Engemann, D. Strohmeier, C. Brodbeck, L. Parkkonen and M. Hämäläinen, MNE software for processing MEG and EEG data, *NeuroImage,* (86) (2013), 446-460.

[15] S. Rusinkiewicz and M. Levoy, Efficient variants of the ICP algorithm, in *Proceedings of the 3rd International Conference on 3-D Digital Imaging and Modeling*, 2001.

[16] B. Fischl, D. H. Salat, E. Busa, M. Albert, M. Dieterich, C. Haselgrove, A. van der Kouwe, R. Killiany, D. Kennedy, S. Klaveness, A. Montillo, N. Makris, B. Rosen and A. M. Dale, Whole brain segmentation: automated labeling of neuroanatomical structures in the human brain, *Neuron*, (33) 3 (2002), pp. 341-355.

[17] T. R. Knösche, Transformation of whole-head MEG recordings between different sensor positions, *Biomedical Engineering / Biomedizinische Technik*, (47) 3 (2002), pp. 59-62.

[18] K. Uutela, S. Taulu and M. S. Hämäläinen, Detecting and correcting for head movements in neuromagnetic measurements, *NeuroImage,* (14) 6 (2001), pp. 1424-1431.

Christof Pieloth *studied Computer Science at Leipzig University of Applied Sciences (Germany). During his master study he focused on Parallel and Distributed Systems. Christof Pieloth finished his study in 2012 with a master's degree.Since then he is working at the Laboratory for Biosignal Processing on real-time processing and analysis ofbrain activity.*

Thomas R. Knösche *studied Theoretical Electrical Engineering at Ilmenau University of Technology (Germany) from 1987 to 1992. In 1991, he finished his PhD with a thesis about the neuroelectromagnetic inverse problem at Technical University of Twente (Netherlands).*

Thomas R. Knösche received his habilitationfrom the Ilmenau University of Technology in 2010. Since 2006 he is head of the research group "MEG and Cortical Networks" at the MPI for Human Cognitive and Brain Sciences in Leipzig.

Burkhard Maess *studied Physics in Leipzig from 1982 to 1987. In 1991 he finished his PhD. Since 1992 he focused on Cognitive Neuroscience and has worked in different labs in Berlin, Jülich and Leipzig (Germany). Since 2000 he is head of the magneto-encephalography group at the MPI for Human Cognitive and Brain Sciences n Leipzig.*

Mirco Fuchs *studied Electrical Engineering at the Leipzig University of Applied Sciences (HTWK Leipzig). After he received his diploma degree in in 2005, he was working in several research projects. Since 2007, he focused on inverse methods for the reconstruction of neuroelectromagnetic sources. Since 2010, he is research assistant at the Laboratory for Biosignal Processing at the HTWK and guest PhD student at the MPI for Human Cognitive and Brain Sciences in Leipzig.*

computing@computingonline.net
www.computingonline.net

ISSN 1727-6209
International Journal of Computing

USE OF A COST-EFFECTIVE NEUROHEADSET EMOTIV EPOC FOR PATTERN RECOGNITION PURPOSES

Aleksandra Kawala-Janik [1)], Jerzy Baranowski [2)], Michal Podpora [1)], Pawel Piatek [2)], Mariusz Pelc [1,3)]

[1)] Faculty of Electrical Engineering, Automatic Opole University of Technology,
ul. Proszkowska 76, 45-756 Opole, Poland,
{a.kawala-janik, m.podpora, m.pelc}@po.opole.pl, http://www.we.po.opole.pl
[2)] AGH University of Science and Technology, Faculty of Electrical Engineering, Automatics,
Computer Science and Biomedical Engineering,
al. Mickiewicza 30, 30-059 Krakow, Poland,
{jb, ppi}@agh.edu.pl, http://www.eaiib.agh.edu.pl
[3)] School of Computing and Mathematical Sciences, University of Greenwich, Old Royal Naval College,
Park Row, SE10 9LS, London, United Kingdom,
m.pelc@greenwich.ac.uk, http://www.cms.gre.ac.uk

Abstract: Application of biomedical signals for the control purposes is currently growing interest of research society. Various biomedical signals enable various control prospects. In this paper application domain of using electroencephalographic signals obtained from an inexpensive Emotiv EPOC headset was described. It is also important to mention the possible implementation of the proposed method on an embedded platform, as it causes some significant limitations due to the little efficiency and low computing power of an embedded system platform. The proposed method enables to extend future application of the BCI system presented in this paper and it also gives more testing flexibility, as the platform can simulate various external environments. It is crucial to mention, that no filtering was done and that the traditional, statistical signal processing methods were in this work neither used, nor described.

Keywords: Electroencephalography (EEG), Brain-Computer Interface (BCI), signal processing, bio-informatics, control, robotics.

1. INTRODUCTION

Implementation of various biomedical signals – in particular EEG – as an information source applied for the purpose of external environments control has become recently growing concern in the scientific world. Application of the EEG signals as a data source for Brain-Computer Interfaces (BCI) enables quick and direct communication between the computer (or any other device) and the brain [1].

Most of the BCI systems require expensive equipment with high computing power and it used complex signal processing methods, what eliminates the majority of the current solutions from their potential implementation on embedded platforms. This is because the analysis of biomedical signals and in particular EEG is very complex due the presence of various artifacts, which can be both internal and external. The signals itself are very sensitive to various disturbances and non-stochastic [2-4].

As these biomedical signals have non-stationary character, this may frequently lead to variation of SNR (Signal-Noise-Ratio), where low SNR can cause insufficient decoding accuracy and as a result affect the overall quality of a BCI system [3-5].

The novelty of the solution described in this work relies on application of basic mathematical operations, such as addition, subtraction, multiplication and division, only. Traditional, sophisticated signal processing methods were not applied. All experiments carried out for the study purpose were conducted in noisy, similar to real-life conditions [6].

2. BRAIN-COMPUTER INTERACTION

Last few decades have brought very thorough exploration of the BCI-related fields of research. BCI systems can be divided into two main groups – invasive (with surgical implantation of electrodes) and non-invasive (e.g. those EEG-based, where no surgical intervention is made). It is also possible to divide the systems into the two varieties – synchronous and asynchronous [1].

Any BCI system's goal is to record the brain activity in order to manage computer or machine actions [7]. In Fig. 1 the main six steps carried out in a typical BCI system were presented, where at the very beginning the cerebral activity is being recorded and then the data is extracted, classified and finally translated into commands, which enable to control a computer [7].

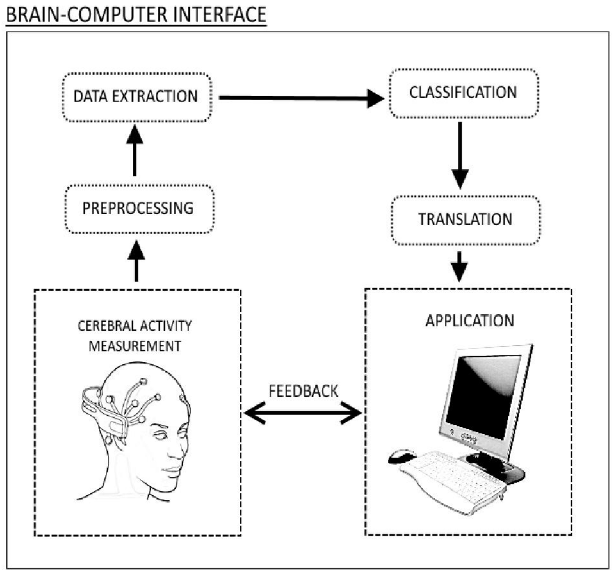

Fig. 1 – Six steps in a typical BCI system.

The BCI system presented in this work is based on EEG, where electrodes are placed on the surface of the scalp, which enables to read signals generated by the electrical activity of the brain [7, 8].

For this study purpose a non-invasive, EEG based Emotiv EPOC headset was applied. As it was important to use user-friendly, cost-effective, commercial headset (Fig. 2) [6, 8, 9].

Fig. 2 – Neuroheadset Emotiv EPOC [9].

3. RESEARCH METHODOLOGY

As mentioned above – Emotiv EPOC headset was applied for this study purpose. This is a 14-channel EEG-based headset [8-10]. It is also important to mention that most of the currently available solution require application of complex signal processing methods, which results in need of an expensive equipment due to the high computing power requirements. The method presented in this paper differs from other most common BCI systems by using basic mathematical operations only and does not require implementation of measurement equipment with high computing capability [6].

All experiments were conducted in similar to real life conditions, as only this would ensure that the proposed solution could be applicable in products such as wheelchair on crowded and noisy streets.

Twenty healthy, anonymous subjects participated in this study (Fig. 3), which had to imagine appropriate hand movement in accordance with the message appearing on the computer screen (Fig. 4). which played a role of a visual stimulus with all necessary instructions displayed on it.

Fig. 3 – Anonymous research participant.

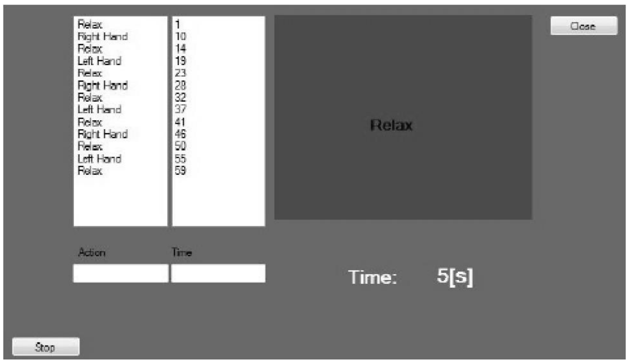

Fig. 4 – Visual stimulus with the tasks to be completed by research participants.

The data was obtained from the two channels only – F3 and F4 (Fig. 5). The electrodes are placed according to the 10-20 electrodes placement standard. The data was recorded during imagery hand movements – right (F3 electrode) and left (F4 electrode).

Equipment used during this research is not a typical medical device and therefore does not register signals with medical precision.

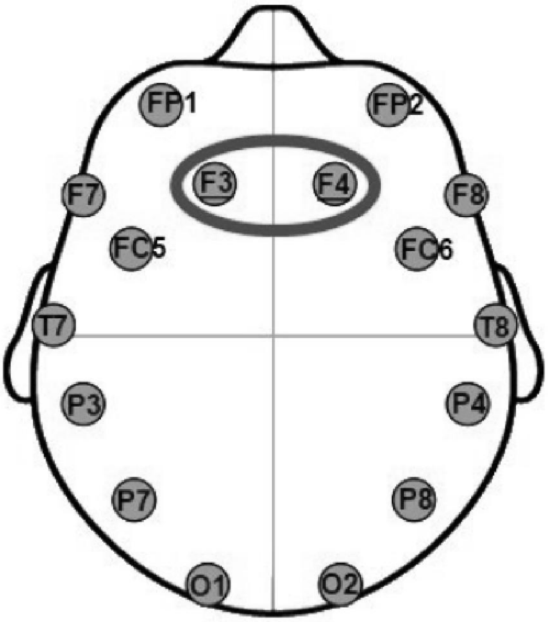

Fig. 5 – Electrodes placement.

The choice of an inexpensive, gaming equipment was made to present possible implementation of this sort of hardware in order to build cheap, but effective Brain-Computer Interface.

The Emotiv EPOC consists of 16 electrodes, where 14 only are placed on scalp and record EEG signal. The sampling rate of the device is 128 Hz and the bandwidth is between 0.2 and 45 Hz, which is fair enough for the investigated frequency ranges [9, 10]. It can also be successfully applied for recognition of user's emotions and has potentially wider use than traditional clinical electroencephalograph [11]. The neuro-headset uses three types of controls – EEG, EMG and Gyroscope [12, 13]. It also has fewer scalp contacts than a typical professional device and potentially less accuracy. Also very little study was carried out in order to test its accuracy compared to the traditional EEG [8, 12, 13].

4. MATHEMATICAL INTERPRETATION OF THE PROPOSED METHOD

As mentioned above – the method can only be presented with the use of basic mathematical operations only (1):

$$\epsilon = \frac{(1-\alpha)}{N}\sum_{k=0}^{N-1}\left[\tilde{s}_i(kT_s) - \tilde{p}_i(kT_s)\right]^2 + \frac{\alpha}{M}\sum_{l=0}^{M-1}\left[\left|\tilde{S}_j(lf_s)\right| - \left|\tilde{P}_j(lf_s)\right|\right]^2, \quad (1)$$

where $t = kT_s$ is the discrete time as $(k = 0,1,...,N-1)$, $\tilde{s}_i(kT_s)$ and $\tilde{p}_i(kT_s)$ for $i = 1,...,r$, are the discrete time representations of the ith signal and its pattern (or model depending on use), respectively, sampled at the frequency $F_s = \frac{1}{T_s}$, where T_s is the sampling interval, $\left|\tilde{S}_j(lf_s)\right|$ and $\left|\tilde{P}_j(lf_s)\right|$ are the single-sided amplitude spectra of $\tilde{s}_i(kT_s)$ and $\tilde{p}_i(kT_s)$ respectively, with f_s being the frequency step-related to (but not necessarily equal) to F_s. The normalisation ensures that $(\tilde{s}_i, \tilde{p}_i, \tilde{S}_j, \tilde{P}_j) \in [0,1]$ and that the values of Є always belong to the [0,1].

It is possible to differentiate two components of signal for the purpose of analysis. The weighted difference between the pattern and the signal is set up for both domains – the time domain and the frequency domain. In case the signal is of bad quality – very noisy, then – as a result – its time-domain representation may not be very useful for the research purposes. In this case the coefficient should be set to the value '1' or very close to '1', so that only the frequency domain component would be taken into account. Typically – as the most optimal solution – the value of the 'α' coefficient should be set to '0.5', which means that the both components are equally important. The novelty of the diagnostic (or pattern recognition) approach adopted for the purpose of this research is an application of a threshold imposed on, which enable to make decisions on the quality of pattern recognition.

5. EXPERIMENTAL RESULTS

For this study purpose all signals were recorded in a noisy, full of disturbances, environment. Fig. 6 illustrated signals obtained from the 'F3'-electrode during right-hand imagery movement. The signals matched. Signals were recorded from two different male, adult subjects – Subject 3 and Subject 7. It is also important to mention, that only raw, unfiltered signals were processed. No filtering at all was done.

In Fig. 7 the same signals, but in a normalised, scaled – [0,1] form were presented.

In both views it is possible to notice 'peaks' present in signals, what may be considered as potential artifacts. However the proposed method contains features of mean-square method. This means that this method has attributes of averaging the values and as a result – the eventual 'peaks', which may occur in signals will be eliminated.

The signals also visualy seem to differ strongly, however it is clearly noticable that they oscilate around similar values.

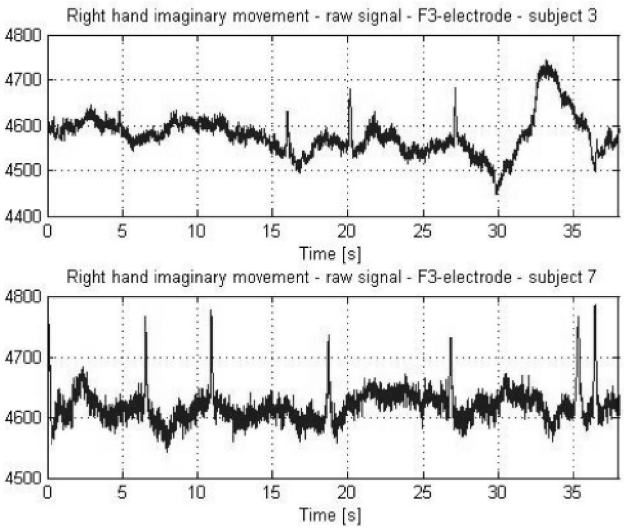

Fig. 6 – Subject 3 and 7 – imagery right-hand movement – 'F3'-electrode.

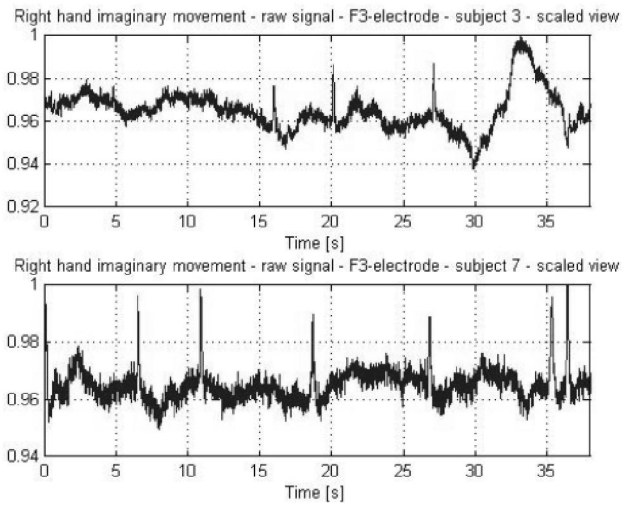

Fig. 7 – Subject 3 and 7 – imagery right-hand movement – 'F3'-electrode – normalised view.

6. RESEARCH CHALLENGES

All the above mentioned numeric procedures were carried out in MATLAB software package. The whole research was challenging due to the non-stationary nature of biomedical signals. Also implementation of the embedded platform has caused significant limitations in choosing appropriate signal processing method. As it also precludes application of advanced neural networks, as the traditional embedded platform's micro controller would not be able to proceed the computing. The conducted research was carried out on a small (for statistic criteria) group of subjects and therefore the obtained results could be unreliable, however it could be consider as a preliminary study (similar to: [14, 15]).

Analysis of efficiency of the proposed solution for the particular candidates has not been done at this stage. As the sophisticated signal processing methods cannot be used as it may cause prohibitive computational burdens. Also the device itself (Emotiv EPOC headset) had some disadvantages, as it was not designed for clinical usage. The obtained signals did not contain full information unlike it is in case the signals are recorded with a typical electroencephalograph. As a result - the recorded EEG signals had also a very low accuracy.

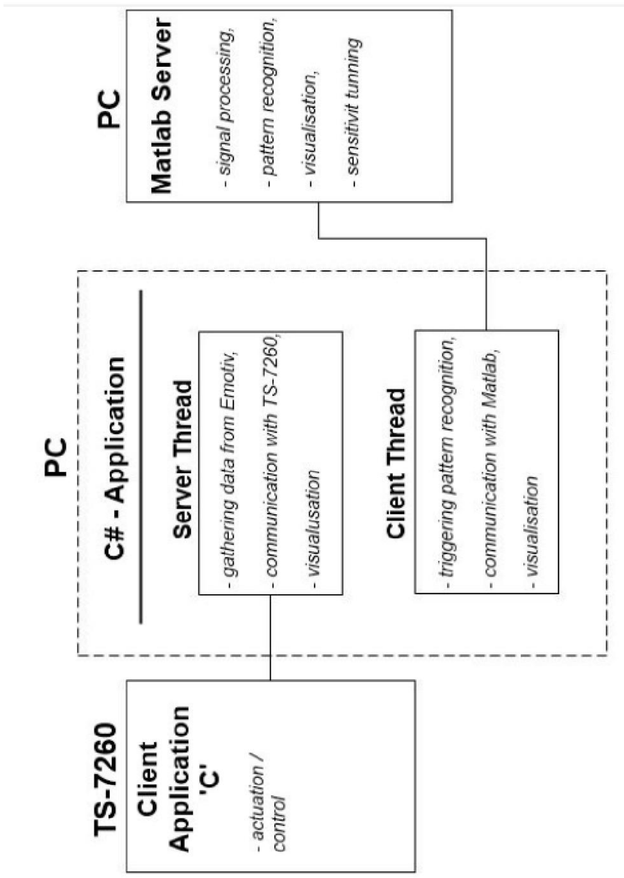

Fig. 8 – Scheme of the communication between the particular BCI components.

As the current approach is based on the fast prototyping scheme. Testbed was based on communication between PC and TS-7260 (embedded platform) and between MATLAB and PC. The main aim of this work was to build a fully working, standalone BCI system with no need of using Matlab or PC. The structure of the BCI system fast prototyping testbed described in this paper was presented in Fig. 8.

In future applications it will be desired to construct a simple embedded system based on a mobile computing platform. Main approach, that is considered is the automatic code generation directly from MATLAB/Simulink with use of Simulink Coder and Matlab Coder toolboxes (http://www.mathworks.com/products/matlab-coder/) [27].

7. CONTRIBUTION OF THE RESEARCH

In this study traditional complex statistical signal processing methods were not involved. The novelty of the proposed solution relies on application of the basic mathematical operations.

The proposed method is simple, novel and what is the most important – efficient. No filtering was done as it did not improve the results (some of the pilot study was done in order to test the effectiveness of filtering – see: [26].

It is also important to mention, that the Emotiv EPOC provides wireless USB connector and has relatively good battery life – up to 12 hours work [16]. The signals recorded with Emotiv EPOC headset are quite noisy [17]. Also – as already mentioned above – Emotiv EEG (or EPOC) is an inexpensive, non-invasive, 'off-the-shelf' wireless EEG neuroheadset, where the raw data stream is locked. Also the recording accuracy is low, however it enables successful implementation in various BCI applications [28]. All the numeric procedures of this work were conducted in MATLAB.

Adopted tools for signal processing could be more sophisticated, although it might led to prohibitive computational burdens, in particular in the embedded system environment selected owing to the lowcost implementation prerequisite.

Also the implementation of Emotiv EPOC headset had some disadvantages, as the device was not used for clinical applications and therefore the accuracy of the registered signal was not very high, however the conducted initial tests proved efficiency and suitability of the implementation of the proposed solution in real-life environments.

As it was mentioned above, equipment used for the research purposes was not designed for clinical use. It is inexpensive and easy to use (also for inexperienced potential user) [1, 18, 19]. The proposed device became very popular recently among other BCI researchers due to its intuitive user interface and low price [18, 19].

Other BCI solutions (eg. Khushaba – [21], Volosyak – [22] or Cholula – [23]) are based on analysis of various brain-signals, such as α or β unlike the proposed by the authors of the hereof paper method, where only the waves are being processed.

Many scientists engaged in analysis of EEG signals state that the frequencies of: δ, θ and α are strongly correlated with drowsiness, fatigue and poor tasks performance [29].

The above mentioned methods also require high computing power, what makes it impossible to implement in traditional embedded platforms.

The novelty of the described method relies also on its simplicity and lack of traditional statistic methods, applied in other BCI systems (e.g. [21-23). For the research purposes only two electrodes were taken into consideration, and as a result only two channels have been used – 'F3' and 'F4' [22].

The proposed method's efficiency is quite high – 91.7% in case signal was gathered in quiet environment, recorded during left hand movement from the electrode placed on 'F4' position, which was suprisingly high. However in case the same signals, from the same electrode were gathered in different conditions – noisy environment – the efficiency dropped to 86.7%. For the signals (both – noisy and quiet environment) obtained during right-hand movement and recorded from the 'F3' electrode – the efficiency was the same – 86.7%. Traditional methods – SSVEP (Steady-State Visual Evoked Potential) or P300 Paradigm oscillate between 69.2% and 100% and require higher computing power [15, 22, 23]. SSVEP BCI solution's overall pattern-recognition efficiency (presented in: [15]) was 84%, which is much lower than the effectivness of the solution proposed by the authors of this paper. Also both SSVEP and P300-based BCIs require implementation of complex signal processing method and therefore would not be suitable for the method used by authors of this publication [15, 23].

Also no filtering was done in this work, as some initial tests have proven that in analysis of signals with limited information data (when the signals have been hardware-preprocessed) filtering 'cuts-off' also the valuable information, what significantly decreases the overall signal processing performance [6, 10, 24].

Also various filtering methods such as adaptive spatio-temporal (AST) algorithms are frequently applied. The advantage of such algorithm is that it reduces the danger of signals overfitting by constructing a low-pass temporal filter with the implementation of two-parameter Gaussian kernel [30]. Using such a sophisticated method, which would also involve some mathematical modelling is was impossible to implement on the embedded platform with a very limited computing.

To sum it all up – the novelty of the proposed solution (despite its simplicity and limitations) relies on repudiation of the traditional signal processing methods based on complex statistics. The use of basic mathematical operations enables potential implementation of the methods in embedded systems with small computing power. The method can be also easily transferred into any programming language – including 'C' or 'Assembler'. During very thorough literature studies similar method have not been found.

8. FUTURE WORK

Further research will be carried out in three main areas. The first one, considers the algorithmic and conceptual improvements. The signal processing algorithm has a potential for development, with advanced techniques. Especially methods of filtering will be reconsider with possible applications of statistical filtering via densitogram [25] or Bayesian filtering [26].

Also pattern recognition and classification algorithms require additional analysis. Currently field is dominated by neural based approaches, which have many drawbacks. Authors consider application of Bayesian classifiers. In order to verify any potential advance in algorithm modification series of additional experiments is needed.

Second area for improvement is focused on hardware realisation of the system. In particular two basic approaches are considered. The first one is to construct a dedicated microcontroler system which will be responsible for data processing and interpretation. This approach has its merits, especially if true real time requirements are present. This is where automatic code generation shines the most, as Simulink algorithms can be smoothly implemented. Main drawbacks are limits to computing power and the requirement of creation of dedicated system, which in low numbers is simply not cost effective. Different approach is to use a mobile embedded platform such as smartphone. In such situation actual electronic circuits are limited to some kind of wireless interface – for example for Bluetooth or WLAN. In such case, smartphone acquires data from the interface and takes care of the processing. What is especially interesting, because of cellular network there is a constant internet access and the potential for cloud computing. It is currently used in such applications like Google Voice Search.

Third avenue for development is the extension of the system by additional methods of biomedical signal acquisition. In particular speech, EMG and EOG. Potential for integration of such systems is unlimited with broad area of applications.

The further study will focus also on improvement of the signal-processing method and application of other bio-signals – in order to extend the possible applicability and ameliorate its effectiveness. It will also involve improvement of the proposed algorithm in order to improve the pattern recognition efficiency. There are also plans for conduction more experiments with the implementation of other inexpensive, easily available on market headsets in order to obtain more data and to make the proposed method more reliable.

As mentioned already above, all numeric procedures were carried out in MATLAB. The further research plans involve building a standalone system, where not only EEG signals will be used, but also other bio- signals such as speech, EMG and EOG.

Research will also be conducted on wider group of subjects in order to make the obtained results more reliable.

Some initial tests (Fig. 9) were already run on adapting the proposed method for EMG signals recorded during simple finger movements. The efficiency of the method was in that case a little bit lower – ca. 85%. Also some initial research regarding simultaneous on-line analysis of EEG and fMRI signals was already conducted [31-33].

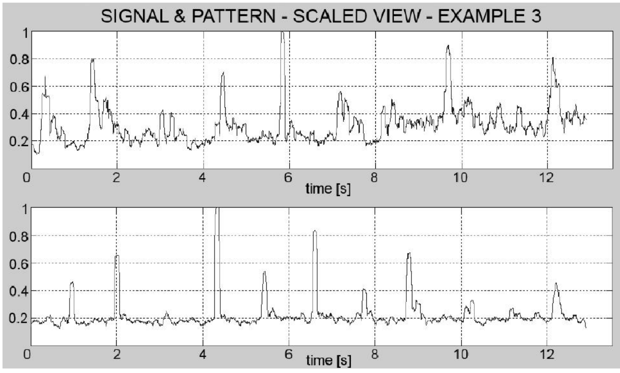

Fig. 9 – Sample of the left (top) and right (bottom) index fingers movements.

6. REFERENCES

[1] Wenjia Ouyang, Kelly Cashion, Vihayan K. Asari, Electroencephalograph based brain machine interface for controlling a robotic arm, *2013 IEEE (AIPR) Applied Imagery Pattern Recognition Workshop: Sensing for Control and Augumentation,* (October 23-25, 2013), pp. 1-7.

[2] K. Blinowska, J. Zygierewicz, *Practical Biomedical Signal Analysis Using MATLAB, Series in Medical Physisc and Biomedical Engineering*, CRC Press, Taylor and Francis Book, 2012.

[3] S. Gao, Y. Wang, X. Gao, B. Hing, Visual and auditory Brain-Computer Interfaces, *IEEE Transactions on Biomedical Engineering*, (Accepted for Publication) (2014).

[4] H. I. Suk, S. W. Lee, A novel Bayesian framework for discriminative feature extraction

in Brain-Computer Interfaces, *IEEE Transactions on Pattern Analysis and Machine Intelligence*, (35) 2 (2013), pp. 286-299.

[5] D. Huang, K. Qian, D.-Y. Fei, W. Jia, X. Chen, Electroencephalography (EEG)-based Brain-Computer Interface (BCI): A 2-D virtual wheelchair control based on Event-Related Desynchronization/Synchronization and state control, *IEEE Transactions on Neural Systems and Rehabilitation Engineering*, (20) 3 (2012), pp. 379-388.

[6] Aleksandra Kawala-Janik, Michal Podpora, Mariusz Pelc, Jerzy Baranowski, Pawel Piatek, Implementation of an inexpensive EEG headset for the pattern recognition purpose, *2013 IEEE (IDAACS) 7th International Conference on Intelligent Data Acquisition and Advanced Computing Systems,* (Berlin, September 12-14, 2013), pp. 399-403.

[7] Simon Grude, Matthew Freeland, Chenguang Yang, Hongbin Ma, Controlling mobile Spykee robot using Emotiv Neuro Headset, *2013 (CCC) 32nd Chinese Control Conference,* (Xi'an, July 26-28, 2013), pp. 5927-5932.

[8] Hidenori Boutani, Mieko Ohsuga, Applicability of the “Emotiv EPOC Neuroheadset” as a user-friendly input interface, *2013 (EMBC) 35th Annual International Conference of the IEEE Engineering in Medicine and Biology Society,* (Osaka, July 3-7, 2013), pp. 1346-1349.

[9] Official website of the Emotiv Inc. Company: *http://www.emotiv.com*

[10] Emotiv Wikia Page: *http://www.emotiv.wikia.com*

[11] R. Bernays, J. Mone, P. Yau, M. Murcia, J. Gonzales-Sanchez, M. E. Chavez-Echeagaray, R. Christopherson, R. Atkinson, Lost in the dark: Emotion adaptation, *2012 (UIST) 25th Annual ACM Symposium on User Interface Software and Technology*.

[12] G. M. Poor, L. M. Leventhal, S. K. Bowling, J. Ringenberg, S. D. Jaffee, Thought Cubes: Exploring the use of an inexpensive Brain-Computer Interface on a mental rotation task, *2011 (ASSETS) 13th International ACM SIGACCESS Conference on Computers and Accessibility.*

[13] C. Vi, S. Subramanian, Detecting Error-related negativity for interaction design, *2012 (CHI) SIGCHI Conference on Human Factors in Computing Systems,* ACM.

[14] A. Vourvopoulos, F. Liarokapis, Brain-controlled NXT robot: Tele-operating a robot through brain electrical activity, *2011 3rd International Conference on Games and Virtual Words for Serious Applications.*

[15] O. Friman, I. Volosyak, A. Graeser, Multiple channel detection of Steady-State Visual Evoked Potentials for Brain-Computer Interfaces, *IEEE Transactions on Biomedical Engineering, (54) 4 (2007).*

[16] J.-M. Seigneur, The Emotional Economy for the Augmented Human, *(AH) 2nd Augmented Human International Conference,* ACM, 2011.

[17] A. T. Campbell, T. Choudhury, S. Hu, H. Lu, M. K. Mukerjee, M. Rabbi, R. D. S. Raizada, NeuroPhone: Brain-Mobile Phone Interface. Using a Wireless EEG Headset. *2010 (MobiHeld) 2nd ACM SIGCOMM workshop on Networking, Systems, and Applications on Mobile Handhelds,* USA (August 2010).

[18] M. van Vliet, A. Robben, N. Chumerin, N. V. Manyakov, A. Combaz, M. M. van Hulle, Designing a Brain-Computer Interface Controlled Video-Game Using Consumer Grade EEG Hardware. *2012 (BRC) Biosignals and Biorobotics Conference*, Brazil (January 2012).

[19] A. Luo, J. Sullivan, A User-Friendly SSVEP-Based Brain-Computer Interface Using a Time-Domain Classifier, *Journal of Neural Engineering*, (7) 2 (2010).

[20] Y. Liu, X. Jiang, T. Cao, F. Wan, P. Un Mak, P.-I. Mak, M. I. Vai, Implementation of SSVEP Based BCI with Emotiv EPOC. *2012 (VECIMS) IEEE International Conference on Virtial Environments Human-Computer Interfaces and Measurement Systems*, China (July 2012).

[21] R. N. Khushaba, S. Kodagoda, G. Dissanayake, L. Greenacre, S. Burke, J. Louviere, A Neuroscientific Approach to Choice Modeling: Electroencephalogram (EEG) and User Preferences, *2012 (IJCNN) the 2012 International Joint Conference on Neural Networks.*

[22] I. Volosyak, Ch. Guger, A. Graeser, Toward BCI Wizard – Best BCI Approach for Each User, *2010 (EMBS) the 32nd Annual International Conference of the IEEE EMBS*, Argentina, (August-September 2010).

[23] G. Rosas-Cholula, J. M. Ramirez-Cortes, V. Alarcon-Aquino, J. Martinez-Carballid, P. Gomez-Gil, On Signal P-300 Detection for BCI Applications Based on Wavelet Analysis and ICA Preprocessing, *2010 Electronics, Robotics and Automotive Mechanics Conference*.

[24] A. Kawala-Janik, Efficiency Evaluation of External Environments Control Using Bio-Signals, *(PhD Dissertation), The University of Greenwich*, 2013.

[25] J. Baranowski, P. Piatek, A. Kawala-Janik, M. Pelc, R. J. Anthony, Application of Kernel Density for Analysis of EEG Signals, *Ubiquitous Computing and Ambient Intelligence, Lecture Notes in Computer Science*, (7656) 2012, pp 403-406.

[26] L.G. Bretthorst, Bayesian Spectrum Analysis and Parameter Estimation, *Lecture Notes in Statistics*, (48) 1988, Springer Verlag, New York.

[27] P. Piatek, D. Marchewka, M. Pauluk, Automatyczna generacja kodu regulatora dla wbudowanego sterownika ukladu magnetycznej lewiacji, *Projektowanie, analiza i implementacja systemow czasu rzeczywistego (red. L. Trybus i S. Samolej)*, WKL, Warszawa, 2011, pp. 187-196. (in Polish)

[28] N. Al-Ghamdi, G. Al-Hudhud, M. Alzamel, A. Al-Wabil, Trials and tribulations of BCI control applications, *Science and Information Conference (SAI) 2013*, pp. 212-217.

[29] Ch.-T. Lin, Ch.-H. Chuang, Ch.-Sh. Huang, Sh.-F. Tsai, Sh.-W. Lu, Y.-H. Chen, L.-W. Ko, Wireless and Wearable EEG Systems for Evaluating Driver Vigilance, *IEEE Transactions on Biomedical Circuits and Systems*, vol. 8, no. 2, 2014, pp. 165-176.

[30] J. Lu, K. Xie, D. McFarland, Adaptive Spatio-Temporal Filtering for Movement Related Potentials in EEG based Brain-Computer Interfaces, *IEEE Transactions of Neural Systems and Rehabilitation Engineering*, Accepted for Publictation in 2014. DOI: 10.1109/TNSRE.2014.2315717.

[31] X. Hongjing, R. Dan, M. S. Cohen, Coupled basis learning and regularized reconstruction for BCG artifact removal in simultaneous EEG-fMRI studies, *2013 IEEE 10th International Symposium on Biomedical Imaging (ISBI)*, 2013, pp. 986-989.

[32] A. Kawala-Janik, M. Podpora, M. Blaszczyszyn, J. Kolanska-Pluska, B. Grochowicz, Combined fMRI- and EEG-based Brain-Computer Interface – Pilot Study, *XXXVII International Conference on Fundamentals of Electrotechnics and Circuit Theory 2014*, p. 72.

[33] A. Kawala-Janik, M. Podpora, J. Kolanska-Pluska, M. Konieczny, B. Grochowicz, Pilot Study on On-Line Analysis of Biomedical Signals Using Labview, *XXXVII International Conference on Fundamentals of Electrotechnics and Circuit Theory 2014*, p. 73.

***Aleksandra Kawala-Janik, Ph.D**. received M.Sc. in Computer Engineering from the Opole University of Technology in Poland in 2007. In 2012 she has completed doctorate in Computing and was awarded in 2013 Ph.D. degree in Computing by the University of Greenwich in London. She has been working as a Lecturer in both Opole University of Technology and University of Greenwich. She has also gained some industrial experience. Currently she is employed as assistant professor at the Department of Robotics and Applied Informatics, Institute of Electromechanical Systems and Industrial Electronics, Faculty of Electrical Engineering, Automatic Control and Informatics, Opole University of Technology. Her research interests include BrainComputer Interfaces, Human-Computer Interaction, Biomedical Signal Processing and Articial Intelligence.*

***Jerzy Baranowski, Ph.D**. He obtained MSc in Control Engineering in 2006 and PhD in technical sciences in 2010. Currently he is an assistant professor in AGH University of Science and Technology at the Department of Automatics and Biomedical Engineering. His main research interests are control theory, Bayesian statistics, numerical methods and optimization.*

***Michal Podpora, Ph.D**. received B.Sc. (2002) and M.Sc. (2004) degrees in Computer Engineering from the Opole University of Technology in Poland, where he was also awarded in 2012 (Ph.D. in Control Engineering and Robotics). Until 2010 he was employed in industry sector as a developer of research software and as a EU-funds fundraiser. Since 2010 he was Research Department Manager and Project Manager of co-financed research project in industry. At the same time (2005-2011) he was employed as K-12 IT teacher. He is also Apple Distinguished Educator. He has been employed as associate professor at the Faculty of Electrical Engineering, Automatic Control and Informatics, Opole University of Technology since 2012. His main research interests include machine vision, vision reasoning, cognitive systems, robotic systems and distributed systems.*

***Pawel Piatek, Ph.D**. He obtained MSc in Control Engineering in 2000 and PhD in technical sciences in 2007. Currently he is an assistant professor in AGH University of Science and Technology at the Department of Automatics and Biomedical Engineering. His main research interests are embedded systems, signal processing and discrete control.*

***Mariusz Pelc, Ph.D**. is currently employed at the University of Greenwich, School of Computing and Mathematical Sciences, Smart Systems Technology Department and also at the Opole University of Technology, Faculty of Electrical Engineering, Automatic Control and Computer Science. His scientific activities are spread across various domains, including automatic control and robotics, modern computer / embedded (control) systems, software systems as well as computer clusters and parallel processing. His most recent scientific activity is focused on autonomic and self-* systems and most of all - validation and verification of such systems, interoperability issues and certification of self-* systems. He has published in total of nearly 50 research papers and 2 books.*

computing@computingonline.net
www.computingonline.net

ISSN 1727-6209
International Journal of Computing

NOISE IMMUNITY RESEARCH FOR NONLINEAR DYNAMICAL SYSTEMS IDENTIFICATION BASED ON VOLTERRA MODEL IN FREQUENCY DOMAIN

Vitaliy Pavlenko [1], Sergei Pavlenko [1], Viktor Speranskyy [2]

[1] ICS, Odessa National Polytechnic University, 65044, 1, Shevchenko av., Odessa, Ukraine, pavlenko_vitalij@mail.ru, psv85@yandex.ru
[2] BEITI, Odessa National Polytechnic University, 65044, 1, Shevchenko av., Odessa, Ukraine, speranskyy@gmail.com, http://study.cc.ua

Abstract: The accuracy and noise immunity of the interpolation method of nonlinear dynamical systems identification based on the Volterra model in the frequency domain is studied in this paper. The polyharmonic signals are used for the testing the method. The algorithmic and software toolkit in Matlab is developed for the identification procedure. This toolkit is used to construct the informational models of test system and communication channel. The model is built as a first-, second- and third-order amplitude–frequency and phase–frequency characteristics. The comparison of obtained characteristics with previous works is given. Wavelet denoising is studied and applied to reduce measurement noise.

Keywords: identification; nonlinear dynamic systems; Volterra models; multifrequency characteristics; polyharmonic signals; wavelet denoising; communication channels.

1. INTRODUCTION

It is necessary to consider technical conditions of the communication channels (CC) operation for effective data transfer. Changes in environmental conditions cause reducing the transmission data rate: in the digital CC – up to a full stop of the transmission, in analog CC – to the noise and distortion of the transmitted signals. The new methods and supporting toolkit are developing to automate the measurement of parameters and taking into account the characteristics of the CC. This toolkit allows obtaining the informational and mathematical model of such nonlinear dynamic object, as the CC [1], i.e. to find the identification problem solution.

Modern continuous CCs are nonlinear stochastic inertial systems. The model in the form of integro–power Volterra series used to identify them [2–5].

The nonlinear and dynamic properties of such system are completely characterized by a sequence of multidimensional weighting functions – Volterra kernels.

Building a model of nonlinear dynamic system in the form of a Volterra series lies in the choice of the test actions form. Also it uses the developed algorithm that allows determining the Volterra kernels and their Fourier–images for the measured responses (multidimensional amplitude–frequency characteristics (AFC) and phase–frequency characteristics (PFC)) to simulate the CC in the time or frequency domain, respectively [6, 7].

The additional research of noise immunity to measurement noise for nonlinear dynamical systems identification method, based on the Volterra model in the frequency domain is proposed. The developed identification toolkit used to build information model of the test nonlinear dynamic object in the form of the first, second and third order model [14] where updated.

2. INTERPOLATION METHOD OF NONLINEAR DYNAMICAL SYSTEMS IDENTIFICATION

The presentation of the “input–output” type nonlinear dynamical system presented by Volterra series were given in previous work [6].

An interpolation method of identification of the nonlinear dynamical system based on Volterra series is used [7–8, 14]. It is used n–fold differentiation of a target signal on parameter–amplitude a of test actions to separate the responses of the nonlinear dynamical system on partial components $\hat{y}_n(t)$ [8].

The $ax(t)$ type test signal is sent to input of the system, where $x(t)$ – any function; $|a|\leq 1$ – scale factor for n–th order partial component allocation $\hat{y}_n(t)$ from the measured response of nonlinear dynamical system $y[ax(t)]$. In such case it is necessary to find n–th private derivative of the response on amplitude a at a=0

$$\hat{y}_n(t) = \underbrace{\int_0^t \dots \int_0^t}_{n\ times} w_n(\tau_1,\dots,\tau_n)\prod_{l=1}^{n} x(t-\tau_l)d\tau_l = \\ = \frac{1}{n!}\frac{\partial^n y\left[a\,x(t)\right]}{\partial a^n}\Bigg|_{a=0} . \quad (1)$$

Partial components of responses $\hat{y}_n(t)$ can be calculated by using the test actions and procedure (1). Diagonal and subdiagonal sections of Volterra kernel are defined on basis of calculated responses.

Formulas for numerical differentiation using central differences for equidistant knots $y_r = y[a_r x(t)] = y[rhx(t)],\ r = -r_1, -r_1+1, \dots, r_2$ with step of computational mesh on amplitude $h=\Delta a$ were received [8].

Certain limitations should be imposed on choice of frequency polyharmonic test signals while determining multidimensional AFC and PFC [6]. That's why the values of AFC and PFC in this "limited" points of multidimensional frequency space can be calculated using interpolation only. In practical realization of nonlinear dynamical systems identification it is needed to minimize quantity of such undefined points at the range of multidimensional frequency characteristics determination. This done to provide a minimum of restrictions on choice of frequency of the test signal. It is shown that existed limitation can be weakened. New limitations on choice of frequency are reducing quantity of undefined points.

It is defined: to obtain Volterra kernels for nonlinear dynamical system in frequency domain the limitations on choice of frequencies of test polyharmonic signals have to be restricted. This restrictions provide inequality of combination frequencies in the test signal harmonics. It is necessary to consider the imposed constraints on choice of the test polyharmonic signal frequencies during determination of multidimensional transfer functions of nonlinear systems. It provides an inequality of combination frequencies in output signal harmonics: $\omega_1 \neq 0$, $\omega_2 \neq 0$ and $\omega_1 \neq \omega_2$ for the second order identification procedure, and $\omega_1 \neq 0$, $\omega_2 \neq 0$, $\omega_3 \neq 0$, $\omega_1 \neq \omega_2$, $\omega_1 \neq \omega_3$, $\omega_2 \neq \omega_3$, $2\omega_1 \neq \omega_2+\omega_3$, $2\omega_2 \neq \omega_1+\omega_3$, $2\omega_3 \neq \omega_1+\omega_2$, $2\omega_1 \neq \omega_2-\omega_3$, $2\omega_2 \neq \omega_1-\omega_3$, $2\omega_3 \neq \omega_1-\omega_2$, $2\omega_1 \neq -\omega_2+\omega_3$, $2\omega_2 \neq -\omega_1+\omega_3$ и $2\omega_3 \neq -\omega_1+\omega_2$ for the third order identification procedure.

3. THE TECHNIQUE OF THE TEST OBJECT IDENTIFICATION

Described method was fully tested on a nonlinear test object (Fig. 1) described by Riccati equation:

$$\frac{dy(t)}{dt} + \alpha y(t) + \beta y^2(t) = u(t)., \quad (2)$$

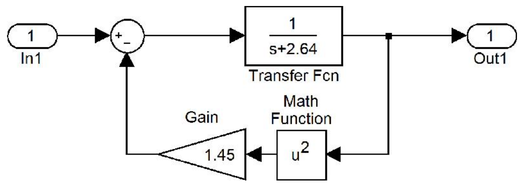

Fig. 1 – Matlab-Simulink model of the test object.

Analytical expressions of AFC and PFC for the first, second and third order model were received and presented in [8].

The main purpose was to identify the multifrequency performances characterizing nonlinear and dynamical properties of nonlinear test object. Volterra model in the form of the second order polynomial is used. Thus, test object properties are characterized by transfer functions of $W_1(j\omega_1)$, $W_2(j\omega_1,j\omega_2)$, $W_3(j\omega_1,j\omega_2,j\omega_3)$ − by Fourier–images of weight functions $w_1(t)$, $w_2(t_1, t_2)$, $w_3(t_1, t_2, t_3)$.

Structure chart of identification procedure – determination of the 1st, 2nd or 3rd order AFC of CC is presented on Fig. 2.

The weighted sum is formed from received signals – responses of each group (Fig. 2). As a result the partial components of CC responses $y_1(t)$, $y_2(t)$ and $y_3(t)$ are got. For each partial component of response the Fourier transform (the FFT is used) is calculated, and from received spectrum only an informative harmonics (which amplitudes represent values of required characteristics of the first, second and third orders AFC) are taken.

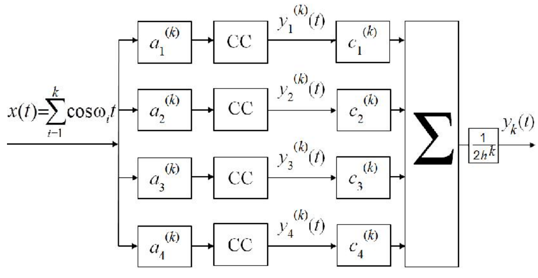

Fig. 2 – The structure chart of identification procedure using the k- order Volterra model in frequency domain, number of experiments N=4, *k* – order of the estimated Volterra kernel.

The first order AFC $|W_1(j\omega_1)|$ and PFC $\arg W_1(j\omega_1)$, where $\omega_1=\omega$ are received by extracting the harmonics with frequency f from the spectrum of the CC partial response $y_1(t)$ to the test signal $x(t)=A/2(\cos\omega t)$.

The second order AFC $|W_2(j\omega_1,j\omega_2)|$ and PFC $\arg W_2(j\omega_1,j\omega_2)$, where $\omega_1=\omega$ and $\omega_2=\omega_1+\Omega_1$, were received by extracting the harmonics with summary frequency $\omega_1+\omega_2$ from the spectrum of the CC partial response $y_2(t)$ to the test signal $x(t)=(A/2)(\cos\omega_1 t+\cos\omega_2 t)$.

The third order AFC $|W_3(j\omega_1,j\omega_2,j\omega_3)|$ and PFC $\arg W_3(j\omega_1,j\omega_2,j\omega_3)$, where $\omega_1=\omega$, $\omega_2=\omega_1+\Omega_1$, $\omega_3=\omega_2+\Omega_2$ were received by extracting the harmonics with summary frequency $\omega_1+\omega_2+\omega_3$ from the spectrum of the CC partial response $y_2(t)$ to the test signal $x(t)=(A/2)(\cos\omega_1 t+\cos\omega_2 t+\cos\omega_3 t)$.

The results (first, second and third order AFC and PFC) which had been received after procedure of identification are represented in Fig. 3–5 (number of experiments for the model N=4).

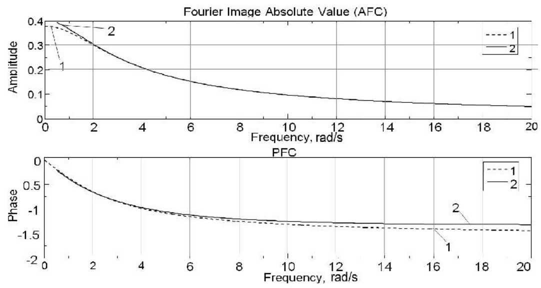

Fig. 3 – First order AFC and PFC of the test object: analytically calculated values (1), section estimation values – number of experiments for the model N=4 (2).

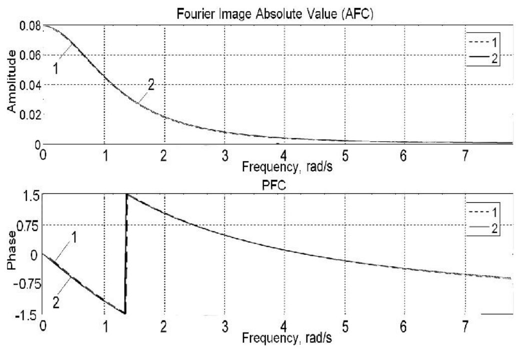

Fig. 4 – Second order AFC and PFC of the test object: analytically calculated values (1), subdiagonal cross–section values with number of experiments for the model N=4 (2), Ω₁=0,01 rad/s.

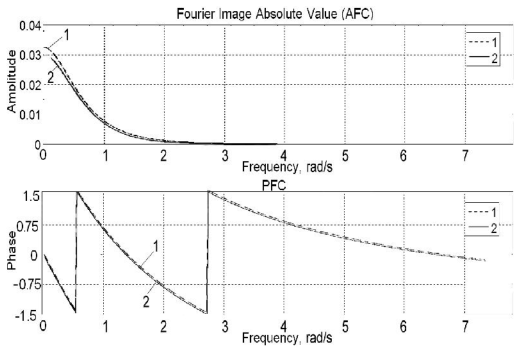

Fig. 5 – Third order AFC and PFC of the test object: analytically calculated values (1), subdiagonal cross-section values with number of experiments for the model N=6 (2), Ω_1=0,01 rad/s, Ω_2=0,1 rad/s.

The surfaces shown on Fig. 6–9 are built from subdiagonal cross–sections which were received separately. Ω_1 was used as growing parameter of identification with different value for each cross–section in second order characteristics. Fixed value of Ω_2 and growing value of Ω_1 were used as parameters of identification to obtain different value for each cross–section in third order characteristics.

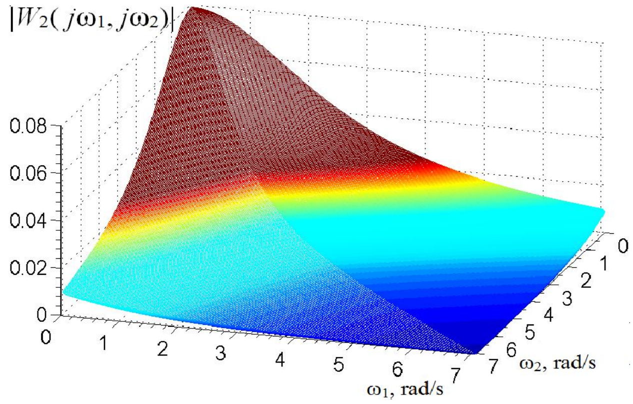

Fig. 6 – Surface of the test object AFC built of the second order subdiagonal cross–sections received for N=4, Ω_1=0,01 rad/s.

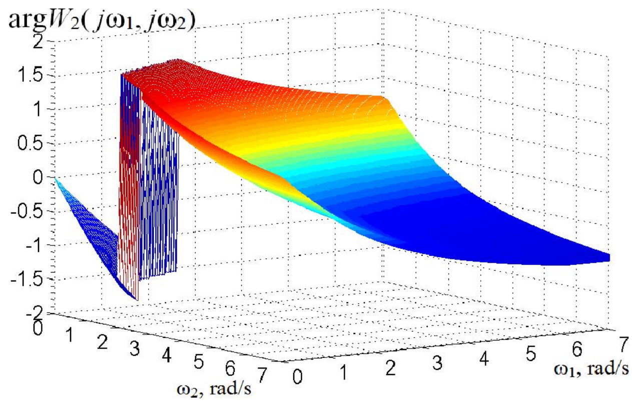

Fig. 7 – Surface of the test object PFC built of the second order subdiagonal cross–sections received for N=4, Ω_1=0,01 rad/s.

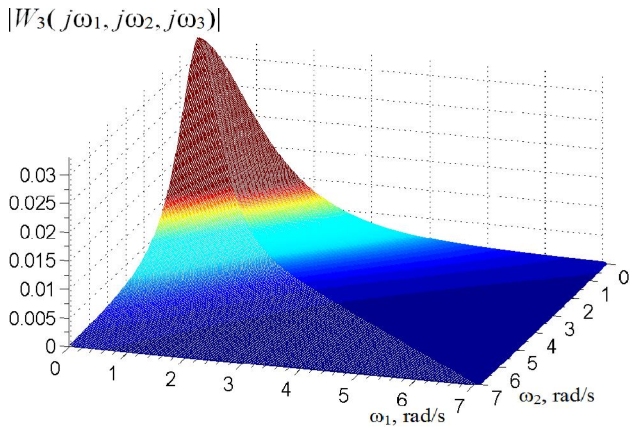

Fig. 8 – Surface of the test object AFC built of the third order subdiagonal cross–sections received for N=6, Ω_1=0,01 rad/s, Ω_2=0,1 rad/s.

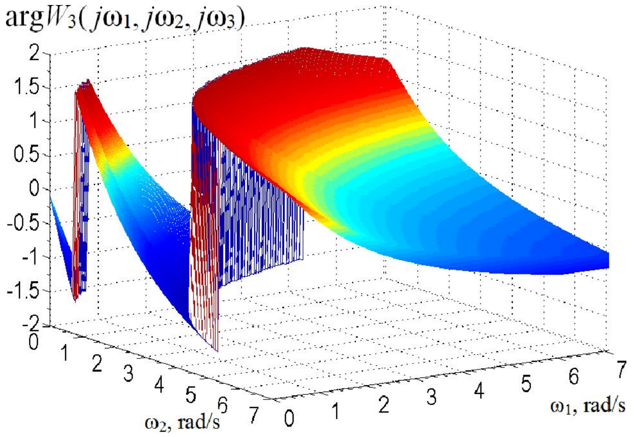

Fig. 9 – Surface of the test object PFC built of the third order subdiagonal cross-sections received for N=6, Ω_1=0,01 rad/s, Ω_2=0,1 rad/s

The second order surfaces for AFC and PFC had been received after procedure of the test object identification and are shown in Fig. 6–7 (number of experiments for the model N=4).

The third order surfaces for AFC and PFC had been received after procedure of the test object identification and are presented in Fig. 8–9 (number of experiments for the model N=6).

Numerical values of identification accuracy using interpolation method for the test object are represented in Table 1.

Table 1. Numerical values of identification accuracy using interpolation method.

Kernel order, k	Experiments quantity, N	AFC relative error, %	PFC relative error, %
1	2	2.1359	2.5420
	4	0.3468	2.0618
	6	0.2957	1.9311
2	2	30.2842	76.8221
	4	2.0452	3.7603
	6	89.2099	5.9438
3	4	10.9810	1.6280
	6	10.7642	1.5522

4. THE STUDY OF NOISE IMMUNITY OF THE IDENTIFICATION METHOD

Experimental research of the noise immunity of the identification method were made. The main purpose was the studying of the noise impact (noise means the inexactness of the measurements) to the characteristics of the test object model using interpolation method in frequency domain.

The first step was the measurement of the level of useful signal after test object (Out2 in Fig. 10). The amplitude of this signal was defined as the 100% of the signal power.

After that procedure the Random Noise signal where added to the test object output signal. This where made to simulate inexactness of the measurements in model. The sum of these two signals for the linear test model is shown in Fig. 11.

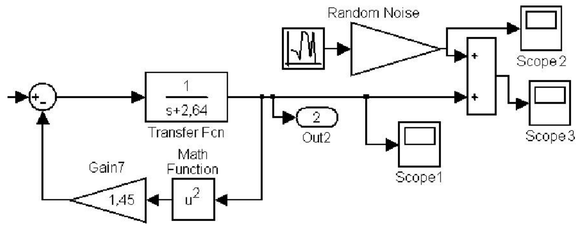

Fig. 10 – The Simulink model of the test object with noise generator and osillosopes.

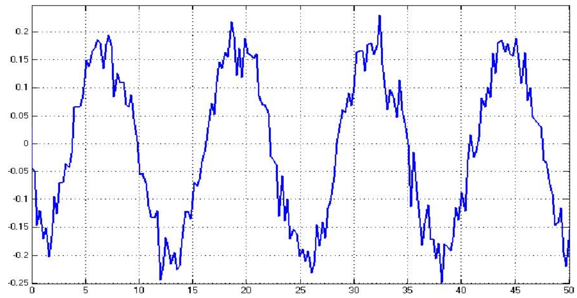

Fig. 11 – The "noised" signal of the test object, the level of noise is 50% of source signal.

The simulations with the test model were made. Different noise levels were defined for different order of the model.

The automatic wavelet denoising were used to reduce the noise impact on final characteristics of the test object. The Daubechie wavelet of the 2 and 3 level were chosen and used for the AFC and PFC denoising respectively [9, 13].

The first order (linear) model was tested with the level of noise 50% and 10% and showed excellent level of noise immunity. The second order (nonlinear) model was tested with the level of noise 10% and 1% and showed good level of noise immunity. The noised (Fig. 12) and de-noised (filtered) (Fig. 13) characteristics (AFC and PFC) with level of noise 10% are presented. The third order (nonlinear) model was tested with the level of noise 10% and 1% and showed good level of noise immunity.

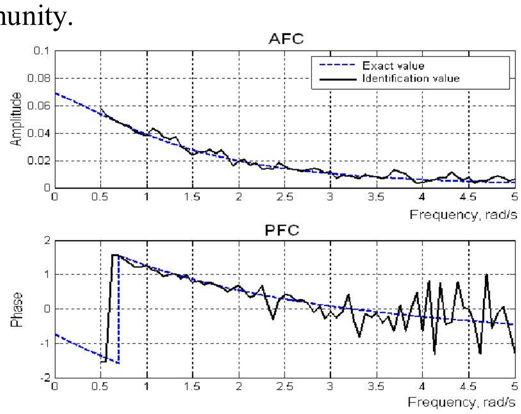

Fig. 12 – Noised characteristics (AFC – top, PFC – bottom) of the 2nd order for the test object model with noise level 10%.

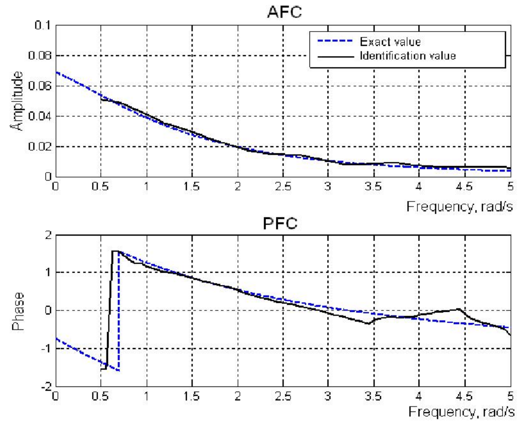

Fig. 13 – Denoised characteristics (AFC – top, PFC – bottom) of the 2nd order for the test object model with noise level 10%

The numerical values of standard deviation (SD) of the identification accuracy before and after wavelet denoising procedure are shown in Table 2.

Table 2. Standard deviation with noise impact.

k	N	Noise level = 10%		Noise level = 1%		Improvement	
		SD for AFC	SD for PFC	SD for AFC	SD for PFC	for AFC, times	for PFC, times
		(without / with denoising)					
1	2	0.000097 /0.000063	0.09031 /0.07541	–	–	**1,540**	1,198
	4	0.000271 /0.000181	0.07804 /0.06433	–	–	1,497	1,213
	6	0.000312 /0.000223	0.12913 /0.09889	–	–	1,399	1,306
2	2	0.000920 /0.000670	0.52063 /0.51465	–	–	1,373	1,012
	4	0.001972 /0.001663	0.28004 /0.06877	–	–	1,186	**4,072**
	6	0.004165 /0.003908	0.39260 /0.19237	–	–	1,066	2,041
3	4	–	–	0.000288 /0.000288	0.89857 /0.61251	1,003	1,467
	6	–	–	0.000461 /0.000352	0.84868 /0.59319	1,310	1,431

The diagrams, showing the improvement of standard deviation for identification accuracy using the automatic wavelet denoising of the received characteristics (AFC and PFC) are shown in Fig. 14 and Fig. 15 respectively.

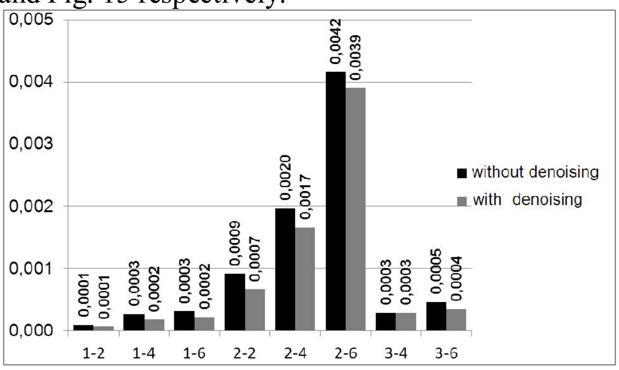

Fig. 14 – Standard deviation changing for AFC using automatic Wavelet-denoising.

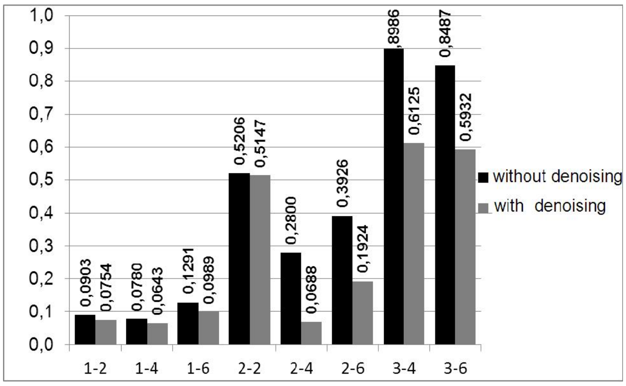

Fig. 15 – Standard deviation changing for PFC using automatic Wavelet-denoising.

5. HARDWARE-SOFTWARE TOOLKIT AND TECHNIQUE OF RADIOFREQUENCY CC IDENTIFICATION

Experimental research of the Ultra High Frequency range CC were done. The main purpose was the identification of multifrequency performances that characterize nonlinear and dynamical properties of the CC. Volterra model in the form of the second order polynomial is used. Thus physical CC properties are characterized by transfer functions of $W_1(j2\pi f)$ and $W_2(j2\pi f_1, j2\pi f_2)$ − by the Fourier–images of weighting functions $w_1(t)$ and $w_2(t_1, t_2)$.

Implementation of identification method on the IBM PC computer basis has been carried out using the developed software in Matlab software. The software allows automating the process of the test signals forming with the given parameters (amplitudes and frequencies). Also this software allows transmitting and receiving signals through an output and input section of PC soundcard, to produce segmentation of a file with the responses to the fragments, corresponding to the CC responses being researched on test polyharmonic effects with different amplitudes.

In experimental research two identical marine transceivers S.P.RADIO A/S SAILOR RT2048 VHF (the range of operational frequencies is 154,4−163,75 MHz) at 16th operational channel and IBM PC with Creative SBLive! soundcards were used. These transceivers are now used at most ships for communication with coast port stations. Sequentially AFC of the first, second and third orders were defined. The method of identification with number of experiments N=4 was applied.

General scheme of a hardware–software complex of the CC identification, based on the data of input–output type experiment was studied in [6].

The CC received responses $y[a_i x(t)]$ to the test signals $a_i x(t)$, compose a group of the signals, which amount is equal to the used number of experiments N (N=4), shown in Fig. 16.

In each following group the signals frequency increases by magnitude of chosen step. A cross–correlation was used to define the beginning of each received response. Information about the form of the test signals given in [7] were used.

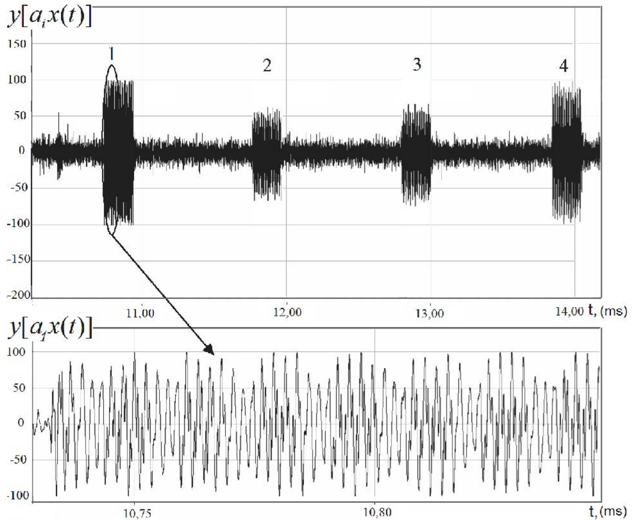

Fig. 16 – The group of signals received from CC with amplitudes: -1 (1); 1 (2); -0,644 (3); 0,644 (4); N=4.

In described experiment with use of sound card the maximum allowed amplitude was A=0,25V (defined experimentally). The range of frequencies was defined by the sound card pass band (20…20000 Hz), and frequencies of the test signals has been chosen from this range, taking into account restrictions specified above. Such parameters were chosen for the experiment: start frequency f_s =125 Hz; final frequency f_e =3125 Hz; a frequency change step Δf=125 Hz; to define AFC of the second order determination, an offset on frequency $F_1=f_2\text{-}f_1$ was increasingly growing from 201 to 3401 Hz with step 100 Hz.

The weighed sum is formed from received signals – responses of each group (Fig. 2). As a result we get partial component s of response of the CC $y_1(t)$ and $y_2(t)$. For each partial component of response a Fourier transform (the FFT is used) is calculated, and from received spectra only an informative harmonics (which amplitudes represents values of required characteristics of the first and second orders AFC) are taken.

The first order AFC $|W_1(j2\pi f)|$ is received by extracting the harmonics with frequency f from the spectrum of the partial response of the CC $y_1(t)$ to the test signal $x(t)=A/2(\cos 2\pi ft)$.

The second order AFC $|W_2(j2\pi f, j2\pi(f+F_1))|$, where $f_1=f$ and $f_2=f+F_1$, was received by extracting the harmonics with summary frequency f_1+f_2 from the spectrum of the partial response of the CC $y_2(t)$ to the test signal $x(t)=(A/2)(\cos 2\pi f_1 t+\cos 2\pi f_2 t)$.

The wavelet noise–suppression was used to smooth the output data of the experiment [9]. The results received after digital data processing of the data of experiments (wavelet "Coiflet" de–noising) for the first, second and third order AFC are presented in Fig. 17–20.

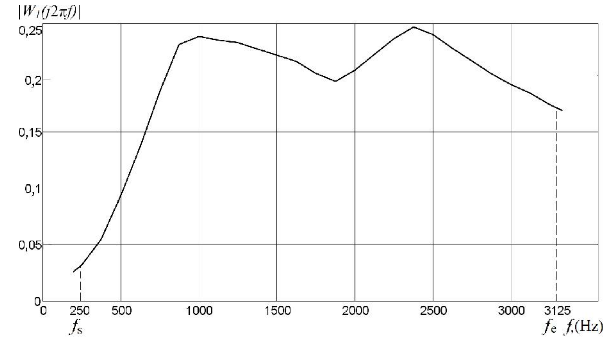

Fig. 17 – AFC of the first order after wavelet "Coiflet" second level denoisingю

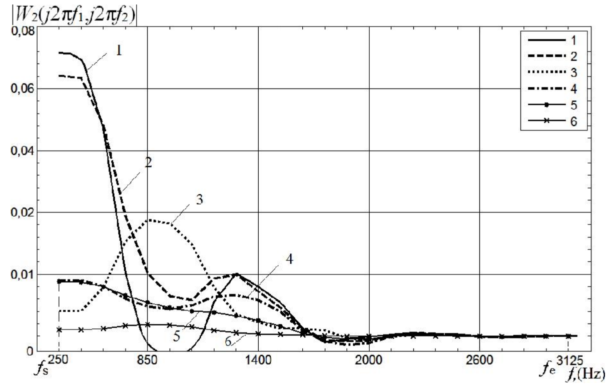

Fig. 18 – Subdiagonal cross–sections of AFCs of the second order after wavelet "Coiflet" second level denoising at different frequencies: 201 (1), 401 (2), 601 (3), 801 (4), 1001 (5), 1401 (6) Hz.

The surfaces shown in Fig. 19–20 were built from subdiagonal cross–sections that have been received separately. A growing parameter of identification Δf with different value for each section was used.

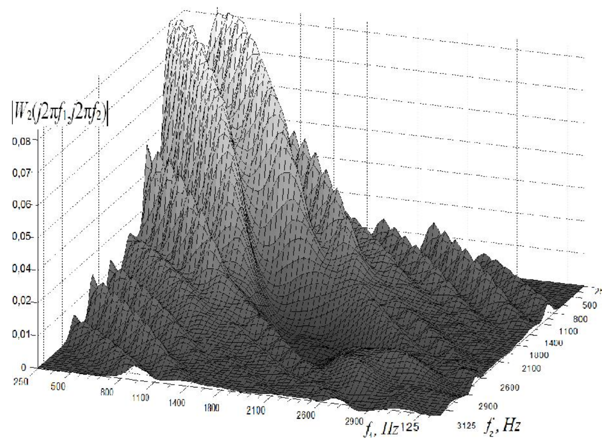

Fig. 19 – Surface built of AFC cross–sections of the second order after wavelet "Coiflet" 3rd level denoising.

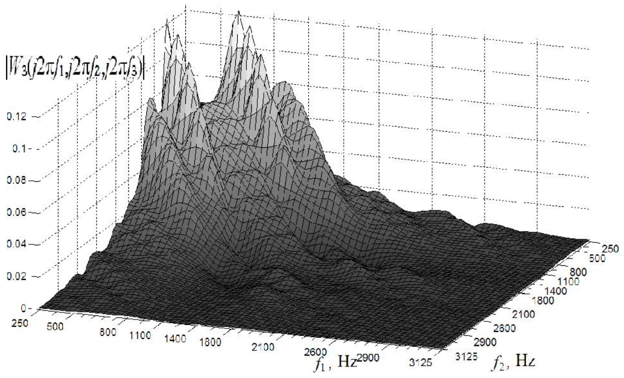

Fig. 20 – Surface built of AFC cross–sections of the third order after wavelet "Coiflet" 3rd level denoising, where $f_3 = f_1 + 100$ Hz.

6. CONCLUSION

The method based on Volterra model using polyharmonic test signals for identification nonlinear dynamical systems is analyzed. The method based on composition of linear responses combination on test signals with different amplitudes were used to differentiate the responses of object for partial components. New values of test signals amplitudes were defined and model were validated using the test object. Excellent accuracy level for received model is achieved as in linear model so in nonlinear ones. Given values are greatly raising the accuracy of identification in compare to amplitudes and coefficients studied in [10, 11]. The identification accuracy of nonlinear part for the test object has grown for 5-20% while the standard deviation in best cases is no more than 10% that means excellent adequacy of used method.

The noise immunity is very high for the linear model, high enough for the second order nonlinear model and has moderate noise immunity for the third order model. The wavelet denoising is very effective and gives the possibility to improve the quality of identification of the noisy measurements up to 1,54 and 4,07 times for the AFC and PFC respectively.

Interpolation method of identification using the hardware methodology used in [11, 12] is applied for constructing of informational Volterra model as an APC of the first and second order for UHF band radio channel. Received results had confirmed significant nonlinearity of characteristics of the tested objects that leads to distortions of signals in different type radio devices.

7. REFERENCES

[1] G. B. Giannakis, E. Serpedin, A bibliography on nonlinear system identification and its applications in signal processing, communications and biomedical engineering, *Signal Processing – EURASIP*, Elsevier Science B.V., (81) 3 (2001), pp. 533–580.

[2] D. T. Westwick, *Methods for the Identification of Multiple–Input Nonlinear Systems, Departments of Electrical Engineering and Biomedical Engineering*, McGill University, Montreal, Quebec, Canada, 1995, pp. 192–232.

[3] F. J. Doyle, R. K. Pearson, B. A. Ogunnaike, *Identification and Control Using Volterra Models,* Published Springer Technology & Industrial Arts, 2001, pp. 58–72.

[4] S. Boyd, Y. S. Jang, L. O. Chua, Measuring Volterra kernels, *IEEE Transactions on Circuits and Systems*, (CAS-30) 8 (1983), pp. 571–578.

[5] K. V. Peddanarappagari, M. Brandt-Pearce, Volterra series approach for optimizing fiber–optic communications system designs, *J. Lightwave Tech.*, (16) 11 (1998), pp. 2046–2055.

[6] V. D. Pavlenko, V. I. Lomovoy, V. O. Speranskyy, Modelling of radio-frequency communication channels using Volterra model, *Proceedings of the 6th IEEE International Conference on Intelligent Data Acquisition and Advanced Computing Systems: Technology and Applications*, Vol. 2, 2011, pp. 574-579.

[7] V. D. Pavlenko, Identification of nonlinear dynamic systems in the form of the Volterra kernels on the basis of the data of pulse response measurements, *Electronic Modeling*, (32) 3 (2010), pp. 3–18. (in Russian).

[8] M. Schetzen, *The Volterra and Wiener Theories of Nonlinear Systems,* Wiley & Sons, New York., 1980, pp. 321–360.

[9] J. G. Goswami, A. K. Chan, *Fundamentals of Wavelets: Theory, Algorithms, and Applications,* Publishing John Wiley & Sons, Inc., 1999, pp. 125–137.

[10] L. V. Danilov, P. N. Mathanov, E. S. Philipov, *The theory of nonlinear electrical circuits,* Published Energoatomizdat, Leningrad, 1990, pp. 136–148 (in Russian).

[11] V. D. Pavlenko, V. O. Speranskyy, Communication channel identification in frequency domain based on the Volterra model, *Proceedings of the International Conference on Computers, Digital Communications and Computing (ICDCC'11)*, Barcelona, Spain, September 15-17, 2011, Published by WSEAS Press, 2011, pp. 218–222.

[12] V. D. Pavlenko, S. V. Pavlenko, V. O. Speranskyy, Interpolation method of nonlinear dynamical systems identification based on Volterra model in frequency domain, *Proceedings of the 7th IEEE International*

Conference on Intelligent Data Acquisition and Advanced Computing Systems: Technology and Applications (IDAACS'2013), Berlin, Germany, 15–17 September 2013, pp. 173–178.

[13] M. Misiti, Y. Misiti, G. Oppenheim, J.-M. Poggi, *Wavelets toolbox users guide, The MathWorks*. Wavelet Toolbox, for use with MATLAB, 2000.

Vitaliy Pavlenko, *D.Sc., senior research associate. Education: 1970 Student, Odessa Polytechnic University, 1973 Post graduate Student, Computers Department, Odessa Polytechnic University. Current position: professor of Computer Systems Institute.*

Scientific interests: Modeling and Simulation for Industrial Applications; Non-parametric Identification of Nonlinear Systems; Theory of the Volterra series; Mathematical methods, models and technologies for complex systems' research; Problems of data and knowledge mining; Statistic Classification; Neural nets for simulation; Diagnostic, Fault detection, Forecasting; Computers Information Technologies; Computer and telecommunication systems; Parallel computing algorithms and methods of parallel programming.

Sergey Pavlenko, *PhD student. Education: 2007 Student, Odessa National Polytechnic University, 2010 Post graduate Student, Computer Systems Department, Odessa National Polytechnic University. Current position: Junior researcher of Energy Management Instititute.*

Scientific interests: Modeling and Simulation for Industrial Applications; Non-parametric Identification of Nonlinear Systems; Theory of the Volterra series; Mathematical methods, models and technologies for complex systems' research; Problems of data and knowledge mining.

Viktor Speranskyy, *PhD student. Education: 2003 Student, Odessa State Academy of Refrigeration, 2007-2012 Post graduate Student, Computer Systems Department, Odessa National Polytechnic University. Current position: senior lecturer of Economic cybernetics and informational technologies department in the Business, Economics and Informational Technologies Institute. Scientific interests: Modeling and Simulation for Industrial Applications; Non-parametric Identification of Nonlinear Systems; Theory of the Volterra series; Mathematical methods, models and technologies for complex systems' research; Computer Information Technologies; Wired and wireless communications; Programming algorithms; Operation systems.*

computing@computingonline.net
www.computingonline.net

ISSN 1727-6209
International Journal of Computing

STUDY OF TWO 3D FACE REPRESENTATION ALGORITHMS USING RANGE IMAGE AND CURVATURE-BASED REPRESENTATIONS

Agata Manolova, Krasimir Tonchev

Faculty of Telecommunications, Technical University of Sofia, 1000 Sofia, 8 Kl. Ohridski Str., Bulgria,
e-mail: amanolova@tu-sofia.bg, k_tonchev@tu-sofia.bg

Abstract: In this paper we present a comparative analysis of two algorithms for image representation with application to recognition of 3D face scans with the presence of facial expressions. We begin with processing of the input point cloud based on curvature analysis and range image representation to achieve a unique representation of the face features. Then, subspace projection using Principal Component Analysis (PCA) and Linear Discriminant Analysis (LDA) is performed. Finally classification with different classifiers will be performed over the 3D face scans dataset with 61 subject with 7 scans per subject (427 scans), namely two "frontal", one "look-up", one "look-down", one "smile", one "laugh", one "random expression". The experimental results show a high recognition rate for the chosen database. They demonstrate the effectiveness of the proposed 3D image representations and subspace projection for 3D face recognition.

Keywords: 3D Face Recognition, Curvature Analysis, Range image representation, Principal Component Analysis, Linear Discriminant Analysis, Kernel Support Vector Machine classifier.

1. INTRODUCTION

Face recognition is a crucial part of many contemporary applications. Recent key applications in fields such as human-computer interface, identity verification, criminal face identification and surveillance systems need a reliable face recognition algorithms. Most of the approaches have focused on the use of 2D images but the decreasing cost of 3D acquisition systems and their increasing quality, together with the greater computational power available nowadays, will make real-time 3D systems for face recognition a commonplace in the near future.

According to [1] it appears that 2D face recognition techniques have exhausted their potential as they stumble on inherent problems of their modality such as differences in pose, lighting, expressions, and other characteristics that can vary between captures of a human face.

Recently, to overcome these challenges 3D facial recognition systems have been developed as a newly emerged biometric technique. It is showing promising results in terms of a high level of accuracy and reliability. Also it is more robust to face variation due to the different factors. A face-based biometric system consists of several subsystems: acquisition system performed by special devices (2D camera, 3D scanner or infrared camera), pre-processing unit, feature extraction unit, database and a recognition unit. In our scenario, an acquisition device may be a 3D-scanner that can record the facial information.

3D face recognition is a challenging task with a large number of proposed solutions [2, 3]. With variations in pose and expression the identification of a face scan based on 3D geometry is difficult.

One common technique on 3D object recognition is based on the correspondence among scene points and model points in order to perform the recognition and to determinate the object pose and location [4]. Among the 3D free-form object descriptors to represent objects is the curvature of the local surface evaluated in each point, which is characterized by the directions in which the normal of the surface changes more and less quickly [5]. In [5], a set of twelve 3D feature extracted from segmented regions using curvature properties of the surface were experimented for face recognition using a database of 8 individual and 3 images per individual obtaining 95,5% recognition rate providing a previous 100% correct feature extraction.

Another popular approach to representing the face is the range image representation where the 3D point cloud is represented as a 2D image. The popularity of this approach is due to the many readily available methods for 2D facial recognition [6]. Also range images are robust to the change of color and illumination, which causes a significant problem in face recognition using 2D intensity images.

The rest of the paper is organized as follows: In the next section we present the technique for pre-processing of point cloud data, curvature analysis and range image representation of the 3D face image data. In Section 3 we present the approach for dimensionality reduction based on PCA and LDA. In that section we have described the classifiers for the subspace projections. In Section 4 we have presented the experimental results for the classification of the processed data with various classification techniques. Finally in section V we will present our future plans to develop these methods.

2. PREPROCESSING OF THE POINT CLOUD DATA, RANGE IMAGE AND CURVATURE-BASED REPRESENTATION

2.1. POINT CLOUD FILTERING

Compared to widely available CMOS and CCD technologies for capturing 2D images, the technology for 3D scanning is still immature in many aspects. There are multiple approaches to acquiring 3D data but all of them have drawbacks. The data acquired with 3D scanners contain undesired noise usually in the form of erroneous measurements or missing measurements. In the first case this noise appears as "spikes" in the data and in the second appears as "holes". An example is illustrated on Fig. 1.

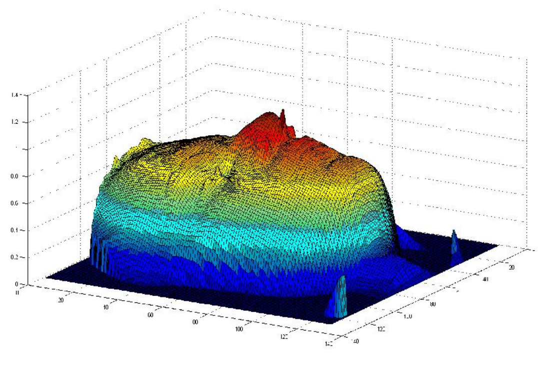

Fig. 1 – Example of spikes in the 3D scan under the nose and on the eye.

Usually samples are missing because the scanner fails to read the reflection of the laser beam at certain point, while the spike-like measurements are usually caused by reflection of wet surfaces such as the eyes [12]. The spikes exist because the laser beam is reflected by a glossy object such as wet skin areas. The holes on the other hand can be seen when the laser beam of the scanner is not reflected. Such situations can rise, for example, when the mouth of the person is open or the pupil of the eye is wide open. It may heavily influence the recognition processes so a preprocessing step is required.

To cope with these issues we apply preprocessing in three steps: face extraction, median filtration and smoothing. Median filtration is used to remove the spike-like measurements. The smoothing is performed using cubic interpolation. All missing points are filled by interpolation based on the closest points. Since the interpolation is applied in a least squares manner, a Gaussian noise is reduced also. Example of profile view of point cloud originated from scanner, filtered with median filter and the extracted face region is presented in Fig. 2.

The scanning process captures the face but also the region around the face including hair, neck, chests etc. These body parts do not contain information relevant to the face recognition process and need to be removed.

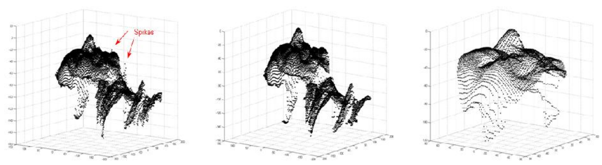

Fig. 2 – (from left to right): Example point cloud representation, filtered version of it and the extracted facial region.

To cope with these drawbacks we apply 3D median filtering of size N_{med} elements. The steps to perform this filtration are as follows: first, for each point $\mathbf{x}_i = [x_i, y_i, z_i]^T$ of the point cloud data the nearest N_{med} points are selected by calculating the Euclidean distance using only the x and y coordinates. Next the z values of these N_{med} points are arranged in increasing order and the value at index $\lfloor N_{med}/2 \rfloor + 1$ is selected. This value represents the median value of the selected N_{med} points, closest to $\mathbf{x}_i$. As a final step, the z_i value of $\mathbf{x}_i$ is replaced with the median value.

This filtration removes the "spikes" and the "holes" and also noise induced by the scanner.

The next step in the preprocessing stage is face extraction (Fig. 1). This step is needed because the scanner captures data of body parts such as neck, shoulders and hair. This step can also be considered as face registration step because all faces are aligned to the same coordinate center.

2.2. RANGE IMAGE REPRESENTATION

A common approach [6, 7] is to use all data points of the point cloud, located inside a sphere with radius R_{FE} and center the tip of the nose. Using this assumption the point with maximum z value is considered as the nose and translation of the 3D point cloud data is made such that this point is the center of 3D coordinate system. After the registration step all faces are aligned to a common coordinate system and are extracted such as to contain relevant and meaningful information only.

An example of range image representation and extracted face region is given on Fig 3. The intensity values of the range images represent inverse distance to the scanner i.e. the brighter the value the closer to the scanner.

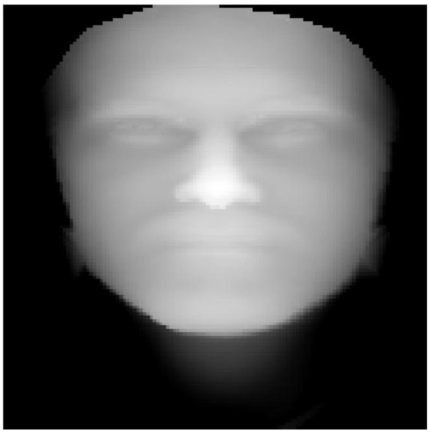

(a)

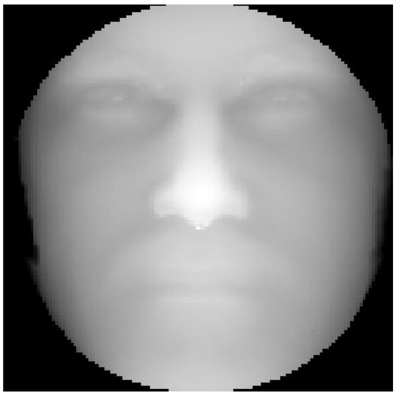

(b)

Fig. 3 – Range image representation of 3D point cloud data from scanner (a) and extracted face (b).

The range images are robust to the change of illumination and color because the value on each point represents the depth value which does not depend on illumination or color.

Also, range images are simple representations of 3D information. The 3D information in 3D mesh images is useful in face recognition, but its data is complex and difficult to handle. It is easy to utilize the 3D information of range images because the information of each point is explicit on a regularly spaced grid.

As a first step to range image representation the minimum and maximum values of the point cloud values are extracted:

$$\begin{aligned} MinX &= \min(x_i), MaxX = \max(x_i) \\ MinY &= \min(y_i), MaxY = \max(y_i) \\ MinZ &= \min(z_i), MaxZ = \max(z_i) \end{aligned} \tag{1}$$

for each point $i = 1,\ldots,N$, where N is the number of points in the point cloud. Next a set of two regular grids, one for x one for y directions, are generated such that there are N_{RI} equally spaced points between $MinX$ and $MaxX$ and $MinY$ and $MaxY$ respectively. These grids define the coordinate system of the range image. Next a linear interpolation is applied to the point cloud data such that the interpolated points lie on the previously defined grid. At the end rescaling of the z values is applied such that $MinZ = 0$ and $MaxZ = 1$. The result is M by M image with intensities in the range [0, 1].

2.3. CURVATURE-BASED REPRESENTATION

One of the main motivations for using curvature representation is their invariance to rotations. Besl and Jain [13] studied the 3D object recognition using range images. They calculated Gaussian curvature and mean curvature and used the signs of these surface curvatures to classify range image regions. Based on this 3D object recognition problem, Gordon devised a solution for a face recognition problem using range images [14].

Formally curvature represents the amount of local bending. The facial point cloud can be considered as 2D continuous surface parameterized over independent variables u, v.

Let S be the facial surface in the form $z = f(x, y)$ with parameterization $Z(u,v) = (u, v, f(u,v))$. The partial derivatives in the directions of the independent variables Z_u, Z_v form a basis for the tangent plane at point $Z(u,v)$. Then the intersection of S with a plane formed by the surface normal n and a vector from the tangent plane is called normal section of S at (u,v) along the direction of the tangent vector. The curvature of the normal section is called normal curvature. Then the principal curvatures $k_1, k_2, (k_1 \geq k_2)$ are the maximum and the minimum of the normal curvatures at point (u,v). Using the principal curvatures we calculate the mean H and the Gaussian curvature K by [8]:

$$K = k_1 k_2 \quad (2)$$

$$H = \frac{1}{2}(k_1 + k_2) \quad (3)$$

These values are calculated for each point of the 3D point cloud and they are the curvature based its representation. On fig. 4 an example of Gaussian and mean curvature representation of range image. Then the feature vector is formed by rearranging them as vectors and concatenation to form single vector.

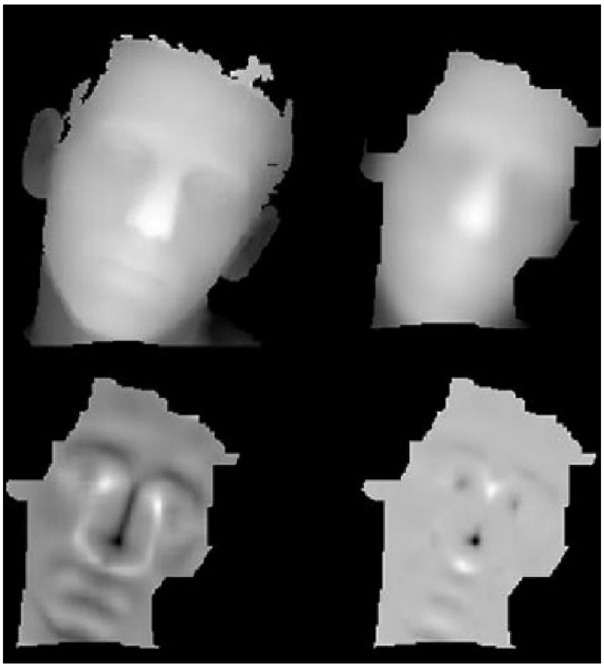

Fig. 4 – Top row, left to right: projected range image and its smoothed version. Second row: mean and Gaussian curvature map [21] (the darker zones are high curvature regions and lighter low curvature regions).

According to [15] this method shows that a great deal of information about facial features that cannot be seen from intensity images is contained in the curvature maps. This approach can deal with faces that differ in size, but needs extension to cope with changes in facial expression.

3. SUBSPACE PROJECTION WITH PCA AND LDA

For the subspace projection step we propose a combination of two very popular approaches for linear dimensionality reduction, namely Principal Component Analysis (PCA) and Linear Discriminant Analysis (LDA).

3.1. PRINCIPAL COMPONENT ANALYSIS

The first approach is unsupervised technique for projection onto a subspace, trying to preserve most of the important information while reducing irrelevant noises.

From statistical point of view PCA seeks linear transformation of type $\mathbf{Y} = \mathbf{W}^{\mathbf{T}}\mathbf{X}$ which results in decorrelated output signals [9], where $\mathbf{X}$ is a matrix of the feature vectors. The major step in PCA is determining the basis $\mathbf{W}$. This basis is calculated by solving the problem of eigenvalues and eigenvectors of the covariance matrix of $\mathbf{X}$:

$$\mathbf{C_X} = E\{(\mathbf{X} - \overline{\mathbf{X}})(\mathbf{X} - \overline{\mathbf{X}})^{\mathbf{T}}\}, \quad (4)$$

where $\overline{\mathbf{X}}$ is the mean value of the data. The solution of the eigenvalue problem is stated as:

$$\mathbf{C_X W} = \mathbf{W}\Lambda \quad (5)$$

Each of the columns of $\mathbf{W}$ represents a normalized eigenvector of $\mathbf{C_X}$ and Λ is diagonal matrix with the eigenvalues on the main diagonal. Dimensionality reduction can be achieved by first rearranging eigenvalues in descending order and then rearranging $\mathbf{W}$ to match Λ. Using the criteria Normalized Residual Mean Square Error (*RMSE*):

$$RMSE(b) = \sum_{i=1}^{b} \lambda_i \Big/ \sum_{i=1}^{p} \lambda_i > T, \quad (6)$$

where T is a threshold representing the fraction of the power of the signal, the most relevant b eigenvectors are selected.

Projecting the data on the PCA basis $\mathbf{W}$ has two advantages. First, this transformation preserves most of the important information and facilitates further calculations since the dimension of the projected data is much lower. Second, removing basis vectors of which the corresponding eigenvalues are lower is similar to filtering out non correlated noises. Thus PCA makes the process more robust to non informative variations.

3.2. LINEAR DISCRIMINANT ANALYSIS

The second technique is supervised and oriented towards classification. It seeks a subspace onto which the projected data can be separated by a hyperplane.

Given c classes $\omega_i, i=1,...,c$ LDA seeks *c-1* discriminating directions of type $y_i = \mathbf{w}_i^{\mathbf{T}}\mathbf{x}, i=1...c-1$, (or in matrix notation $\mathbf{y}=\mathbf{W}^{\mathbf{T}}\mathbf{x}$), where $\mathbf{x}$ is a PCA feature vector [9]. It is assumed that the dimensionality of the image space is $d \geq c$, which defines $\mathbf{W}$ as a rectangular matrix. Thus, LDA is a projection in a space with lower dimensionality.

The basis $\mathbf{W}$ is calculated by solving:

$$J(\mathbf{W}) = \arg\max_{\mathrm{w}} \frac{|\mathbf{W}^{\mathbf{T}}\mathbf{S}_B\mathbf{W}|}{|\mathbf{W}^{\mathbf{T}}\mathbf{S}_W\mathbf{W}|} \tag{7}$$

$\mathbf{S}_W$ is called within-class scatter matrix representing the scatter of each class and $\mathbf{S}_B$ is between-class scatter matrix representing the scatter between the mean vectors of each class:

$$\mathbf{S}_W = \sum_{i=1}^{c}\mathbf{S}_i \text{ ,where } \mathbf{S}_i = \sum_{\mathbf{x}\in\omega_i}(\mathbf{x}-\mathbf{m}_i)(\mathbf{x}-\mathbf{m}_i)^{\mathbf{T}} \tag{8}$$

$$\mathbf{S}_B = \sum_{i=1}^{c} n_i(\mathbf{m}_i-\mathbf{m})(\mathbf{m}_i-\mathbf{m})^{\mathbf{T}} \tag{9}$$

The vector $\mathbf{m}$ is the mean value of the data and $\mathbf{m}_i$ is the mean vector of the *i*-th class. The scalar n_i defines the priors for *i*-th class. The matrix $\mathbf{S}_B$ is sum of *c* matrices with rank one where at most *c-1* of these matrices may be independent. Thus there exist not more than *c-1* nonzero eigenvalues with their respective eigenvectors.

The solution of (8) is calculated by solving the generalized eigenvalue problem:

$$\mathbf{S}_B\mathbf{w}_i = \lambda_i\mathbf{S}_W\mathbf{w}_i \tag{10}$$

for each basis vector $\mathbf{w}_i$, $i=1,...,c$, corresponding to the largest *c* eigenvalues $\lambda_i, i=1,...,c$.

Once the dimension of the data is reduced for the range image representation technique and the curvature-based representation using the feature vectors we apply multiple class classification using different classifiers to test the effectiveness of these two approaches.

4. EXPERIMENTAL RESULTS

We performed tests of the proposed approach using the "SHape REtrieval Contest 2008: 3D Face Scans" (SHREC) database [11]. All subjects in this database are Caucasian, scanned with Minolta Vi-700 laser range scanner.

There are seven scans per subject, two are with neutral expression and the rest are with expression. Thus there are total 61 subject with 7 scans per subject (427 scans), namely two "frontal", one "look-up", one "look-down", one "smile", one "laugh", one "random expression".

SHREC scans are normalized for pose variations and a simple hole filling algorithm is applied. Moreover the tip of the nose is centered at the origin of the 3D coordinate system. This kind of normalization reduces the dependency of irrelevant variations and emphasize on the actual 3D face recognition. A sample of the database is presented on Fig. 5.

For both experiment we selected experimentally the radius of the sphere in the Face extraction step to be and the size of the median filter window to be 5x5.

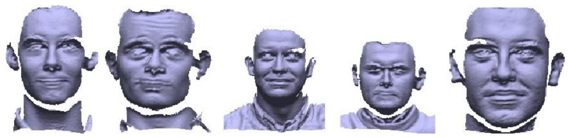

Fig. 5 – Sample from the 3D face scans of SHape REtrieval Contest 2008.

We performed two experiments on the point cloud face scans. In Experiment 1 we used the first two scans with frontal view (neutral expression) for training and the rest of the scans for testing. In Experiment 2 we used 2 frontal scans, one scan with smiling expression and one "random expression" scan for training and the rest for testing.

For the experiments we used Matlab Pattern Recognition Toolbox PRTools 4.2.4 (http://prtools.org/) [16] and the LIBSVM package (http://www.csie.ntu.edu.tw/~cjlin/libsvm/) [17] for the kernel Support Vector Classifier.

For our classification task we use several standard classifiers.

We apply nearest neighbors classifier (KNN) for classification of unknown point cloud into one of the available classes. This classifier is relatively simple technique which assigns the class label of the unknown data based on the closest training samples.

Closeness is defined by the distance between the samples and the class label assignment is made by selecting the class label of the majority of the closest KNN samples. In our approach we use the advantages of the Euclidean measure to compute the distance between samples and we tested the approach by varying the number of neighbors between 1, 3 and 5. Only the best results for the recognition rate are presented [22].

Minimum least square linear classifier (Fisher classifier), normal densities based quadratic (multi-class) classifier (QDC) and Naïve Bayes classifier are also used in the experiment.

The normal based quadratic classifier assumes that the classes are described by multi-normal distributions each with its own covariance matrix. If the covariance matrices are singular we use a regularized version of this classifier by enlarging the diagonal values of the matrix [20].

The Fisher linear discriminant is obtained maximizing the ratio of between-scatter to within-scatter – the Fisher criterion, which for two classes is basically the normal based linear classifier. If the covariance matrix is singular we use a regularized version of this classifier by enlarging the diagonal values of the matrix [20].

The naive Bayes classifier has several properties that make it useful in practice. One of the most important is the separation of the class conditional feature distributions which means that each distribution can be independently estimated as a one dimensional distribution. This helps solve the problem of the curse of dimensionality, such as the need for datasets that scale exponentially with the number of features [19].

We also applied kernel-based SVM. Each kernel defines an implicit transformation from objective space into a usually higher dimensional feature space. We applied kernel Support Vector Machines with the pure distance substitution linear kernel (k_{lin}) and the Gaussian radial basis kernel (k_{rbf}). Depending on the chosen kernel, the geometry of this induced feature space can be very specific. Using RBF kernels for example, the points in feature space all lie on a hyper sphere around the origin with a radius one [18]. One of the main characteristics of kernel-based SVM is that their runtime and space complexity is basically independent of the dimensionality of the input space, but rather scales with the number of data points used for training. In our case we use only a fraction of the dataset for training.

The values of the penalty error C and the parameter for the Gaussian radial basis kernel are logarithmically varying along a suitable grid and only the best recognition rates are presented. Because this is multiclass recognition problem we used the "one versus all" procedure for the Support Vector Machines where classification is done by a max-wins voting strategy.

For the size of the range images we selected $N_{RI} = 64$, thus the range images space is of size 4096. We preserve 95% of the energy of the PCA eigenvalues which results in 107 eigenvectors, i.e. 107 dimensional feature spaces.

The results for the range image representation in terms of recognition rate in % are presented in Table 1.

Table 1. Experimental results for the range image representation in terms of recognition rate in %.

Classifier	Recognition Rate Experiment 1	Recognition Rate Experiment 2
Fisher classifier	71,93	77,56
QDC	81.64	89,43
Naïve Bayes	78,88	86.24
KNN	91.78	95.45
SVM k_{lin}	64.92	75,93
SVM k_{rbf}	93.36	96.64

On Fig. 6 is represented the training set for Experiment 2 in function of the first two features to demonstrate the highly nonlinear data representation.

For the curvature-based representation after preserving 95% of the energy of the eigenvectors i.e. T = 0.95 the resultant PCA basis is with 112 eigenvectors.

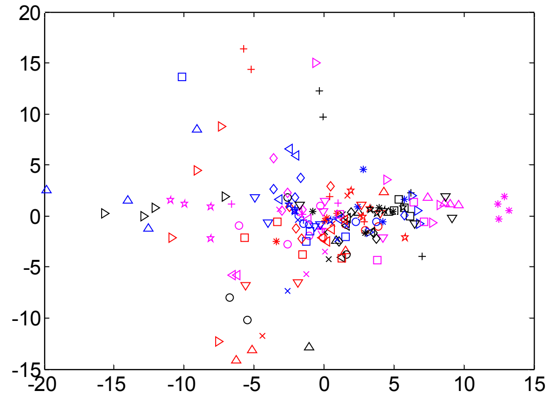

Fig. 6 – The training set for Experiment 2 in function of the first two features.

The results for the curvature-based image representation in terms of recognition rate in % are presented in Table 2 below.

Table 2. Experimental results for the curvature-based image representation in terms of recognition rate in %.

Classifier	Recognition Rate Experiment 1	Recognition Rate Experiment 2
Fisher classifier	63.93	69.22
QDC	76.38	83.65
Naïve Bayes	72.68	79.22
KNN	78.78	85.16
SVM k_{lin}	69.56	74.87
SVM k_{rbf}	87.12	91.56

5. CONCLUSION

In this paper we have presented comparative analysis to 3D Face recognition techniques based on range image and curvature-based image representations.

The 3D range image representation technique results in easy to handle data because the value on each point represents the depth information. The range images are robust to the change of illumination and color.

The curvature-based representation is robust to faces that differ in size, but needs extension to cope with changes in facial expression as the results for the recognition rate show.

The experimental results show a high recognition rate for the SHREC 3D Face database. These experiments demonstrate the effectiveness of the proposed 3D image representations and subspace projection for 3D face recognition. The recognition is successful with most classifiers but the best classifier performance in the two representations is the SVM Gaussian radial basis kernel. The linear classifiers such as Fisher and SVM k_{lin} perform less well than the other nonlinear classifiers, this is due to the highly nonlinear data representation.

In the future additional tests will be performed adding more classification techniques to try and confirm the method's robustness against additive noise. Also different test will be included with different number of retained feature vectors. There is a need of improving the curvature-based representation to take into account the changes in facial expression.

ACKNOWLEDGMENT

This work was sponsored by the Ministry of Education and Science of Bulgaria, National Foundation "Science and Research", Slovenian-Bulgarian R&D joint project, NSF Grant DNTS/Slovenia 01/08 – "Fast and Reliable 3D Face Recognition".

6. REFERENCES

[1] G. Eason, B. Noble, and I. N. Sneddon, Three-dimensional face recognition in the presence of facial expressions: an annotated deformable model approach, *Journal of IEEE Transactions on Pattern Analysis and Machine Intelligence*, (29) 4 (April 2007), pp. 640-649.

[2] K. Bowyer, K. Chang, P. Flynn, A survey of approaches and challenges in 3D and multi-modal 3D + 2D face recognition, *Computer Vision and Image Understanding*, (101) 1 (2006), pp. 1–15.

[3] A. Scheenstra, A. Ruifrok, R. C. Veltkamp, A survey of 3D face recognition methods, in *AVBPA*, 2005, pp. 891–899.

[4] R. Campbel, P. Flynn, A survey of free-form object representation and recognition techniques, *Computer Vision and Image Understanding*, (81) (2001), pp. 166-210.

[5] P. Hallinan, G. Gordon, A. Yuille, P. Giblin, D. Mumford, *Two and Three-dimensional patterns of the face*, Ed. A. K. Peters, 1999.

[6] B. Gökberk, H. Dutağacı, A. Ulaş, L. Akarun, B. Sankur, Representation plurality and fusion for 3D face recognition, *IEEE Transactions on Systems, Man, and Cybernetics-Part B: Cybernetics*, (38) 1 (2008), pp. 155-173.

[7] A. Mian, M. Bennamoun, R. Owens, An efficient multimodal 2D-3D hybrid approach to automatic face recognition, *IEEE Transactions on Pattern Analysis and Machine Intelligence*, (29) 11 (2007), pp. 1927-1943.

[8] H. Tanaka, M. Ikeda, H. Chiaki, Curvature-based face surface recognition using spherical correlation, Principal directions for curved object recognition, *Proceedings of the Third IEEE International Conference on Automatic Face and Gesture Recognition*, 1998, pp. 372-377, 1998.

[9] K. Fukunaga, *Statistical Pattern Recognition,* Academic Press, NY, 1989.

[10] G. Shakhnarovish, T. Darrell, P. Indyk, ed., *Nearest-Neighbor Methods in Learning and Vision*, MIT Press, 2005.

[11] F. Haar, M. Daoudi, R. Veltkamp, SHape REtrieval contest 2008: 3D face scans, *Proceedings of the IEEE International Conference on Shape Modeling and Applications*, 2008, pp. 225-226.

[12] A.B. Moreno, A. Sanchez, J.F. Vlez, F.J. Daz, Face recognition using 3D surface-extracted descriptors, *Proceedings of the Irish Machine Vision and Image Processing Conference*, 2003.

[13] P. Besl and R. Jain, Invariant surface characteristics for 3D object recognition in range images, *Computer Vision, Graphics and Image Processing*, (33) (1986), pp. 33-80.

[14] G. Gordon, Face recognition based on depth maps and surface curvature, *Geometric Methods in Computer Vision*, (SPIE 1570) (July 1991), pp. 1–12.

[15] J. Lee, *3D face recognition using range images, literature survey report*, Department of Electrical and Computer Engineering, The University of Texas, Austin, 2005.

[16] F. van der Heijden, R. P.W. Duin, D. de Ridder and D. M.J. Tax, *Classification, parameter estimation and state estimation, an engineering*

approach using Matlab, John Wiley & Sons, 2004.
[17] C.-C. Chang and C.-J. Lin. LIBSVM: a library for support vector machines, *ACM Transactions on Intelligent Systems and Technology*, (2) 3 (2011), pp. 1-27.
[18] M. Eigensatz, *Insights into the Geometry of the Gaussian Kernel and an Application in Geometric Modeling*, Master thesis, Swiss Federal Institute of Technology Zurich, March 13, 2006.
[19] Harry Zhang, The optimality of naive bayes, *Proceedings of the Conference FLAIRS*, Miami Beach, Florida, USA, 2004, pp. 562-567.
[20] E. Pękalska and R.P.W. Duin, Classifiers for dissimilarity-based pattern recognition, in: A. Sanfeliu, J.J. Villanueva, M. Vanrell, R. Alquezar, A.K. Jain, J. Kittler (eds.), *Proceedings of the 15th International Conference on Pattern Recognition ICPR15*, Barcelona, Spain, September 3-7, 2000.
[21] A. Colombo, C. Cusano, R. Schettini, 3D face detection using curvature analysis, *Pattern Recognition*, (39) 3 (March 2006), pp. 444–455.
[22] K. Tonchev, A. Manolova, I. Paliy, Comparative Analysis of 3D Face Recognition Algorithms Using Range Image and Curvature-Based Representations, *The 7th IEEE International Conference on Intelligent Data Acquisition and Advanced Computing Systems: Technology and Applications (IDAACS'2013)*, 12-14 September 2013, Berlin, Germany, Vol. 1, pp. 394-398.

Ass. Prof. Agata Manolova*, is the Assistant Professor with the Faculty of Telecommunications at the Technical University of Sofia (TU-Sofia), Bulgaria. She finished her PhD conjointly between the TU-Sofia and the University of Grenoble, France. Her domains of interest are Pattern Recognition, Computer Vision, Statistics, Image and Video processing. Dr. Manolova has participated in several scientific projects both national and international concerning object and human action recognition in video sequences, compression of multispectral and hyper spectral images, developing an online educational system for the students at the TU-Sofia. In 2013-2014 she was invited scholar with a Fulbright Visiting Scholar grant in the Computer Science Department at University of Arkansas at Little Rock, USA.*

Krasimir Tonchev*, is a PhD student at the Department of Radio communications and Video Technologies, Faculty of Telecommunications, technical University of Sofia, Bulgaria. His main interests are Kernel-based Support Vector Machines, age and gender recognition, 3D face models, computer vision. He has participated in several scientific projects both national and international for the development of reliable face recognition methods. With collaboration with other authors he has published several papers in conferences such as WSEAS, IDAACS and others.*

computing@computingonline.net
www.computingonline.net

ISSN 1727-6209
International Journal of Computing

SENSOR BASED ALGORITHMS FOR DEAD RECKONING: A COMPARISON OF TWO APPROACHES FOR SMARTPHONES

Daniel Caspari [1], Mircea Strutu [2], Lucas Riedhammer [1], Uwe Grossmann [1]

[1] Fachhochschule Dortmund, Emil-Figge-Strasse 44, www.mbms.fh-dortmund.de
{daniel.caspari, uwe.grossmann}@fh-dortmund.de, lucas-cedric.riedhammer001@stud.fh-dortmund.de
[2] Politehnica University of Bucharest, Splaiul Independentei 313, strutu_mircea@yahoo.com, www.upb.ro

Abstract: The implementation of a reliable indoor localization system can be the starting point for a variety of much desired applications. Either for efficient patient monitoring inside a hospital or as an automatic guide inside a museum, a working localization solution can be useful. Smartphone technology represents a powerful and user friendly tool in order to achieve adequate indoor positioning. This paper explores the potential of using smartphone sensor data (accelerometer and compass) in order to track the location of the person holding the device using dead reckoning algorithms. Two different approaches are under scrutiny in order to assess their performance in different real life inspired scenarios.

Keywords: Smartphone based indoor localization; dead reckoning; accelerometer sensors; fft; peak detection; smartphone; distance; indoor; positioning.

1. INTRODUCTION

Smartphone technology enables the possibility to develop a vast range of applications that can benefit from its ever increasing computing power, internet connectivity and interesting sensor capabilities. One of the problems that pose a great interest not only for private persons, but also for several public institutions is smartphone aided localization. This allows people to have an entirely new set of possibilities to interact with the surrounding environment by implementing location aware information systems.

Modern museums need to adapt to the needs and tastes of their guests. Therefore, one of the solutions they would like to have is a self-guidance system for smartphone devices. This would offer their visitors a great deal of freedom, giving them the possibility to move independently (without the aid of a human guide) and receive data about the exhibits they encounter, on their own familiar hand held device.

Assessing the gadget's location is no longer a problem for outdoor applications thanks to the advanced Global Positioning System (GPS). On the other hand, indoor localization does not benefit from the advantages of a universal approach.

Every indoor location has its own particularities regarding its geometry, construction materials, dimensions and wireless infrastructure. A vast diversity of approaches has been used in order to solve the localization problem in respect with each of the particular features listed above.

The only localization solution that holds regardless of the surrounding environment is dead reckoning (DR). In this case, the current position is determined by adding the distance travelled in a given time to the last known position, in the direction of movement. The travelled distance is a function of speed and time, while the direction of movement is determined using a compass [19].

This method was formerly used in seafaring, and has only recently been used for pedestrians, based on foot-mounted accelerometers [10, 17]. In the latter case, it uses acceleration readings for step recognition.

The reason why this method is more general than the others is that it only relies on the integrated sensors of the mobile device. This consequently implies that there is no need for a special setting and its' only limitations are related to the sensor's accuracy and the necessary processing power to run the localization algorithm.

The purpose of this article is to determine if such a smartphone based localization system can be useful for indoor applications. In order to do so, two localization methods for dead reckoning have been considered. In this paper they are called Peak and FFT (Fast Fourier Transformation based method). Both methods are based on a given step size and a determined starting point. The performance analysis takes into account that the algorithms may perform differently from one scenario to another.

Therefore, after a short description of the two methods, a series of demonstrative tests will be depicted in order to determine if this is indeed a working solution, capable of fairly accurate indoor positioning. Next, a series of tests designed to determine the strengths and weaknesses of each algorithm will be described. These will include testing with different walking velocities, different holding positions or even different devices. A comparative statistical analysis will be available. Finally, the presented data will be evaluated and conclusions will be drawn.

2. RELATED WORK

Several implementation methods for localization have been discussed. Some popular approaches include signal fingerprinting [11], triangulation [3] and dead reckoning [2]. Each of the proposed solutions has its strengths and weaknesses.

The first approach to this problem has been carried out using Wi-Fi signal fingerprinting. The previous experience from [6] showed that "adapted algorithms can be used in large and dynamically changing environments and multi-level buildings". As we can find out from [13], fingerprinting can be time consuming, and easily becomes invalidated when physical conditions change, e.g. the number of people in the vicinity or new office equipment, thereby requiring new measurements to keep the calibration database up to date.

The approach of dead reckoning is not completely new, but had been used before for gait pattern recognition [14]. A good overview was given by Harle [7]. The survey discusses the implementation of different Pedestrian Dead Reckoning (PDR) systems, their advantages and disadvantages. In addition, it gives a comprehensive overview of the existing step detection methods and describes the standardized Internal Navigation System (INS) solution for PDR.

Mikov et al. achieved good accuracy in estimating the travelled distance relying only on the accelerometer data [15]. However, their results are based on data gathered using a special device, employing a non-standard sensor.

Strutu et al. presented a method which relies only on accelerometer and compass data, sensors which are generally available for virtually any smartphone [21]. Due to a step detection algorithm (based on peak determination), it was possible to assess the position of the person holding the device. During the determination of this technique's performance, it was assumed that the starting point of each path is known (by reading an NFC tag) and that the step length is dependent only to the individual's height. Also, the tests were only intended to present that steps can be determined if the smartphone is used in a hand held position.

Because these hypotheses were only covering a small part of the possible real life scenarios, the efforts have been concentrated on determining possible ways in which the algorithm can be used for more complex situations. In this regard, a new distance estimation method based on Fast Fourier Transformation was tested [4].

Thus, in this article, two methods of DR will be compared. The first one will be called Peak method and the other Fast Fourier (FFT) method. They both rely on the acceleration data provided by the acceleration sensor of an Android smartphone and use the provided compass data to estimate the direction of movement. However, as the method used for determining the walking direction is the same, this article focuses on the distance estimation.

3. METHODS

Dead reckoning (DR) "is the process of estimating the current position of a user based upon a previously known position, and advancing that position based upon measured or estimated speeds over elapsed time and course" [19]. For smartphones the method works using compass and acceleration sensors. The direction of movement of a smartphone holder can be obtained by its compass sensor, while the movement itself can be detected by the acceleration sensor. Analyzing the time signal of acceleration data yields steps frequencies. Combining these with the step length results in the velocity of the movement. Hence, travelled distance can be determined knowing the velocity and elapsed time.

The time signal of the acceleration sensor is recorded in three orthogonal directions (Fig. 1), left / right, forward / backward, up / down.

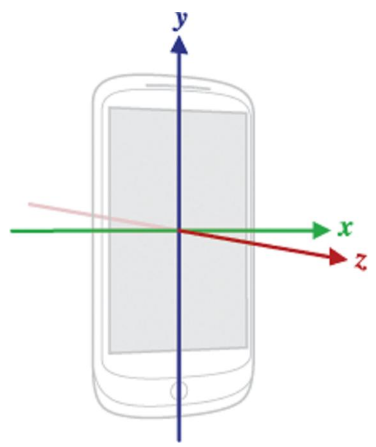

Fig. 1 – Axes of a smartphone [16].

3.1. PEAK METHOD

The Peak method uses the length of the acceleration vector *(m_i)* as a measurement of the accelerometer data. The idea is that a step can be identified as a high peak in the time signal of the acceleration vectors. Assuming that there has to be a minimal time interval between two consecutive steps and that the measured acceleration in case of a step is significant larger than other possible accelerations (e.g. hand movement); a step is only counted when these requirements are met.

In real life scenarios there are different holding positions for a smartphone, meaning concentrating on only one axis is not useful. Hence, the time signal from all 3 acceleration axes is transferred into one corresponding value time signal using (1).

$$m_i = \sqrt{x_i^2 + y_i^2 + z_i^2}\ ;\ i = 1, \ldots, k, \qquad (1)$$

Therefore, in order to have an estimation of the entire acceleration, the signal's magnitude is used (Fig. 2).

In order to get the correct number of steps using only accelerometer data, a series of checks are imposed that result in identifying the highest points (peaks) which consequently can be considered to be step marks. Using this method, step counting is possible. For each step walking direction should also be assessed (compass reading) in order to determine the user's path.

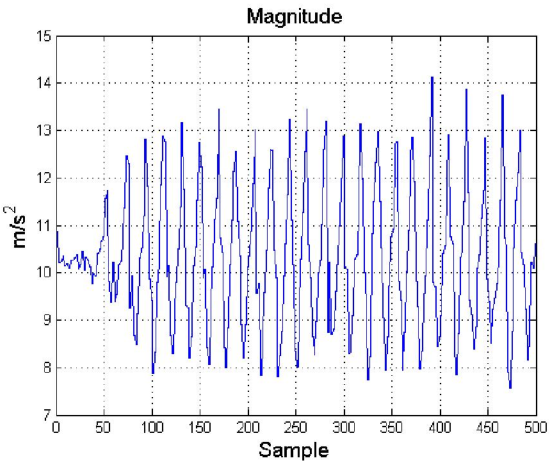

Fig. 2 – Length of acceleration vector vs. time.

Step Counting Algorithm

1. Start application – extract x, y, z (axis accelerometer data) and compass heading;
2. Calculate each sample's magnitude by using (1);
3. Determination of the first peak in the value time signal.
4. Comparing the value of the peak to a given threshold.
5. Comparing the value of the peak to a moving average threshold. The threshold consists of an average of a specific number of previous samples.
6. Comparing the time between this peak and the next to a given threshold.
7. The peak is considered to be a valid step.
8. The next peak in the value time signal is looked at and the algorithm starts at 4.

If a sample validates all the conditions above, the number of steps is increased and an average heading is assigned to the newly found step. (The assigned heading is considered to be the average value of the heading registered by the last few samples before the peak and the peak itself).

The covered distance is calculated by using (2).

$$d_{peak} = step_{count} * step_{size}, \qquad (2)$$

where d_{peak} (cm) is the determined travelled distance, $step_{count}$ the number of identified steps and $step_{size}$ (cm) the assumed step size over the time interval.

3.2. FFT METHOD

Another approach for analyzing recorded acceleration values is based on transforming the time signal of acceleration data (1) firstly into a homogeny time acceleration signal and then into frequency domain using Fast Fourier Transformation. A moving time window of 2.56 or 3.2 sec width is used, which slides over the time signal (see Fig. 3, upper part). The resolution is sample frequency through sample count per time window. The two red vertical bars indicate the current time window. The signal within this window will be transformed to frequency domain.

The idea is to determine a step frequency representative for one window as the dominant frequency (unique maximum) within the frequency range of 0-4 Hz of the according normalized frequency power spectrum (NFPS). The frequency power spectrum is normalized according to its maximum value within the 0-4 Hz interval (see Fig. 3, lower part). As normal step frequencies are below 3 Hz a range of 0-4 Hz (app. 10 km/h) should be sufficient. Furthermore, frequencies not belonging to the step frequency spectrum are filtered out.

If there is a NFPS value of 1 within the frequency range 0-4 Hz and no other frequencies exist with NFPS values above a given threshold value (see Fig. 3, lower part, red line), the frequency with

NFPS value 1 is interpreted as the dominant frequency, and thus interpreted as the step frequency of the according time window. In any other case the frequency for this time window will be discarded. The percentage of discarded frequencies is about 10% for all tests.

This step frequency is then correlated to the starting point of the corresponding time window. If there is no unique maximum above the threshold value within the range of 0-4 Hz, no step frequency can be determined. Figure 3 (middle part) shows the calculated step frequencies (CSF) over the already processed time interval.

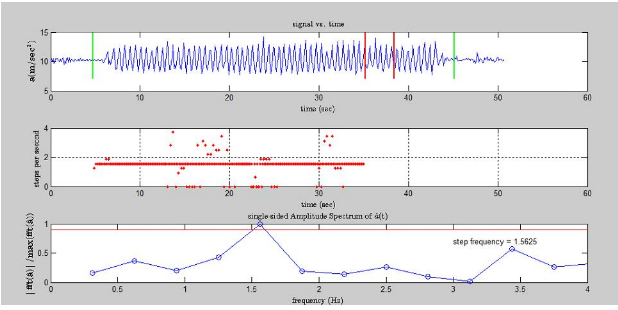

Fig. 3 – Acceleration-Time Signal (top), Calculated step frequency vs. time (middle), Normalized power frequency spectrum (bottom).

Dividing a received step frequency by the sampling rate of the time signal and then multiplying with the step size yields the covered distance between two sample time points. Formula (3) shows the accumulated covered distance over all time points i of the time signal.

$$d_{fft} = \sum_{i} \frac{step_{freq}(i)}{fs} * step_{size}, \quad (3)$$

where d_{fft} (cm) represents the covered distance, $step_{freq}(i)$ (Hz) the step frequency at time point i, $step_{size}$ (cm) the assumed average step size and fs (Hz) the time signal's sampling rate.

4. TEST ENVIRONMENT

Tests have been carried out using two smartphones of different types (HTC One X; Samsung Galaxy Nexus) both with Android 4.3.2. In case of the accelerometer the HTC One X has the newer BMP250 while Samsung Galaxy Nexus has BMP220. The basic functionality of both sensors is the same, but the BMP250 is improved in terms of accuracy and output noise. For the exact differences please see the original data sheets provided by Bosch [4].

The developed test application records real time data from the smartphone acceleration sensor, together with a time stamp and offers the possibility to mark the time signal in order to emphasize different events during testing. The same data is used for both above mentioned methods and was processed with Matlab©.

The Android System provided the acceleration data but used a different library to access the acceleration sensor on each device. On HTC One X, the Android System uses “The Panasonic Android Open Source Project” library while, on Samsung Galaxy Nexus, the “Invensense Motion Processing Library” is used. As the test application uses the sensor data provided by the Android system, it must be assumed that the provided data is preprocessed by those libraries. Due to limitations of the Android System, the accelerometer sensor and compass cannot be used in order to achieve homogeneous sampling rates. The average sampling rate has been 10 Hz.

Both devices are capable of Near Field Communication (NFC). NFC is working in close distance about 1-4 cm. By reading a NFC tag with known position the position of the reading device is identified.

Since the building used for the initial tests was no longer available, later tests had been conducted in another indoor location (inside one of our university’s buildings).

All tests were carried out by one person in order to minimize differences through different step characteristics.

5. TESTS

5.1. INITIAL TESTS

The initial tests had been conducted inside of a faculty building of the University of Applied Sciences and Arts Dortmund using a pathway of roughly 44 meters (Fig. 4). These were used as an experimental background for a previous paper [21], as proof of concept and using only the Peak method. For these tests a HTC One X smartphone has been used, which was held horizontally within the palm in front of the test person.

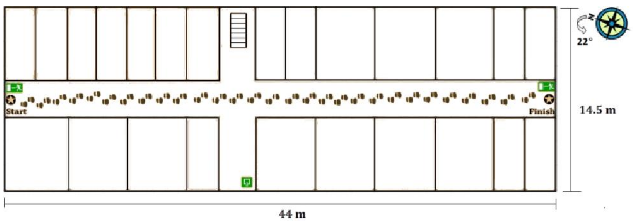

Fig. 4 – Test scenario with 60 steps in straight line (around 44 meters).

The first experiments' goal has been to identify the values needed for the calibration parameters. In order to do so, 8 experiments were performed consisting of 60 steps in straight line having on average around 44.1 meters. The distance was calculated using (2) with an assumed step size of 0.73 m. The average number of steps achieved is 59.75 with a calculated distance of 44.1 m. The average error summing the error by compass offset and missed steps has been 3.1 meters (around 7%). Also it was noticed that the device has a compass deviation of 3° which can just be recalibrated. With this recalibration there was an error of 0.52 meters. Therefore, it can be concluded that with proper calibration, compass errors can be considerably reduced.

Next, a test scenario based on the same calibration parameters is shown. The test consists of 60 steps taken in straight direction with 2 missing steps. It is presented in Fig. 5. Using a peak algorithm implemented in Matlab©, it can be seen exactly which steps have been missed and the overall error (Fig. 5).

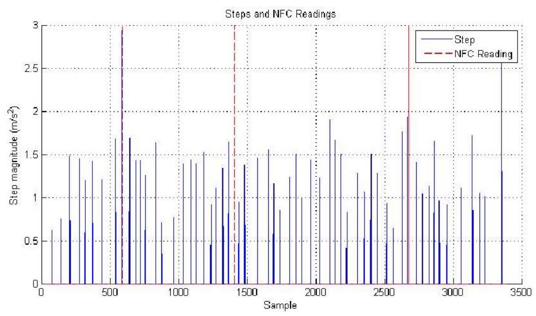

Fig. 5 – A graphical representation of steps in regard to their position inside the sample data vector and NFC tag readings.

NFC has been used in order to compare the results between tests with or without recalibration. Different numbers of (location recalibrating) NFC tag readings and tests with no NFC tag readings have been conducted.

The first case taken into account does not consider any NFC readings (Fig. 6). The number of steps is 58 with a calculated distance of 42.3 m. The total difference between endpoint and calculated endpoint (DEP) is 3.07 m.

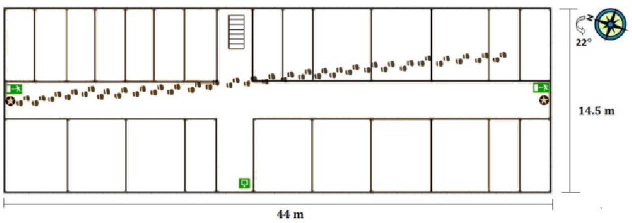

Fig. 6 – Tracking position without NFC tags.

In order to determine the benefit of NFC recalibration, as a second case one NFC tag has been used after 25 steps (Fig. 7). As the algorithm only covers for 24 steps and there is a heading error of around 3°, the NFC reading manages to correct this error. Overall, the DEP is now just 1.39 m (compared to 3.07 m without NFC).

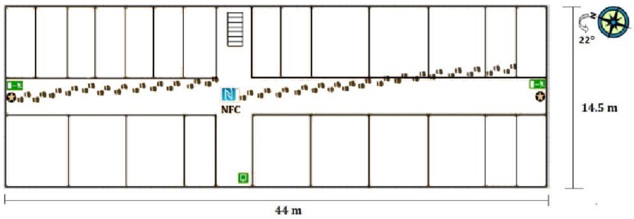

Fig. 7 – Tracking position using one NFC tag.

As third case, estimating the error by using 3 NFC tags positioned as depicted in Fig. 8 has been tested. The first NFC tag is positioned after 10 steps. As the algorithm only found 9 steps, it will help recover for the lost distance. The second NFC tag is positioned after 25 steps (out of which the algorithm can identify only 24) but, because the step loss occurred before the first NFC tag, the only remaining error is due to the heading offset. The third NFC tag also needs to account only for the heading error because there are no further lost steps. The DEP is 0.81 m, mainly because of the lost step during the last interval. All the results are considered with no prior compass calibration.

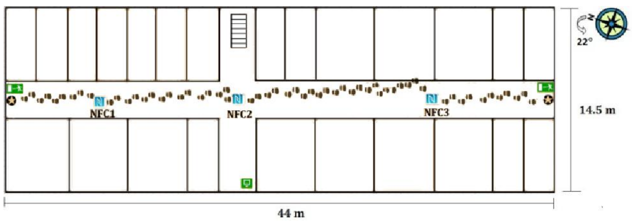

Fig. 8 – Tracking positions using 3 NFC tags.

Using NFC tags to reassess the location of the tester made a big difference in the overall error. This method is therefore useful and creates the opportunity to integrate it as part of the dead reckoning tracking system. The results of the experiments are highlighted in Table 1.

Table 1. Step Counting improved by NFC – 60 Steps.

Case	Detected Steps	Calculated distance (m)	DEP (m)	Error (%)	Remark
1	58	42.3	3.07	7	No NFC Tag
2	58	42.3	1.39	3	1 NFC Tag
3	58	42.3	0.81	1	3 NFC Tags

The objective was to implement the localization system inside a large room where people are free to move in any direction. Therefore, it should provide accurate information even if the visitors would have a trajectory resembling the one depicted in Fig. 9.

The test shows how a more complicated trajectory can be tracked using the algorithm and gives a rough indication about the validity of the received data. The red line represents the real path and the green dots are the steps taken, therefore reconstructing the path.

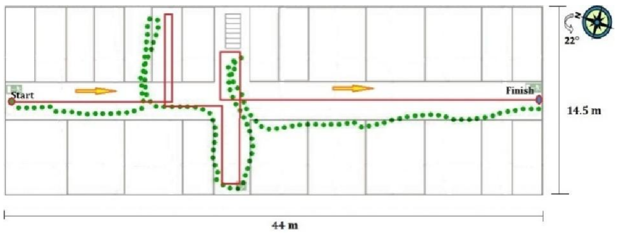

Fig. 9 – Simulated position using magnitude and compass readings in a scenario resembling a real life visitor activity.

Therefore, the initial tests conclusion has been that without using NFC tag readings, the determined location is not accurate enough in order to move through long distances or time. However, localization is possible for several meters, giving the visitor the possibility to freely enjoy the exhibits.

5.2. COMPARING FFT ALGORITHM AND PEAK ALGORITHM

The following test's purpose was comparing both algorithms regarding accuracy of determining step frequency and accumulated covered distance. As no changes at the parameter of the FFT method were made during the tests, the Peak method uses different thresholds for each device.

The test person walked along a straight line of 40 m length (Fig. 10, blue dotted line) with homogenous velocity and counted the performed steps. The mean step frequency (MSF) is calculated by dividing the counted steps by the walked time.

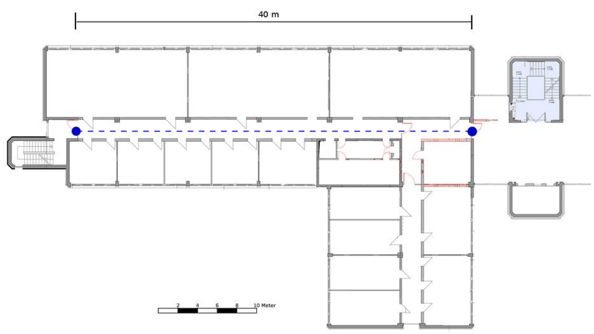

Fig. 10 – Testing area (office building), straight line of 40m length (dotted blue line).

The step frequency parameter is used as a base for comparison between the two algorithms, offering the possibility to directly evaluate their performances based on a common parameter. The Peak method provides a step frequency as the inverse of the time interval between two peaks, i.e. there is a step frequency for every peak time point. FFT provides step frequencies for every sample time point. According to sample rate and the width of the time window used, the FFT method yields a resolution of step frequencies of 0.3125 Hz. In order to compare the results of both methods, the cumulative distribution of the ratio of calculated step frequency (CSF) to mean step frequency (MSF) is plotted.

There are several different test scenarios. All tests were carried out with both smartphones and at least twice.

The influences of three holding scenarios for the smartphones were examined. Firstly, the smartphone was held horizontally within the open hand in front of the test person. Secondly, the device was carried within the pocket of the test person's trousers. Thirdly, the test person was holding the smartphone in the hand, but swinging the arm as normal while walking and not watching the smartphone's display.

Moreover, we examined the influence of different velocities (slow/medium/fast). In case of slow velocity the test person needed 74 steps and 61 sec, i.e. velocity = 0.66 m/sec and MSF = 1.21 Hz. In case of medium velocity it was 63 steps and 40 sec, i.e. velocity = 1.00 m/sec and MSF = 1.58 Hz, and in case of fast velocity 48 steps and 28 sec, i.e. velocity = 1.42 m/sec and MSF = 1.71 Hz.

The following figures present the ratio of CSF to MSF of both methods. The MSF is obtained by dividing the total number of steps counted during walking the test line by the total walking time.

1) Comparing two devices

This test was carried out with medium velocity and the smartphone held horizontally within the open hand in front of the test person.

Fig. 11 shows the results in case of using the Peak method with both devices. The first quartile shows a ratio of 0.65 in case of HTC One X and 0.7 in case of Samsung Galaxy Nexus. The second and third quartile shows a ratio of 0.85 respectively 0.95 for both devices. At 90% the ratio is 1 in case of HTC One X and 1.4 in case of Samsung Galaxy Nexus.

The Peak method is underestimating step frequency with both devices.

The results using the FFT method are presented in Fig. 12. The ratio of the first quartile shows 0.8 for both devices. The second quartile shows 0.9 in case of Samsung Galaxy Nexus and 0.95 in case of HTC One X. The third quartile shows 0.95 in case of

Samsung Galaxy Nexus and 1 for HTC One X. At 90% the ratio shows 1 for Samsung Galaxy Nexus and 1.8 for HTC One X.

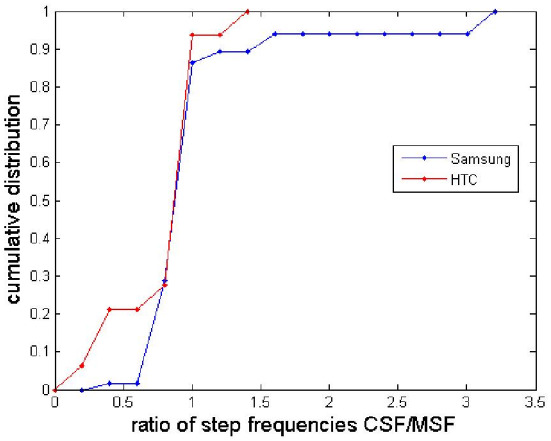

Fig. 11 – Peak method, medium velocity, HTC One X (MSF: 1.56Hz) and Samsung Galaxy Nexus (MSF: 1.49Hz).

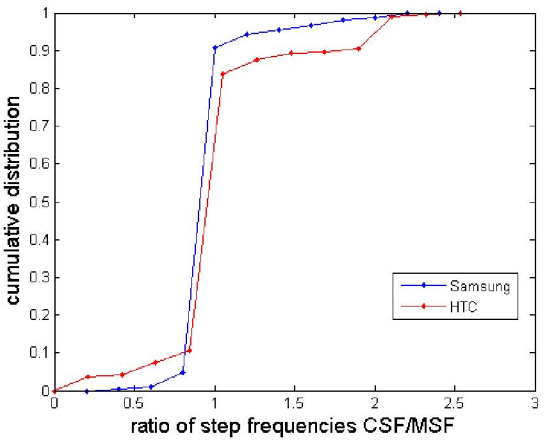

Fig. 12 – FFT method, medium velocity, HTC One X (MSF: 1.56 Hz) and Samsung Galaxy Nexus (MSF: 1.49 Hz).

The FFT method underestimates step frequencies, but not to the same amount as the Peak method.

As shown in Fig. 11 and Fig. 12 the ratio of CSF to MSF is more spread for the HTC One X than for the Samsung Galaxy Nexus.

Both devices are able to obtain a unique step frequency with both methods, albeit Samsung Galaxy Nexus performs better.

In the following presentation of results only the data obtained by Samsung Galaxy Nexus will be used. The data from HTC One X is more spread but essentially similar.

2) The influence of different velocities

The next figures show the results of tests using the Samsung Galaxy Nexus with three different velocities: slow (MSF: 1.21 Hz), medium (MSF: 1.58 Hz) and fast (MSF: 1.71 Hz) and the smartphone held horizontally within the open hand in front of the test person.

Fig. 13 shows the results of the Peak method.

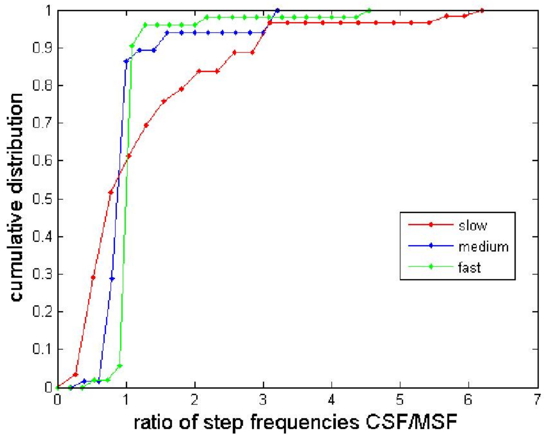

Fig. 13 – Peak method, different velocities, Samsung Galaxy Nexus.

The first quartile shows a ratio of 0.45, 0.65 and 0.9 in case of slow, medium and fast velocity. The second quartile shows a ratio of 0.7, 0.8 and 0.95 in case of slow, medium and fast velocity. The third quartile shows a ratio of 1.5, 0.9 and 1 in case of slow, medium and fast velocity. At 90% the ratio for slow, medium and fast velocity shows 2.8, 1.4 and 1.1.

A nearly constant step frequency can be calculated while walking with medium and fast velocities, but the method is calculating varying step frequencies while walking slowly.

Fig. 14 presents the results using the FFT method. The first quartile shows a ratio of 0.9 in case of slow and medium and 0.95 in case of fast velocity. The second quartile shows a ratio of 0.95 in case of medium and 1 in case of slow and fast velocity. The third quartile shows a ratio of 1.8, 1 and 1.05 in case of slow, medium and fast velocity. At 90% the ratio for slow, medium and fast velocity shows 2.8, 1.05 and 1.1.

The FFT method is able to calculate distinct step frequencies while walking with medium and fast velocities, but with slow velocities results are more erratic.

As the Peak method is mostly underestimating and rarely overestimating, the FFT method is more overestimating. Furthermore, both methods have problems when used with slow velocities. Both methods perform almost equally in the case of medium and fast velocity.

3) Different holding positions of the smartphone

For these tests a medium velocity (MSF: 1.58 Hz) was used. The smartphone was held either horizontally within the open hand in front of the test person (see Fig. 11 and 12) or it was held in the hand, but the arm was swinging as while walking (see Fig. 15) or the device was carried in the pocket (See Fig. 16).

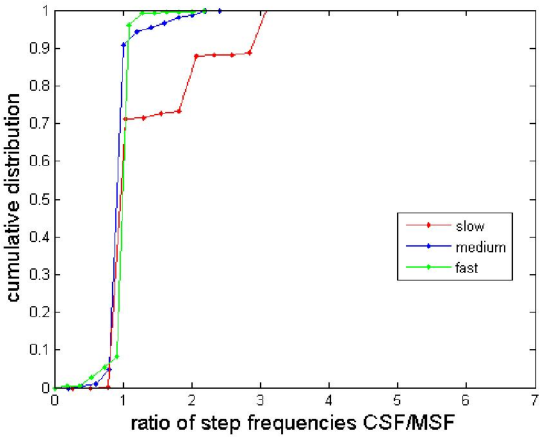

Fig. 14 – FFT method, different velocities, Samsung Galaxy Nexus.

Fig. 15 shows results in case of swinging the arm as during walking. This case represents walking without watching the display for the whole time.

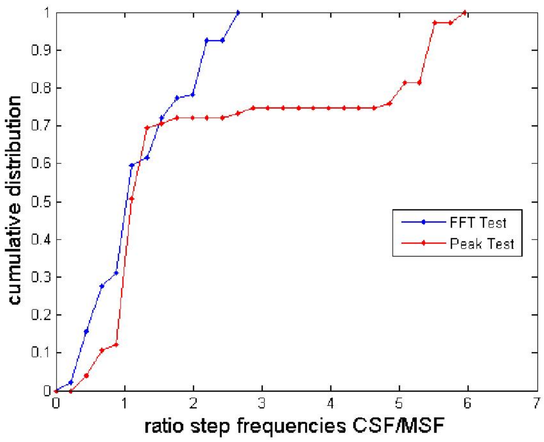

Fig. 15 – Peak and FFT method, arm swinging while walking, Samsung Galaxy Nexus.

In case of the Peak method the first quartile has a ratio of 1 while for the FFT method it shows 0.6. The second quartile shows a ratio of 1.05 in case of the Peak method and 1 for the FFT method. The third quartile shows a ratio of 5 in case of the Peak method and 1.6 in case of the FFT method. At 90% the ratio of the Peak and the FFT methods is 5.4 and 2.2.

Fig. 16 shows the results for the case of carrying the device in the pocket of the test person's trousers.

At the first quartile the Peak method has a ratio of 1.2 while the FFT method has 0.4. The second quartile shows a ratio of 1.5 for the Peak method and 1 for the FFT method. The third quartile shows a ratio of 4.6 in case of the Peak method and 1.05 in case of the FFT method. At 90% the ratio is 5.7 in case of the Peak method and 1.05 in case of the FFT method.

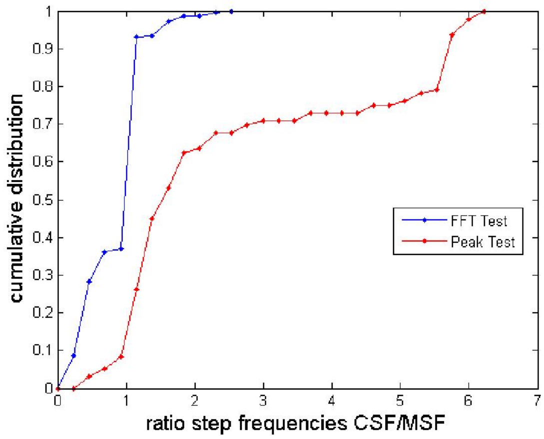

Fig. 16 – Peak and FFT method, device in the pocket, Samsung Galaxy Nexus.

For both tests, the FFT method performs better than the Peak method. While the FFT method underestimates in the results, the Peak method overestimates.

4) Comparing covered distance calculations of both methods

For comparing the resulting distances calculated by both methods one test was performed twice with medium velocity. The test consisted of walking a straight line of 40 m (see Fig. 10) with medium velocity. Performing this test several times shows differences of elapsed time of app. 1 sec. The measuring device was held in the horizontal position in front of the test person. In order not to interfere with problems related to the step size, the determined step length has been used, calculated from walked distance and counted steps by using formulas (2) and (3).

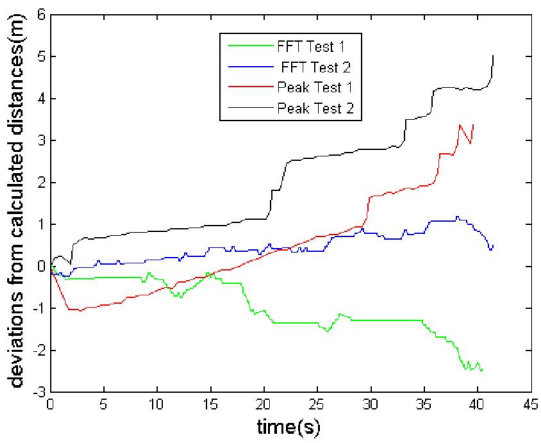

Fig. 17 – Time dependency of deviation of calculated distance from covered distance.

Fig. 17 represents the deviation of calculated distance to covered distance over time. All tests show different progressions of deviation over time. Up to 18 seconds the absolute value of deviation is lower than 1 m. After 20 seconds the absolute value of deviation tends to increase for both methods with Peak method overestimating the covered distance and FTT method partly underestimating covered distance.

6. CONCLUSION AND FUTURE WORK

The results lead to the conclusion that dead-reckoning with both methods can be used, in principle, for smartphones as a positioning method between two secured positions. However, results diverge using either peak or FFT method or using different devices. The discrepancies of results in using different devices can be led back to the different accelerometer sensors of the two devices. Moreover, both devices uses different libraries to access the accelerometer data.

Furthermore results vary due to velocity. Both methods are more erratic with slow velocities. In addition the FFT method seems to perform better in calculating characteristic step frequencies. The FFT method seems to be more robust while walking with swinging the device or carrying the device in the pocket.

As shown by Fig. 17, the absolute value of deviations tends to increase over time, independent of the used method. Both methods estimate the covered distance with an accuracy of about +/-1m up to 16-20 seconds. After this time, the calculated positions should be considered as unreliable und need to be recalibrated by another method.

In comparison of both methods, distinctly more computing power is needed in case of the FFT method than in case of the Peak method. Though smartphones are capable of providing this computing power, the FFT method still has the disadvantage of reducing battery power more quickly.

Comparing to other papers the results seem to be reasonable. The results are partially worse, but the methods can be used to provide positioning. As Alzantot et al. [2] pointed out, using of the shelf smartphones for Dead Reckoning will lead to more errata. Alzantot et al. used standard smartphones among others, but get better results while walking with device swinging or in pocket. Like Mikov [15], if using slower walking velocities the results degrade. The results are comparable to those of Link [13] and Pratama [17].

The presented algorithms have the potential to work as a backup solution for movement tracking inside a large hall or a different indoor location where no other means of localization are possible. This offers the opportunity for a location aware information system to extend its applicability to areas which could not have been previously covered by other localization systems.

Our initial experiments suggest that the error can be kept inside tolerable margins if the position is e.g. periodically recalibrated using a NFC tag. However, the algorithm works even without NFC tag reading for a limited distance. Despite of the small range of 1-4cm, still some possible attack options on visitor devices are conceivable. An imaginable attack could be the manipulation of a NFC tag containing a target URL, which is used for content retrieval or positioning. Visitors could be directed to a website containing malicious software. This may be prevented by using Read-Only tags. Using NFC does not cause a significant threat for the smartphone.

In further experiments, the robustness of the method against the influence of more complex paths should be assessed. In these cases, changes of direction of movement will be included and the compass sensor needs to be analyzed and integrated into the method. Furthermore, possibilities of improving the resolution of the frequency spectrum should be investigated in order to improve differentiation of step frequency and thus speed accuracy.

7. REFERENCES

[1] D. Alvarez, R. C. Gonzalez, A. Lopez, J. C. Alvarez, Comparison of step length estimators from weareable accelerometer devices, *Proceedings of the 28th IEEE Annual International Conference on Engineering in Medicine and Biology Society, EMBS'06*, 2006, pp. 5964–5967

[2] M. Alzantot, M. Youssef, Uptime: ubiquitous pedestrian tracking using mobile phones, *Proceedings of the IEEE Wireless Communications and Networking Conference (WCNC)*, 2012, pp. 3204-3209.

[3] A. Bahillo, S. Mazuelas, J. Prieto, P. Fernández, R.M. Lorenzo, and E.J. Abril, Hybrid RSS-RTT localization scheme for wireless networks, *Proceedings of the IEEE International Conference on Indoor Positioning and Indoor Navigation (IPIN)*, 2010, pp. 1-7.

[4] Robert Bosch GmbH, Data Sheets, www.bosch-sensortech.com

[5] BMA220 http://ae-bst.resource.bosch.com/media/products/dokumente/bma220/BST-BMA220-DS003-08.pdf

[6] BMA250 http://ae-bst.resource.bosch.com/media/products/dokumente/bma250/bst-bma250-ds002-05.pdf

[7] D. Caspari, J. Pickert, U. Grossmann, Positionsbestimmung mittels Dead Reckoning (Koppeln) und Schrittfrequenz-Erkennung, 10. Konferenz Wireless Communication and Information, 24./25.10.2013, Berlin, 2013.

[8] S. Gansemer, U. Grossmann, S. Hakobyan, RSSI-based Euclidean distance algorithm for indoor positioning adapted for the use in dynamically changing WLAN environments and multi-level buildings, *Proceedings of the International Conference on Indoor Positioning and Indoor Navigation (IPIN)*, 2010, pp. 1-6.

[9] R. Harle, A survey of indoor inertial positioning systems for pedestrians, *IEEE Communications Surveys & Tutorials*, (15) 3 (2013) pp. 1281-1293.

[10] Y. Hatano, Use of the pedometer for promoting daily walking exercise, *Int. Council Health Phys. Educ. Recreat.*, (29) (1993), pp.4-8.

[11] J. Jahn, U. Batzer, J. Seitz, L. Patino-Studencka, J. Gutierrez Boronat, Comparison and evaluation of acceleration based step length estimators for handheld devices, *Proceedings of the International Conference on Indoor Positioning and Indoor Navigation (IPIN)*, 2010, pp. 1–6.

[12] S. W. Jeen, W. L. Che, T. C. Yang, and J. H. Yu,"Walking pattern classification and walking distance estimation algorithms using gait phase information, *IEEE Transactions on Biomedical Engineering*, (59) 10 (2012), pp. 2884–2892.

[13] Y. Kim, Y. Chon, and H. Cha, Smartphone-based collaborative and autonomous radio fingerprinting, *IEEE Transactions on Systems, Man, and Cybernetics, Part C: Applications and Reviews*, (42) 1 (2012), pp. 112-122.

[14] H. Leppakoski, J. Collin, J. Takala, Pedestrian navigation based on inertial sensors, indoor map, and WLAN signals, *Proceedings of the IEEE International Conference on Acoustics, Speech and Signal Processing (ICASSP)*, 2012, pp. 1569-1572.

[15] J.A.B. Link, P. Smith, N. Viol, and K. Wehrle, Footpath: Accurate map-based indoor navigation using smartphones, *Proceedings of the IEEE International Conference on Indoor Positioning and Indoor Navigation (IPIN)*, 2011, pp. 1-8.

[16] J. Mantyjarv, M. Lindholm, E. Vildjiounaite, S.M. Makela, & H.A. Ailisto, Identifying users of portable devices from gait pattern with accelerometers, *Proceedings of the IEEE International Conference on Acoustics, Speech, and Signal Processing (ICASSP'05)*, March 2005, Vol. 2, pp. ii-973.

[17] A. Mikov, A. Moschevikin, A. Fedorov, and A. Sikora, A localization system using inertial measurement units from wireless commercial hand-held devices, *Proceedings of the International Conference on Indoor Positioning and Indoor Navigation (IPIN'2013)*, October 2013, pp. 857–863.

[18] PmWiki, axis_device.png, from http://media2mult.uos.de/pmwiki/fields/pgs10/index.php?n=Main.SensorenAndroid", 17.04.2013.

[19] A. Pratama, R. Widyawan, and R. Hidayat, Smartphone-based pedestrian dead reckoning as an indoor positioning system, *Proceedings of the International Conference on System Engineering and Technology (ICSET)*, 2012, pp. 1–6.

[20] T. Sayeed, A. Sama, A. Catala, J. Cabestany, Comparison and adaptation of step length and gait speed estimators from single belt worn accelerometer positioned on lateral side of the body, *Proceedings of the IEEE 8th International Symposium on Intelligent Signal Processing (WISP'13)*, 2013, pp. 14–20.

[21] A. Serra, D. Carboni, and V. Marotto, Indoor pedestrian navigation system using a modern smartphone pedestrian navigation system using a modern smartphone, *Proceedings of the MobileHCI'2010*, September 7-10, 2010, pp. 397–398.

[22] S. H. Shin, C. G. Park, J. W. Kim, H. S. Hong, J.M. Lee, Adaptive step length estimation algorithm using low-cost MEMS inertial sensors, Proceedings of the IEEE Sensors Applications Symposium SAS'07, 2007, pp. 1-5.

[23] M. Strutu, D. Caspari, J. Pickert, U. Grossmann, and D. Popescu, Pedestrian smartphone based localization for large indoor areas, Proceedings of the 7th IEEE International Conference on Intelligent Data Acquisition and Advanced Computing Systems: Technology and Applications, Berlin, 12-14 September, 2013, pp. 450-454.

Daniel Caspari, *B.Sc. Studies of computer science at University of Applied Sciences and Arts, Dortmund. Current position: research associate at Business Department of University of Applied Sciences and Arts, Dortmund. focus of research: location based services.*

Dr. Mircea Strutu, *PhD in Systems Engineering (Politehnica University Bucharest). Current position: research associate at Systems Engineering Department of Politehnica University Bucharest. Focus of research: wireless sensor networks, signal processing, location based services.*

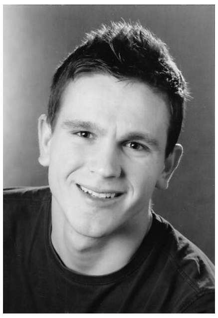

Lucas Riedhammer, *cand. inf. Graduate in computer science at University of Applied Sciences and Arts, Dortmund. Current position: research associate at Business Department of University of Applied Sciences and Arts, Dortmund. Focus of research: location based services.*

Prof. Dr. Uwe Grossmann. *Diploma in mathematics and information technology, Bochum University, Germany, PhD in mathematics, Bochum University, Germany, research associate at Essen University and Max-Planck-Institute Dortmund, project manager computer aided manufacturing at MBP Software & Systems Gmbh. Current position: professor of mathematics and business computing at University of Applied Sciences and Arts, Dortmund; speaker of research group 'mobile business – mobile systems. Focus of research: mobile business/commerce, location based services, mobile/wireless systems, localization/positioning*

computing@computingonline.net
www.computingonline.net

ISSN 1727-6209
International Journal of Computing

AGENT-BASED MODELING OF THE E-LEARNING USERS' BEHAVIOR

Viktor Artemenko

Lviv Academy of Commerce,
str. Tugan-Baranovsky, 10, Lviv, 79005, Ukraine
e-mail: artem@lac.lviv.ua

Abstract: In this paper the methodological and technical approaches are considered to construct the agent-based model (ABM) with built-in artificial neural networks. This model describes the user's behavior of electronic or distance learning in a virtual environment of one of universities. Design of ABM aims to support a development of Web analytics (learning analytics) on the basis of computer experiments evaluating the trends of the knowledge creation and dissemination for e-Learning users. In research AnyLogic software, which is one of the most popular packages for agent-based modeling, is proposed for implementing the created model, and package STATISTICA Neural Networks is proposed for constructing the neural networks.

Keywords: e-Learning, agent-based models, artificial neural networks, software for agent-based modeling.

1. INTRODUCTION

Information and communication technologies (ICT) have a significant impact on almost every aspect of our lives. Under favorable conditions, ICTs become tools of socio-economic development, job creation and continuous improvement of quality of life. Giving each person an opportunity to have access to information and knowledge and to contribute to this field is an important element of inclusive information society, lifelong learning based on ICTs and distance learning technologies.

Distance learning or e-Learning can be seen as an example of a system that consists of agents and has the features of a living structure, as there is a constant exchange of information and knowledge between agents and learning management system.

The term "agent" is widely used in the literature. For example computer models, in which agents are the objects of modeling, called agent-based models or abbreviated ABM [1].

In this article we aim to describe the role and the place of ABM. Among specialized publications dealing with the ABM issues we can refer to the following two [2, 3] and online journals: "Journal of Artificial Societies and Social Simulation" or in short JASSS [4], "Agent-Based Computational Economics" [5] and "Artificial Society" [6]. These sources are devoted to problems of simulation in the social and economic sciences, and development of methodology to obtain new knowledge on the basis of computer experiments with ABM. The ultimate goal of the ABM design is to collect a certain set of rules to conduct specific agents representing an artificial community. Encyclopedia Wikipedia defines this concept as: "Artificial Society is the specific agent-based computational model for computer simulation in social analysis".

Among the ABM software the most popular packages are SWARM and AnyLogic. The first package is a collection of open source software libraries created at the Institute of Santa Fe and available on its website [7]. Some of the libraries are written using scripting language to ensure the use of graphical tools. AnyLogic is a commercial package. Its special AnyLogic agent based library allows specifying the required functionality of the model's agents [8-10].

Analysis of the known examples of agent-based models leads to the following conclusions.

1. Agent is a theoretical abstraction used in the agent-based models in order to represent actors, members of the artificial society, who make decisions with a certain degree of autonomy. The agent can "live" in time, to have a graphical image, respond to actions from the sensors, external programs or specific agents-users.

2. The vast majority of agent-based models are abstract and the main purpose of their creation is a scientific interest, which means the usage of conditional data to test new tools.

3. Among the agent-based models, considering the real phenomena, only a small part is related to the interactions of agents in the field of education.

In our research we aim to study in details approaches, presented earlier in [11], to the agent-based modeling of the e-learning users' behavior with help of artificial neural networks. The creation of such agent-based model is aimed at preparing analytics, which would show trends in the production and dissemination of knowledge of users in distance courses. The results of the ABM testing are based on using the following software: AnyLogic and STATISTICA Neural Networks.

2. APPROACHES TO THE CONSTRUCTION OF AGENT-BASED MODEL OF E-LEARNING USERS

Specifications task of ABM development aimed at creating an artificial society in which interacting agents of such types: A1 – authors of distance courses, A2 – tutors involved in the learning process and A3 – students, users of distance courses. We assume that the agents of artificial society are functioned autonomously. They make decisions, perform actions and interact with other agents of e-learning. Any decision of the agent is sufficient to effect the action. To implement the same interaction is necessary a group decision. Group decisions are subject to certain rules, which must be specified in this case.

Thus, the rules, designed for the agents, who interact in a two-dimensional virtual environment, play the key role in the ABM development.

It is important to note that in our case, during the computer simulation experiments with the means of AnyLogic, two-dimensional virtual environment is presented as a rectangular lattice, which consists of 100 columns and 100 rows (see Fig. 9). The interactions between e-Learning agents take place in each cell (x, y). The virtual environment is limited by the parameters, which are designed on the basis of the analyzed simulation period, namely academic semester (100 days). Any agent that reaches the limits of the simulation period "dies". By that time the authors and tutors of the distance courses fully produce and transmit knowledge, and students receive the full amount of that knowledge.

The move of the analyzed agents in this environment is determined by their behavior during the production and dissemination of knowledge. The main tools in the specification of the behavior of agents are the following variables: timers and statecharts. These variables reflect characteristics of the analyzed agents. Timers can be setup to a certain time, to program when the action will take place. Statecharts allow visually present the behavior of the agents over the time under the influence of events or conditions. They consist of a graphical description of states and transitions between them. Any complex logic behavior of agents in AnyLogic models can be expressed by using a combination of statecharts, algebraic equations, variables, timers and program code in Java.

Statechart allows graphically specify the space between states of the agent behavior algorithms, factors that are driving the transitions from one state to another, as well as the actions that occur when states are changing. Statechart are compliant to UML standards. They store graphics, performance attributes and semantics, which are defined by UML (Unified Modeling Language). Statechart in AnyLogic can support the following types of events: 1) signal – the agent can send a signal to another agent to tell him or her something, 2) timeout – over a given period of time in the statechart nothing happens, 3) event of transition – an event in which the Boolean value indicates "true".

The position of the agent in a virtual environment is defined by variables x and y. The agent moves randomly in the process of computer simulation experiments. Each agent initially moves in the direction to the axis X, causing the method RandomMove, and then along to the axis Y, causing this method again. Method RandomMove uses a simple numerical generator of mathematical library Java. It defines the value -1 for the move back; 0 – for the standing still or +1 – for the move forward (AnyLogic allows you to use other random number generators in calibrating ABM). Henceforth, these movements are formalized by using statecharts (see Fig. 6-8).

The movement of agents in a virtual environment is determined by the agents' network or by the location type. There are two the most commonly used among them:

1. *Random placement* – agents are connected by chance, each agent is determined by the specified number of connections.
2. *According to the distance* –agents are connected with each other if the distance between them is less than the specified range of connection (only in the continuous environment).

In our research we use the first type of agents' placement. Therefore, the location of the agents at time "0" is determined by variables x and y. The initial values of variables are determined randomly in a rectangular lattice on the basis of statistical data, which describes the actions of agents (see below). Directions of their movement are determined by the rules given in statecharts (see Fig. 6-8). The movement of students is defined by statecharts as well. The example of their interaction with the authors of e-learning courses is presented in Fig. 8.

Please note that the concept of the *time modeling* is a base in the agent-based modeling. This time is a relatively logical time, which is defined in terms of the behavior of all objects in the model. It consists of a starting time, start date and end date. Two last dates are set by the built-in AnyLogic calendar. Start time is determined by “0” in the settings of computer experiments. This fact explains the expression t+0, which is implied in the following formulas (1)-(12).

Therefore, the key assumptions in the agent-based modeling are as follows:

- in terms of decision-making, agents e-learning move in a two-dimensional space and having a finite horizon of vision;
- agents of the distance courses interact in a virtual environment by the defined rules, have a finite lifetime;
- goal of author of distance course (agent first type) – produce as much knowledge and transmit them to the tutor and students, goal of tutor (agent second type) – to spread knowledge among the greatest possible number of students, and goal of students (third type of agent) – as much as possible to use knowledge.

Behavior of agents e-learning can be described as follows.

Behavior of the author of a distance course. Author of a distance course moves with some predetermined speed in a random direction to search for other agents of e-learning. The search explained by the fact that the demand for training courses for the choice of the student, including and distance learning courses, largely determined by the “Run Games” author of a distance course's, that is, its advertising proposed “by Hartley” information, which can reduce the uncertainty of the agents, the recipients of such information. The author's task is to bring the course to other agents of e-learning. If the line of sight was another agent, the following happens. Author of a distance course rushes to him, until the distance will not be minimal. Then there is their stop, where there are three possible cases.

1. At a meeting of the two authors of distance learning courses for both is proportional to the amount of knowledge gain knowledge of the interlocutor. After the meeting, agents differ and some time available for subsequent contacts.

2. At a meeting with a tutor from the author of a distance course knowledge gain occurs and growth occurs indicator characterizing the transfer of knowledge. At tutor knowledge gain is proportional to the amount of knowledge of the author of a distance course.

3. At a meeting with the student at the author of a distance course is increase (significantly less than at a meeting with the tutor) of the transmitted knowledge, and the student, in turn, increase consumption of knowledge.

The behavior of a tutor. The tutor also moves randomly. Meeting with the author of a distance course described above. At a meeting with another tutor is a mutual exchange of experience, that is, both the amount of knowledge grows proportionally to the volume of knowledge interlocutor. At a meeting with the student is learning, in which the tutor grows in value of the variable, showing the amount of transferred knowledge, the student accordingly their consumption.

The behavior of a student. The interactions of a student with the author and tutor of a distance course described above. At a meeting between the students is an exchange of knowledge is proportional to the accumulated knowledge of the interlocutor.

If an agent sees several other agents, he rushes to the one that gives the maximum gain his objective function.

A formal description of the model.

Legend: a_i – number of the author's of a distance course; a_j – number of the tutor; a_s – number of the student, members of a distance course; $k(t,a_i), k(t,a_j), k(t,a_s)$ – volumes accumulated or available knowledge of the author, tutor and student; $w(t,a_i), w(t,a_j), w(t,a_s)$ – volumes transferred to other agents of knowledge by the author, tutor and student, respectively; x – coordinate along the abscissa (varies depending on the speed); y – coordinate along the ordinate (varies depending on the speed); vx – speed along the horizontal axis (may change when the agent saw interlocutor – the maximum speed); vy – speed on the y-axis (may change if the agent saw the interlocutor – the maximum speed, and after a conversation with the agent); $d1, d2, d3, d4, d5, d6$ – share knowledge, which is passed from agent to agent; L_a – lifetime agent *a*; K_i, K_j, K_s – the total volumes knowledge produced by the authors, tutors, students of distance learning courses, respectively; K – total amount of knowledge in the analyzed virtual web center; p_i, p_j, p_s – probability of appearance the author, tutor and student of a distance course respectively.

Behaviour the author’s of a distance course a_i at the time *t* leads to a state which is described by the following set of parameters: $k(t, a_i), w(t, a_i), x, y, vx, vy$.

Tutor and student status is defined similarly.

The meeting of the two authors of a distance learning courses is described as follows:

$$k(t+0,a_{i1}) = k(t,a_{i1}) + d1k(t,a_{i2}), \quad (1)$$

$$k(t+0,a_{i2}) = k(t,a_{i2}) + d1k(t,a_{i1}), \quad (2)$$

$w(t,a_{i1}), w(t,a_{i2})$ remain the same.

Meeting the author and tutor of a distance course:

$$w(t+0,a_i) = w(t,a_i) + d2k(t,a_i), \quad (3)$$

$$k(t+0,a_j) = k(t,a_j) + d3k(t,a_i), \quad (4)$$

$k(t,a_i), w(t,a_j)$ remain the same.

The meeting between the author and a student of a distance course:

$$w(t+0,a_i) = w(t,a_i) + d4k(t,a_i), \quad (5)$$

$$k(t+0,a_s) = k(t,a_s) + d4k(t,a_i), \quad (6)$$

$k(t,a_i)$ remain the same.

The meeting between the tutor and the student:

$$w(t+0,a_j) = w(t,a_j) + d5k(t,a_j), \quad (7)$$

$$k(t+0,a_s) = k(t,a_s) + d5k(t,a_j), \quad (8)$$

$k(t,a_j)$ remain the same.

The meeting of two students:

$$k(t+0,a_{s1}) = k(t,a_{s1}) + d6k(t,a_{s2}), \quad (9)$$

$$k(t+0,a_{s2}) = k(t,a_{s2}) + d6k(t,a_{s1}), \quad (10)$$

$$w(t+0,a_{s1}) = w(t,a_{s1}) + d6k(t,a_{s2}), \quad (11)$$

$$w(t+0,a_{s2}) = w(t,a_{s2}) + d6k(t,a_{s1}). \quad (12)$$

Results of agent-based modeling in a SWARM environment are presented in the paper [12].

We aim to investigate the effectiveness of the AnyLogic package for designing a hybrid agent-based model, which assesses knowledge of the users of distance learning courses on the basis of neural networks, which belong to the new frontier of artificial intelligence. The review of scientific papers in this area [2, 3] suggests that the results of neural networks, which are based on a large number of observations, reflect reality better than expert models, which survey a small number of experts, or fuzzy logic systems, which use the rules laid down by several people.

The conceptual scheme of hybrid ABM of the users of e-learning is presented on the Fig. 1.

From this figure, one may see that in the process of construction of ABM three artificial societies are going to be considered. Each of societies presents the set of agents who are decision-makers in the process of production and dissemination of the knowledge in the virtual environment (Learning Management System – LMS) Moodle. The support of decisions is provided by the means of artificial neural networks. The support of decisions is provided by the means of artificial neural networks.

With the purpose of designing artificial neural networks, we use the data from the activity of web-centre users in one of Ukraine's higher education institutions [13]. Based on the number of clicks, published in the Moodle event log system, it is possible to monitor the performance of the e-learning agents over the past twelve months. It is possible to monitor how the distance course resources were viewed, updated, or what was deleted and added to the tasks. Our research uses the data which characterizes 117000 actions by more than 500 agents. Almost 10% of the agents are authors, approximately 20% are tutors, and the rest are students.

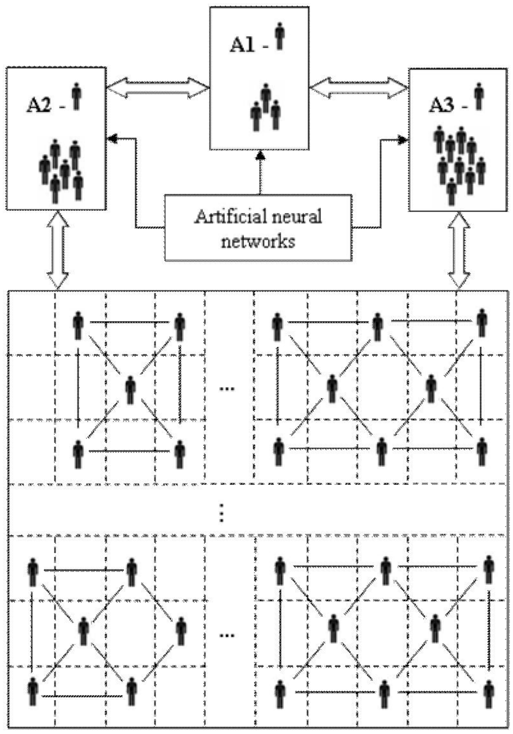

Fig. 1 – The conceptual scheme of hybrid ABM of the users of e-learning

All the data describing the clicks in the event log of the Moodle e-learning management system are divided into the following nonoverlapping click activity data groups: (1) the authors of distance course, (2) tutors and (3) students, participating in the distance course.

On the basis of these data, the number of clicks of j-type agent $\tilde{x}^{(j)}$ $(j=1,2,3)$ is determined. Each group includes a provisional reference value $\tilde{x}_0^{(j)}$ which is defined within the specified interval of this indicator (between the smallest and the largest possible value of $\tilde{x}_{\min}^{(j)}$ and $\tilde{x}_{\max}^{(j)}$ accordingly) and corresponds to better quality. In this case, expert opinions or certain normative indicators may be considered provisional reference values.

Each of the analyzed parameters of a certain $x^{(j)}$ $(j=1,2,3)$ group is provided by conversion

$$x^{(j)} = 1 - \frac{\left|\tilde{x}^{(j)} - \tilde{x}_0^{(j)}\right|}{\max\left\{\left(\tilde{x}_0^{(j)} - \tilde{x}_{\min}^{(j)}\right), \left(\tilde{x}_{\max}^{(j)} - \tilde{x}_0^{(j)}\right)\right\}}, \quad (13)$$

in which the area of its possible values is defined as a range $[0,1]$. In this case, the zero value of the transformed indicator $x^{(j)}$ will signify the smallest quality of the defined specification while the unit value will indicate the highest quality.

So, if the indicators of a number of clicks are specified under the defined above groups, then it is possible to pass on to the specified $x^{(j)}$ parameters, linked with the input variables $\tilde{x}^{(j)}$ by using transformation (13) above.

Clearly, for each j-group the normalized variable $x^{(j)}$ can range from $x^{(j)} = 0$ (which corresponds to the worst quality) to $x^{(j)} = 1$ (which corresponds to the best quality).

On the basis of transformation results (13) we can proceed to the construction of artificial neural networks. This problem is solved in two stages:

1) by choosing type (architecture) of the network,
2) by selection of network weights (training).

In Fig. 2 are shown these stages of construction and the use of artificial neural networks for subsequent incorporation in ABM.

On the first stage, for each type of e-learning agents (or group), we choose the most effective architecture of neural network. The most popular and well-studied architectures are as follows: multilayer perceptron, linear networks, probabilistic neural networks, generalized regression neural network and others.

On the second stage we have to “teach” the chosen network: that is to find such values of its weights so the network can work satisfactorily. There are specific “teaching” algorithms developed for much architecture, which allow adjusting network weights in a certain way (see Table 1).

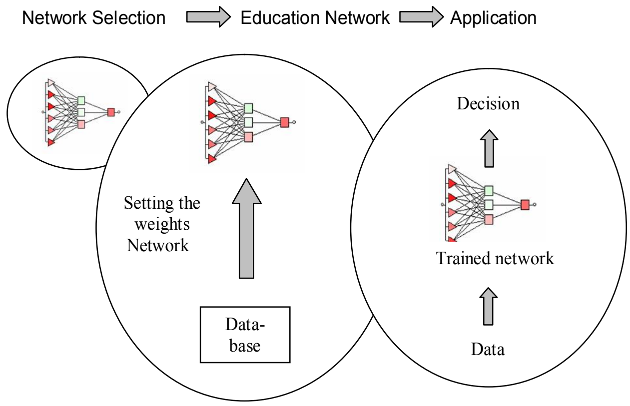

Fig. 2 – Stages of construction and application of neural networks

Table 1. The main types of neural networks and algorithms for their teaching.

Multilayer perceptron (MP)	**Radial basis function (RBF)**
The three-layered MP (there is 1 hidden layer) simulates a problem of almost any complexity. MP network can be trained on the basis of such algorithms: - Conjugate gradient method, - Quasi-Newton, - Levenberg-Marquardt, - Converse and Rapid spread, - Delta-delta with a dash.	These networks have an input layer, hidden layer with radial elements and an output layer of linear elements. RBF relatively quick to learn on-the basis of linear optimization. You can also use the learning algorithms and MP. However, RBF is larger than the multilayer perceptron and therefore are slower.
Linear network (LAN) LAN has only two layers: input and output, the latter has a linear post-synaptic potential function and the activation function. Linear network is better trained by the method of pseudoinverse. This method optimizes the last layer of any network, if it is linear.	**Bayesian networks (PNN, GRNN):** - probabilistic neural network is used only in classification issues, - the generalized regression neural network is used only in regression issues. These networks are trained on the basis of cluster algorithms: k-means, etc.

It's important to note, that the network contains the information estimating production trends and the dissemination of knowledge by agents. This information is recoded from the set of e-learning agents' clicks. Therefore, the quality of network teaching depends on the number of examples in the training set, as well as on how well these examples describe the task.

We have chosen the *STATISTICA Neural Networks* package among other software that is designed to build neural networks [14]. There is a tool called “Problem Solver” in the package, which provides for the construction of neural networks sets with superior characteristics. "Network Constructor", which includes neural networks selection and teaching with the consideration of advanced users requirements, can also be applied.

Fig. 3 shows examples of artificial neural networks developed by means of *STATISTICA Neural Networks* for a hybrid agent-based model.

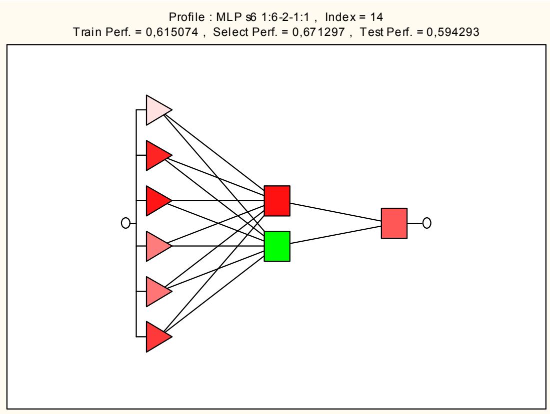

a)

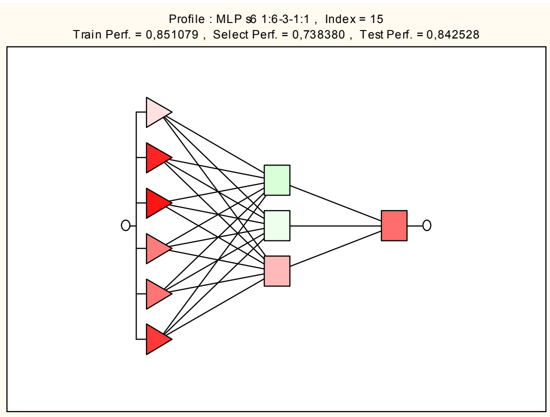

в)

Fig. 3 – Network architectures of master-making STATISTICA Neural Networks

From Fig. 3 one may see that neural networks have identical architecture which is represented by multilayer perceptrons. The differences between these neural networks are in the number of hidden layer neurons and some other parameters.

Numerical values of parameters of neural networks, shown in Fig. 3, are not as important, as the emphasis in this paper is made on the methodological approaches to the development of hybrid ABM. Therefore, we do not need to focus on the technical issues of implementing the neural networks, just simply list below their main purpose for the created agent-based model.

❖ Neural network # 1 (NN#1) determines the activity of agents of the first type based on the forecasting of the possible number of clicks and thus evaluates the level of the knowledge produced and distributed by the e-learning course authors.

❖ Neural network # 2 (NN#2) determines the activity of the second type of agents on the basis of forecasting the possible number of clicks and thus evaluates the level of knowledge distributed by the tutors of a e-learning course.

❖ Neural network # 3 (NN#3) determines the activity of three types of agents on the basis of forecasting the possible number of clicks and thus evaluates the level of knowledge consumed by students participating in e-learning.

So the neural network allegedly accepts a decision of e-learning agents, obtaining an input variable characterizing the growth in usefulness and value of knowledge for the participants of an artificial society of this type. The number of clicks, measured with allowances made for long term threshold values, allows for assessing trends of knowledge production and dissemination in the hybrid agent-based model by agents on the basis of the activity results of each e-learning user.

Note also that *STATISTICA Neural Networks* has a code generator, a separate module that provides this package with an opportunity to create the equivalent of a teaching network as a non-compiled code in C/C++ or Visual Basic. Every calculation and installation of artificial neural network is unlocked and available for viewing user, copy or relevant changes.

Code fragments of a neural network, developed this way, can be embedded as functions for code use in other applications. A huge advantage of this feature is that the *STATISTICA Neural Networks* does not need to be installed on the computer where the generated code is executed.

3. THE IMPLEMENTATION OF A PROTOTYPE HYBRID ABM WITH ANYLOGIC

Agent-based hybrid model was developed in the *AnyLogic* environment. Among utility tools are variables, timers and statecharts (flow charts or diagrams). Variables reflect the change in the characteristics of e-learning course agents. Timers are set for a specific time interval, after which the specified action will be performed. Statecharts make possible to visually present agent's behaviour in time, under the influence of events or conditions, which consists of graphic states and transitions between them. Any complex behavioural logic of the agents in the hybrid model designed in *AnyLogic* can be expressed by a combination of utility tools, as well as embedded code functions of three previously designed neural networks.

To create *AnyLogic* model, we have to create classes of active objects (or use *AnyLogic* library of facilities). With recognition the active objects we create template and particular objects, built in accordance with this template (active object). Those objects can be used as elements of other active objects: avtorDK [..], tutor [..], student [..]. One class is always the root class in *AnyLogic* model. For this root class we generate a copy in the ABM hybrid. The predefined name for the copy is **"Main"**. *AnyLogic* system starts execution with this copy.

Variables which are used to describe the hybrid model have the same structure. The diagram in Fig. 4 explains the variables.

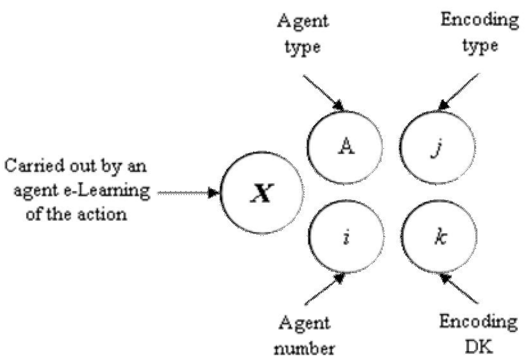

Fig. 4 – Identification of variables in the ABM.

X indicates the action (click), carried by the e-learning agent. Examples of such actions could be as follows: P – browse the resources and tasks in distance course (DK); O – update resources and assignments in DK; D – add resources and tasks in DK; U – remove resources and tasks in DK. As a rule, it is clear from the context which action is involved.

The index *k* determines the electronic distance learning course in which the agent performs its action. The agent's number is marked with the index *i*, and *j* is the index which indicates the type of agent (A1 – author, A2 – tutor, A3 – student).

Fig. 5 shows an example of agent behaviour specification, which reflects the interaction between authors of distance learning courses, tutors and students participating in e-learning.

As can be seen from Fig. 5, the "Entry action" defines the mutual action of the agents using an artificial neural network #1 (NN#1) above. This network sends the message with a prediction about the amount of clicks by the authors of electronic distance courses to all e-learning agents and thus evaluating the level of produced and distributed knowledge.

Exit action provides for the following three cases.

1. During a contact of two authors distance courses both increase knowledge proportionally with the interlocutor's knowledge that is presented on the Fig. 6.

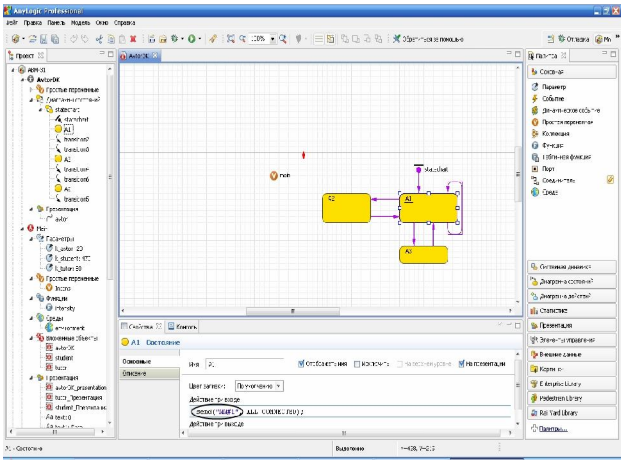

Fig. 5 – Agent-Based Model Specification Example.

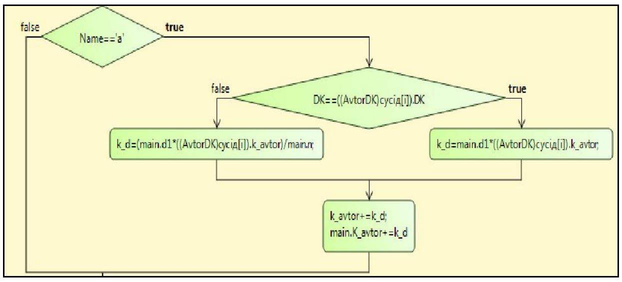

Fig. 6 – Statechart of knowledge transfer algorithm – if AvtorDK meet with AvtorDK.

2. When the distance course author contacts a tutor, he does not gain any knowledge, although the knowledge transfer indicator increases. The tutor gains knowledge proportionally to the author's knowledge of the distance course (Fig. 7).

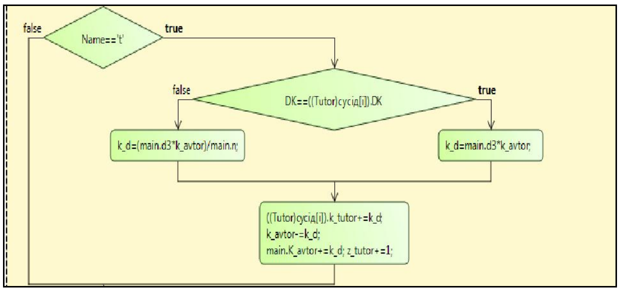

Fig. 7 – Statechart of knowledge transfer algorithm – if AvtorDK meet with Tutor.

3. When the author contacts a student, he gains substantially less knowledge than from contacting with the e-learning course tutor. At the same time the student's knowledge consumption increases (Fig. 8).

Behaviour of Tutor's (A2) and student's (A3) is described in the first Model using neural networks #2 and #3 above.

The designed agent-based model for e-learning allows participants to observe visually their actions.

To view the values of characteristic variables for any agent, you can use the control panel system to pause the simulation.

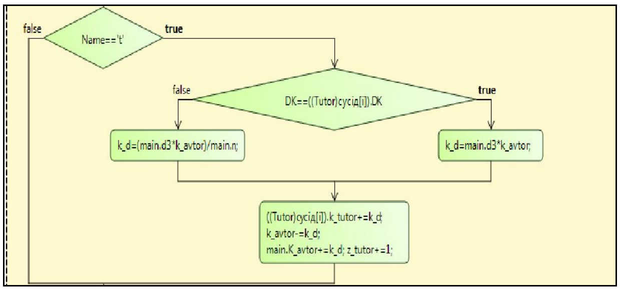

Fig. 8 – Statechart of knowledge transfer algorithm – if AuthorDK meet with Students.

With the help of created model, we may see how much knowledge per type of agent was produced in general and on average (Fig. 9).

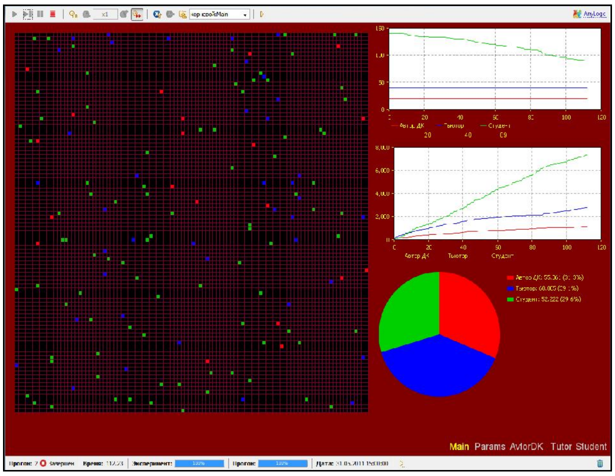

Fig. 9 – The main window of computer experiments.

Here, the upper graph shows the dynamics of change in the number of agents of each type. The X axis shows time of courses, and the axis Y – number of agents. The middle graph represents the amount of knowledge produced by each type of agents. Such a large number of consumed knowledge among the students, represented in the graph, is due to the fact that students rate in comparison with others is remarkably higher: number of students – 140, number of tutors – 40, DK authors – 20. The pie chart represents the average number of produced and consumed knowledge for each type of agents.

We can also observe the statistics of the residual amount of knowledge and the number of meetings each agent after of computer simulation experiments (Fig. 10).

Substantive interpretation of diagrams is shown (see Fig. 10). The top chart shows the amount of knowledge (variable k_avtor) for each AvtorDK. Other charts below describe the number of meetings of each agent with other types of agents. For example agent A(3), for which the value variable k_avtor = 30.304, met in computer simulations 0 times with other DK authors, 3 times with other tutors, and 14 times with the students.

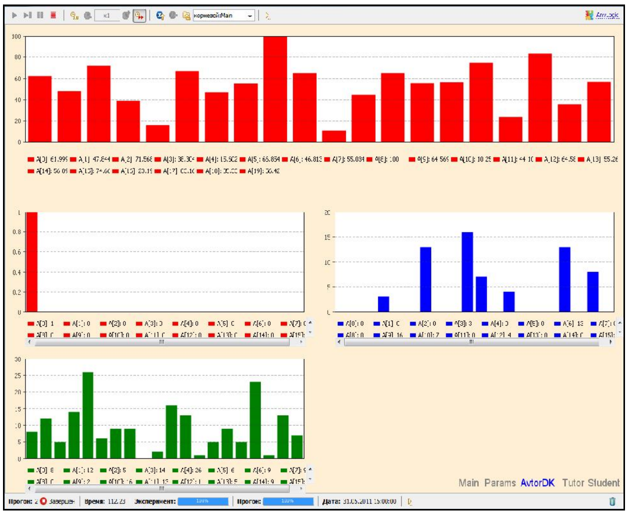

Fig. 10 – Diagrams balance of knowledge and meeting agents on the example of Authors DK.

Such diagrams of the meetings with respect to transfers of knowledge in a learning management system Moodle can be observed for other e-learning agents. In Fig. 10 tabs for tutor and student are presented as well.

Fig. 11 illustrates some results of a simple experiment with a designed agent-based model hybrid, which assesses the knowledge of e-learning users. The results of the knowledge and the e-learning contact between agents are illustrated through the example of a specific (fourth) tutor.

Ideally, a hybrid agent-based model with integrated neural networks allows describing data of layers, and providing analytics.

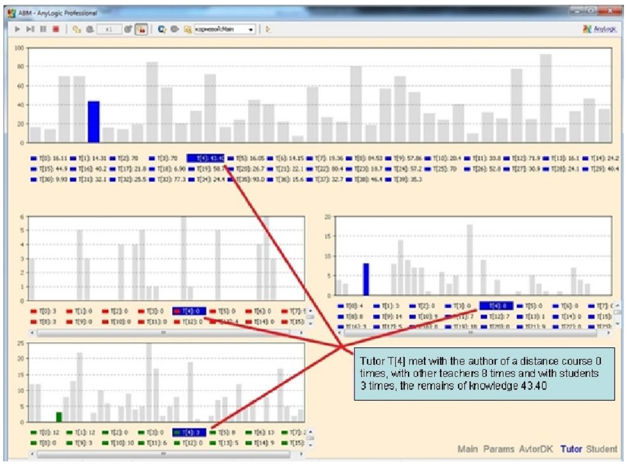

Fig. 11 – Diagrams of the resulting knowledge on the example tutors of the distance course.

We use the multiple data sets and analytical tools in a single interface for the visualization and data presentation. This helps in analysis of patterns of production and knowledge dissemination of e-learning agents.

4. CONCLUSIONS

Thus, analysis of the results of the completed research allows making the following conclusions:

1. It is extremely important to promote a dialogue between researchers and practitioners to create new tools and methodologies supporting the development of Web analytics (or learning analytics) in the field of e-learning.
2. Both agent-based models and artificial neural networks are effective tools for developing Web analytics (learning analytics) in e-learning.
3. Using those tools above can lead to improving distance e-learning courses aimed at creating adaptive mechanisms of interaction between agents of e-learning: webinars, brainstorming and thematic discussions on the forums.

In the future we plan to modernize the ABM model that would take into account:

– all formalized description of the model code for conduct analyzed agents (1) – (12);

– interactions with agents of the university administration and upper-level management – the Ministry of Education and Science of Ukraine.

5. REFERENCES

[1] V.L. Makarov, A.R. Bakhtizin, The new tools in the social sciences – an agent-based model: general description and specific examples, *Economics and Management*, (12) 50 (2009), pp. 13-25 (in Russian).

[2] A.R. Bakhtizin, *Agent-based models of the economy*, ZAO "Publisher "Economy", Moscow, 2008, 279 p. (in Russian).

[3] V.L. Makarov, A.R. Bakhtizin, *Social simulation – a breakthrough new computer (agent-based models)*, Economics, Moscow, 2013, 295 p. (in Russian).

[4] *Journal of Artificial Societies and Social Simulation*. http://jasss.soc.surrey.ac.uk/JASSS.html.

[5] *Agent-based Computational Economics*: http://www.econ.iastate.edu/tesfatsi/ace.htm.

[6] *Journal of Artificial Societies*. http://www.artsoc.ru/ (in Russian).

[7] Website Santa Fe Institute. http://www.santafe.edu.

[8] Anylogic Simulation Software. http://www.anylogic.com/.

[9] Y. Karpov, *Simulation modeling systems. Introduction to modeling with AnyLogic 5*, BHV-Petersburg, St. Petersburg, 2005, 400 p. (in Russian).

[10] A. Borschev, From system dynamics and traditional IT – to practical agent-based models: causes, technology and tools. http://www.gpss.ru/paper/borshevarc.pdf. (in Russian).

[11] V. Artemenko, Web Analytics in e-Learning: agent-based and neural network approaches, *Proceedings of the 2013 IEEE 7th International Computing on Intelligent Data Acquisition and Advanced Computing Systems: Technology and Applications*. Vol. 2, Berlin, Germany (September 12-14, 2013), pp. 774-780.

[12] V. Artemenko. Computer modeling of communicative interactions of e-Learning agents, *Educational Technology & Society*, (13) 2 (2010), pp. 345-354. http://ifets.ieee.org/russian/depository/v13_i2/pdf/12r.pdf. (in Russian).

[13] Website of web-center of Lviv Academy of Commerce (LAC). http://virt.lac.lviv.ua. (in Ukrainian).

[14] *STATISTICA* Automated Neural Networks – Site StatSoft is now a part of Dell. http://www.statsoft.com/Products/STATISTICA/Automated-Neural-Networks.

***Viktor Artemenko**, In 1974 graduated from Ivan Franko National University of Lviv, Faculty of Economics. In 1979-82 studied at the graduate shcool of the Central Economics and Mathematics Institute (CEMI, Moscow) at the Academy of Sciences of the USSR.*

In 1982 defended his PhD thesis in economics. Since 1982 he is working at Lviv Academy of Commerce (LAC) as an assistant professor. In 1994-2009 was the head of the Management Information Systems department at LAC. Since 2006 is the head of the UNESCO Chair branch "New information technologies in education for all". Research interests: management of efficiency of regional development of Ukraine, construction and monitoring of life quality indicators, ICT, e-Learning.

Keisuke Kato, Vitaly Klyuev. Password Protection: End User Security Behavior, *International Journal of Computing*, Vol. 13, Issue 1, 2014, pp. 8-16.

Password authentication is one of essential services in our life for protecting data. In other words, we may loose a lot of money, sensitive data, etc., if passwords leak out. Thus, we have to understand clearly what is important for creating and/or changing passwords. Our goal is to analyze key issues for setting passwords. We surveyed 262 students of the University of Aizu, Japan. We discussed key security problems, main password protection issues and techniques, and misunderstandings about passwords by end users. Furthermore, we compared the obtained data with results provided by the National Institute of Standard Technology (NIST) and others. The results can help the users set stronger passwords

Christof Pieloth, Thomas R. Knösche, Burkhard Maess, Mirco Fuchs. Online Distributed Source Localization from EEG/MEG Data, *International Journal of Computing*, Vol. 13, Issue 1, 2014, pp. 17-24.

Electroencephalography (EEG) and Magnetoencephalography (MEG) provide insight into neuronal processes in the brain in a real-time scale. This renders these modalities particularly interesting for online analysis methods, e.g. to visualize brain activity in real-time. Brain activity can be modeled in terms of a source distribution found by solving the bioelectromagnetic inverse problem, e.g. using linear source reconstruction methods. Such methods are particularly suitable to be used on modern highly parallel processing systems, such as widely available graphic processing units (GPUs). We present a system that, according to its modular scheme, can be configured in a very flexible way using graphical building blocks. Different preprocessing algorithms together with a linear source reconstruction method can be used for online analysis. The algorithms use both CPU and GPU resources. We tested our system in a simulation and in a realistic experiment.

Aleksandra Kawala-Janik, Jerzy Baranowski, Michal Podpora, Pawel Piatek, Mariusz Pelc. Use of a Cost-Effective Neuroheadset Emotiv EPOC for Pattern Recognition Purposes, *International Journal of Computing*, Vol. 13, Issue 1, 2014, pp. 25-33.

Application of biomedical signals for the control purposes is currently growing interest of research society. Various biomedical signals enable various control prospects. In this paper application domain of using electroencephalographic signals obtained from an inexpensive Emotiv EPOC headset was described. It is also important to mention the possible implementation of the proposed method on an embedded platform, as it causes some significant limitations due to the little efficiency and low computing power of an embedded system platform. The proposed method enables to extend future application of the BCI system presented in this paper and it also gives more testing flexibility, as the platform can simulate various external environments. It is crucial to mention, that no filtering was done and that the traditional, statistical signal processing methods were in this work neither used, nor described.

Vitaliy Pavlenko, Sergei Pavlenko, Viktor Speranskyy. Noise Immunity Research for Nonlinear Dynamical Systems Identification Based on Volterra Model in Frequency Domain, *International Journal of Computing*, Vol. 13, Issue 1, 2014, pp. 34-41.

The accuracy and noise immunity of the interpolation method of nonlinear dynamical systems identification based on the Volterra model in the frequency domain is studied in this paper. The polyharmonic signals are used for the testing the method. The algorithmic and software toolkit in Matlab is developed for the identification procedure. This toolkit is used to construct the informational models of test system and communication channel. The model is built as a first-, second- and third-order amplitude–frequency and phase–frequency characteristics. The comparison of obtained characteristics with previous works is given. Wavelet denoising is studied and applied to reduce measurement noise.

Agata Manolova, Krasimir Tonchev. Study of Two 3D Face Representation Algorithms Using Range Image and Curvature-Based Representations, *International Journal of Computing*, Vol. 13, Issue 1, 2014, pp. 42-49.

In this paper we present a comparative analysis of two algorithms for image representation with application to recognition of 3D face scans with the presence of facial expressions. We begin with processing of the input point cloud based on curvature analysis and range image representation to achieve a unique representation of the face features. Then, subspace projection using Principal Component Analysis (PCA) and Linear Discriminant Analysis (LDA) is performed. Finally classification with different classifiers will be performed over the 3D face scans dataset with 61 subject with 7 scans per subject (427 scans), namely two "frontal", one "look-up", one "look-down", one "smile", one "laugh", one "random expression". The experimental results show a high recognition rate for the chosen database. They demonstrate the effectiveness of the proposed 3D image representations and subspace projection for 3D face recognition.

Daniel Caspari, Mircea Strutu, Lucas Riedhammer, Uwe Grossmann. Sensor Based Algorithms for Dead Reckoning: A comparison of two approaches for smartphones, *International Journal of Computing*, Vol. 13, Issue 1, 2014, pp. 50-60.

The implementation of a reliable indoor localization system can be the starting point for a variety of much desired applications. Either for efficient patient monitoring inside a hospital or as an automatic guide inside a museum, a working localization solution can be useful. Smartphone technology represents a powerful and user friendly tool in order to achieve adequate indoor positioning. This paper explores the potential of using smartphone sensor data (accelerometer and compass) in order to track the location of the person holding the device using dead reckoning algorithms. Two different approaches are under scrutiny in order to assess their performance in different real life inspired scenarios.

Viktor Artemenko. Agent-Based Modeling of the E-Learning Users' Behavior, *International Journal of Computing*, Vol. 13, Issue 1, 2014, pp. 61-69.

In this paper the methodological and technical approaches are considered to construct the agent-based model (ABM) with built-in artificial neural networks. This model describes the user's behavior of electronic or distance learning in a virtual environment of one of universities. Design of ABM aims to support a development of Web analytics (learning analytics) on the basis of computer experiments evaluating the trends of the knowledge creation and dissemination for e-Learning users. In research AnyLogic software, which is one of the most popular packages for agent-based modeling, is proposed for implementing the created model, and package STATISTICA Neural Networks is proposed for constructing the neural networks.

Keisuke Kato, VitalyKlyuev. Захист за допомогою паролю: «захисна» поведінка кінцевого користувача, *Міжнародний журнал «Комп'ютинг»*, том. 13, випуск 1, 2014, с. 8-16.

Аутентифікація за допомогою паролю є однією з основних послуг для захисту даних в нашому житті. Іншими словами, можна втратити багато грошей, конфіденційних даних і т.п., якщо не буде паролю. Таким чином, треба чітко зрозуміти, що важливо для створення та/або зміни паролю. Наша мета полягала в аналізі ключових проблем для установки паролів. Нами опитано 262 студентів університету в Айдзу, Японія. Обговорено ключові проблеми безпеки, основні питання та методи захисту за допомогою паролю і нерозуміння паролів кінцевими користувачами. Крім того, проведено порівняння отриманих даних з результатами, представленими Національним інститутом технологічних стандартів (NIST) та іншими. Результати можуть допомогти користувачам встановлювати надійні паролі.

Christof Pieloth, Thomas R. Knosche, Burkhard Maess, Mirco Fuchs. Локалізація розподілених онлайн джерел з ЕЕГ та МЕГ даних, *Міжнародний журнал «Комп'ютинг»*, том. 13, випуск 1, 2014, с. 17-24.

Електроенцефалографія (ЕЕГ) і магнітоенцефалографія (МЕГ) забезпечують дослідження нейронних процесів у корі головного мозку в режимі реального часу. Ці можливості особливо цікаві для методів онлайн аналізу, наприклад, для візуалізації активності мозку в реальному часі. Активність мозку може бути змодельована з точки зору розподіленого джерела, знайденого шляхом вирішення біоелектромагнітного зворотнього завдання, наприклад, використовуючи лінійні методи відновлення лінійного джерела. Такі методи є зокрема спроможні для використання в сучасних високоефективних паралельних системах обробки даних, таких як широкодоступні графічні процесори. Запропоновано систему з модульною структурою, яка може формуватись дуже гнучким способом шляхом використання графічних модулів. Для онлайн-аналізу можуть використовуватися різні алгоритми попередньої обробки даних разом із методом відновлення лінійного джерела. Для виконання алгоритмів використовують ресурси як центрального так і графічного процесора. Система протестована як в режимі симуляції, так і в реальному експерименті.

Aleksandra Kawala-Janik, Jerzy Baranowski, Michal Podpora, Pawel Piatek, Mariusz Pelc. Використання рентабельного Neuroheadset Emotiv EPOC для розпізнавання цілей, *Міжнародний журнал «Комп'ютинг»*, том. 13, випуск 1, 2014, с. 25-33.

В даний час зростає інтерес наукового суспільства до застосування біомедичних сигналів з метою управління. Різні біомедичні сигнали спричиняють різні перспективи управління. У даній статті описано сферу застосування електроенцефалографічних сигналів, отриманих за допомогою недорогої платформи Emotiv EPOC. Важливо також згадати можливу реалізацію запропонованого методу на вбудованих платформах, так як це викликає деякі істотні обмеження у зв'язку з низькою ефективністю та малою обчислювальною потужністю платформи вбудованих систем. Запропонований метод дозволяє в майбутньому розширити розробленої системи і це додатково покращує гнучкість у тестуванні, так як платформа може імітувати різні зовнішні середовища. Потрібно зазначити, що в цій роботі не було здійснено фільтрації, і що не описано традиційні, статистичні методи обробки сигналів, які тут використані.

Віталій Павленко, Сергій Павленко, Віктор Сперанський. Дослідження завадостійкості ідентифікації нелінійних динамічних систем на основі моделі Вольтерра в частотній області, *Міжнародний журнал «Комп'ютинг»*, том. 13, випуск 1, 2014, с. 34-41.

Досліджено точність і завадостійкість інтерполяційного методу ідентифікації нелінійних динамічних систем на основі моделі Вольтерра в частотній області. Для тестування використовуються полігармонічні сигнали. Для проведення процедури ідентифікації в Matlab розроблено алгоритмічні і програмні інструментальні засоби. Розроблені засоби використовуються для побудови інформаційних моделей тестової системи та комунікаційного каналу. Модель побудовано у вигляді амплітудно-частотних і фазо-частотних характеристик першого, другого та третього порядків. Наведено порівняння отриманих характеристик з попередніми роботами. Виконано дослідження і застосування вейвлет-фільтрації для зменшення впливу шумів вимірів.

Agata Manolova, Krasimir Tonchev. Вивчення двох 3D алгоритмів представлення облич, використовуючи діапазон та кривизну представлень зображень, *Міжнародний журнал «Комп'ютинг»*, том. 13, випуск 1, 2014, с. 42-49.

У цій статті представлено порівняльний аналіз двох алгоритмів представлення зображення шляхом розпізнавання трьохмірних (3D) сканованих облич в умовах наявності міміки. Спочатку проводиться аналіз кривизни і діапазону представлення зображень для досягнення цілісного представлення особливостей обличчя. Після цього здійснюється проекція підпростору із застосуванням аналізу головних компонент (PCA - Principal Component Analysis) та лінійного дискримінантного аналізу (LDA - Linear Discriminant Analysis). Наприкінці виконується класифікація за допомогою різних класифікаторів на вибірці 3D сканіву зображень облич. Вибірка містить зображення 61 особи. Для кожної особи використовуються 7 зображень: два „фронтальних", одне „погляд вгору", одне „погляд вниз", одне „усмішка", одне „сміх", одне „випадковий вираз обличчя". Отримані результати показують високу процент розпізнавання для вибраної вибірки. Вони демонструють ефективність запропонованих 3D представлень зображень та проекції підпростору для розпізнавання 3D облич.

Daniel Caspari, Mircea Strutu, Lucas Riedhammer, Uwe Grossmann. Датчик на основі алгоритмів для точного розрахунку: Порівняння двох підходів для смартфонів, *Міжнародний журнал «Комп'ютинг»*, том. 13, випуск 1, 2014, с. 50-60.

Реалізація надійної системи локалізації в приміщенні може стати відправною точкою для цілого ряду необхідних додатків. Така локалізація може бути корисною як для ефективного моніторингу стану пацієнта в лікарні, так і як автоматичний навігатор в музеї. Смартфони на сьогодні є потужним та зручним інструментом для визначення точного місцезнаходження. Стаття розглядає можливість використання даних сенсора смартфону (акселерометра та компасу) для того, щоб відстежити місцезнаходження особи з використанням алгоритмів навігації. В статті вивчаються два різних підходи з метою оцінки їх ефективності в різних реальних життєвих ситуаціях.

Віктор Артеменко. Агентнобазоване моделювання поведінки користувачів електронного навчання, *Міжнародний журнал «Комп'ютинг»*, том. 13, випуск 1, 2014, с. 61-69.

У цій роботі розглянуто методологічні та методичні підходи щодо побудови агент-орієнтованої моделі (АОМ) із вбудованими штучними нейронними мережами. Ця модель описує поведінку користувачів електронного або дистанційного навчання у віртуальному середовищі одного з університетів. Розроблення АОМ спрямовано на підтримку веб-аналітики (навчальної аналітики) на базі комп'ютерних експериментів оцінювання тенденцій створення та розповсюдження знань користувачів електронного навчання. Для реалізації створюваної моделі запропоновано програмне забезпечення, зокрема пакет AnyLogic – один із найбільш популярних для агентного моделювання, і пакет STATISTICA Neural Networks для побудови нейронних мереж.

Keisuke Kato, Vitaly Klyuev. Защита с помощью пароля: «защитное» поведение конечного пользователя, *Международный журнал «Компьютинг»*, том. 12, выпуск 3, 2014, с. 8-16.

Аутентификация с помощью пароля является одной из основных услуг для защиты данных в нашей жизни. Иными словами, можно потерять много денег, конфиденциальных данных и т.п., если не будет пароля. Таким образом, надо четко понять, что важно для создания и/или изменения пароля. Наша цель заключалась в анализе ключевых проблем для установки паролей. Нами опрошено 262 студентов университета в Айдзу, Япония. Обсуждены ключевые проблемы безопасности, основные вопросы и методы защиты при помощи пароля и непонимание паролей конечными пользователями. Кроме того, проведено сравнение полученных данных с результатами, представленными Национальным институтом технологических стандартов (NIST) и другими. Результаты могут помочь пользователям устанавливать надежные пароли.

Christof Pieloth, Thomas R. Knosche, Burkhard Maess, Mirco Fuchs. Локализация распределенных онлайн источников с ЭЭГ и МЭГ данных, *Международный журнал «Компьютинг»*, том. 12, выпуск 3, 2014, с. 17-24.

Электроэнцефалография (ЭЭГ) и магнитоэнцефалография (МЭГ) обеспечивают исследования нейронных процессов в коре головного мозга в режиме реального времени. Эти возможности особенно интересны для методов онлайн анализа, например, для визуализации активности мозга в реальном времени. Активность мозга может быть смоделирована с точки зрения распределенного источника, найденного путем решения биоэлектромагнитного обратной задачи, например, используя линейные методы восстановления линейного источника. Такие методы, в частности, способны для использования в современных высокоэффективных параллельных системах обработки данных, таких как широкодоступные графические процессоры. Предложена система с модульной структурой, которая может формироваться очень гибким способом путем использования графических модулей. Для онлайн-анализа могут использоваться различные алгоритмы предварительной обработки данных вместе с методом восстановления линейного источника. Для выполнения алгоритмов используют ресурсы как центрального так и графического процессора. Система протестирована как в режиме симуляции, так и в реальном эксперименте.

Aleksandra Kawala-Janik, Jerzy Baranowski, Michal Podpora, Pawel Piatek, Mariusz Pelc. Использование рентабельного Neuroheadset Emotiv EPOC для распознавания целей, *Международный журнал «Компьютинг»*, том. 12, выпуск 3, 2014, с. 25-33.

В настоящее время растет интерес научного общества к применению биомедицинских сигналов с целью управления. Различные биомедицинские сигналы вызывают различные перспективы управления. В данной статье описано сферу применения электроэнцефалографических сигналов, полученных с помощью недорогой платформы Emotiv EPOC. Важно также упомянуть возможной реализации предложенного метода на встроенных платформах, так как это вызывает некоторые существенные ограничения в связи с низкой эффективностью и малой вычислительной мощностью платформы встроенных систем. Предложенный метод позволяет в будущем расширить разработанной системы и это дополнительно улучшает гибкость в тестировании, так как платформа может имитировать различные внешние среды. Нужно отметить, что в этой работе не было осуществлено фильтрации, и не описаны традиционные, статистические методы обработки сигналов, которые здесь использованы.

Виталий Павленко, Сергей Павленко, Виктор Сперанський. Исследование помехоустойчивости идентификации нелинейных динамических систем на основе модели Вольтерра в частотной области, *Международный журнал «Компьютинг»*, том. 12, выпуск 3, 2014, с. 34-41.

Исследуется точность и помехоустойчивость интерполяционного метода идентификации нелинейных динамических систем на основе модели Вольтерра в частотной области. Для тестирования используются полигармонические сигналы. Для проведения процедуры идентификации в Matlab разработаны алгоритмические и программные инструментальные средства. Разработанные средства используются для построения информационных моделей тестовой системы и канала связи. Модель построена в виде амплитудно-частотных и фазо-частотных характеристик первого, второго и третьего порядков. Приведено сравнение полученных характеристик с предыдущими работами.

Произведены исследование и применение вейвлет-фильтрации для уменьшения влияния шумов измерений.

Agata Manolova, Krasimir Tonchev. Изучение двух 3D алгоритмов представления лиц, используя диапазон и кривизну представлений изображений, ***Международный журнал «Компьютинг»*****, том. 12, выпуск 3, 2014, с. 42-49.**

В этой статье представлены сравнительный анализ двух алгоритмов представления изображения путем распознавания трехмерных (3D) сканированных лиц в условиях наличия мимики. Сначала проводится анализ кривизны и диапазона представления изображений для достижения целостного представления особенностей лица. После этого осуществляется проекция подпространства с анализом главных компонент (PCA - Principal Component Analysis) и линейного дискриминантного анализа (LDA - Linear Discriminant Analysis). В конце производится классификация с помощью различных классификаторов на выборке 3D сканиву изображений лиц. Выборка содержит изображения 61 человека. Для каждого лица используются 7 изображений: два "фронтальных", одно "взгляд вверх", одно "взгляд вниз", одно "улыбка", одно "смех", одно "случайное выражение лица". Полученные результаты показывают высокий процент распознавания для выбранной выборки. Они демонстрируют эффективность предложенных 3D представлений изображений и проекции подпространства для распознавания 3D лиц.

Daniel Caspari, Mircea Strutu, Lucas Riedhammer, Uwe Grossmann. Алгоритмы на основе сенсорных данных для навигации: Сравнение двух подходов для смартфонов, ***Международный журнал «Компьютинг»*****, том. 12, выпуск 3, 2014, с. 50-60.**

Реализация надежной системы локализации в помещении может стать отправной точкой для целого ряда необходимых приложений. Такая локализация может быть полезной как для эффективного мониторинга состояния пациента в больнице, так и как автоматический навигатор в музее. Смартфоны на сегодня является мощным и удобным инструментом для определения точного местонахождения. Статья рассматривает возможность использования данных сенсора смартфона (акселерометра и компаса) для того, чтобы отследить местонахождение лица с использованием алгоритмов навигации. В статье изучаются два различных подхода для оценки их эффективности в различных реальных жизненных ситуациях.

Виктор Артеменко. Агентнобазированное моделирование поведения пользователей электронного обучения, ***Международный журнал «Компьютинг»*****, том. 12, выпуск 3, 2014, с. 61-69.**

В этой работе рассмотрены методологические и методические подходы к построению агент-ориентированной модели (АОМ) со встроенными искусственными нейронными сетями. Эта модель описывает поведение пользователей электронного или дистанционного обучения в виртуальной среде одного из университетов. Разработка ABM направлена на поддержку веб-аналитики (учебной аналитики) на базе компьютерных экспериментов оценки тенденций создания и распространения знаний пользователей электронного обучения. Для реализации создаваемой модели предложено программное обеспечение, в частности пакет AnyLogic – один из самых популярных для агентного моделирования, и пакет STATISTICA Neural Networks для построения нейронных сетей.

Authors Guidelines

Authors are encouraged to submit high quality, original work in English only that has not appeared in, nor is under consideration by, other journals. Extended versions of papers that have previously published in conference proceedings may also be considered (this must be indicated at the time of submission). Authors must submit their manuscript as a .doc, .docx, .rtf or .pdf file by e-mail to:

International Journal of Computing
Research Institute for Intelligent Computer Systems
Ternopil National Economic University
3 Peremogy Square,
Ternopil 46020, Ukraine
Phone: +380 (352) 43-5050 ext. 12-234
Fax: +380 (352) 47-5053
E-mail: **computing@computingonline.net** or **computing.journal@gmail.com**

Submission of .pdf file is highly appreciated instead of the hard copy.

In case of any technical problems, contact us at **computing@computingonline.net** or **computing.journal@gmail.com**.

Journal Topics:

- Algorithms and Data Structure, Software Tools and Environments
- Bio-Informatics
- Computational Intelligence
- Computer Modeling and Simulation
- Cyber and Homeland Security
- Data Communications and Networking
- Data Mining, Knowledge Bases and Ontology
- Digital Signal Processing
- Distributed Systems and Remote Control
- Education in Computing
- Embedded Systems
- High Performance Computing and GRIDS
- Image Processing and Pattern Recognition
- Intelligent Robotics Systems
- Internet of Things
- IT Project Management
- Wireless Systems

Article Formatting

Essential title page information

• Title. Paper title has to be informative and not more than 50 characters. Please avoid abbreviations and formulae where possible.

• Authors' names and affiliations. Where the family name may be ambiguous (e.g., a double name), please indicate this clearly. Present authors' affiliation addresses (where the actual work was done) below the names. Indicate all affiliations with a lower-case superscript letter immediately after the author's name and in front of the appropriate address. Provide the full postal address of each affiliation, including the country name and, if available, the e-mail address of each author. Please designate a corresponding author.

Abstract

A concise and factual abstract is required. The abstract should state briefly the purpose of the research, the principal results and major conclusions. An abstract is often presented separately from the article, so it must be able to stand alone. For this reason, References should be avoided, but if essential, then cite the author(s) and year(s). Also, non-standard or uncommon abbreviations should be avoided, but if essential they must be defined at their first mention in the abstract itself.

Keywords
Immediately after the abstract, provide a maximum of 6 keywords, using American spelling and avoiding general and plural terms and multiple concepts (avoid, for example, 'and', 'of'). Be sparing with abbreviations: only abbreviations firmly established in the field may be eligible. These keywords will be used for indexing purposes.

Introduction
There needs to be an adequate summary of references to describe the current state-of-the-art or a summary of the results.

Material and methods
Provide sufficient detail to allow the work to be reproduced. Methods already published should be indicated by a reference: only relevant modifications should be described.

Results
Results should be clear and concise.

Conclusions
The main conclusions of the study may be presented in a short Conclusions section, which may stand alone or form a subsection of a Discussion or Results and Discussion section.

Acknowledgements
Collate acknowledgements in a separate section at the end of the article before the references and do not, therefore, include them on the title page, as a footnote to the title or otherwise. List here those individuals who provided help during the research (e.g., providing language help, writing assistance or proof reading the article, etc.).

Subdivision
Divide your paper into clearly defined and numbered sections. Subsections should be numbered 1.1, 1.2, etc. (the abstract is not included in section numbering). Use this numbering also for internal cross-referencing: do not just refer to 'the text'. Any subsection may be given a brief heading. Each heading should appear on its own separate line.

Formulae
Mathematical expressions and Greek or other symbols must be written clearly with ample spacing.

Units
Follow internationally accepted rules and conventions: use the international system of units (SI). If other units are mentioned, please give their equivalent in SI.

Footnotes
Footnotes should be used sparingly. Number them consecutively throughout the article, using superscript Arabic numbers. Many wordprocessors build footnotes into the text, and this feature may be used. Should this not be the case, indicate the position of footnotes in the text and present the footnotes themselves separately at the end of the article. Do not include footnotes in the Reference list.

References
References must appear as a separate bibliography at the end of the paper, numbered by numerals in square brackets.

References to papers published in languages other than English must be translated into English indicating the original language given in brackets in the end of the reference e.g. (in German).

References in the text are indicated in square brackets. Journal titles must not be abbreviated. Please give journal volumes, issues (numbers) and page numbers. *Examples:*

Reference to a journal publication:

[1] J. van der Geer, J. A. J. Hanraads, R. A. Lupton, The art of writing a scientific article, J. Sci. Commun., (16) 3 (2000), pp. 51-59.

Reference to a book:

[2] W. Strunk Jr., E. B. White, The Elements of Style, third ed., Macmillan, New York, 1979, 350 p.

Reference to a chapter in an edited book:
[3] G. R. Mettam, L. B. Adams, How to prepare an electronic version of your article, in: B.S. Jones, R.Z. Smith (Eds.), Introduction to the Electronic Age, E-Publishing Inc., New York, 1999, pp. 281-304.
Reference to a conference proceedings:
[4] Chu-Hsing Lin, Jung-Chun Liu and Chun-Wei Liao, Energy analysis of multimedia video decoding on mobile handheld devices, 2007 International Conference on Multimedia and Ubiquitous Engineering, Seoul, Korea (April 26-28, 2007), pp. 120-125.
Reference to online publications:
[5] I. M. Martin, M. A. Alves, G. G. Peixoto and M. C. Rezende, Radar cross section measurements and simulations of a model airplane in the X-band, Piers Online, (4) 5 (2009), pp. 377-380, available online on www.example.com/martin.pdf, accessed June 2010.

Figures

Electronic version in EPS (Encapsulated Postscript) is preferred. The illustrations must be sharp, noise free and of good contrast.

Please do not:

- Supply files that are optimised for screen use (e.g., GIF, BMP, PICT, WPG); the resolution is too low;
- Supply files that are too low in resolution;
- Submit graphics that are disproportionately large for the content.

Plagiarism

The submissions will be checked on plagiarism and self-plagiarism on a regular basis, using the iThenticate plagiarism detection software, to ensure the originality of published material.

Each submitted paper is assigned to a three members of the Editorial Board for handling. The refereeing is done by anonymous reviewers.

When the paper is accepted, the authors will be required to electronically submit source files of the paper in MS Word. Each figure must also be supplied in two separate files, one in figure's original graphical format, and another in Postscript (.PS or .EPS) or .TIFF format.

The Technical Editor will send page proofs to the contact author for proofreading, usually by e-mail. The author is assumed to send the revised paper back within 10 days; otherwise the paper will be published without proofreading.

Copyright Notice

International Journal of Computing is an open access journal. Authors who publish with this journal agree to the following terms:

- Authors retain copyright and grant the journal right of first publication with the work simultaneously licensed under a Creative Commons Attribution License that allows others to share the work with an acknowledgement of the work's authorship and initial publication in this journal.
- Authors are able to enter into separate, additional contractual arrangements for the non-exclusive distribution of the journal's published version of the work (e.g., post it to an institutional repository or publish it in a book), with an acknowledgement of its initial publication in this journal.
- Authors are permitted and encouraged to post their work online (e.g., in institutional repositories or on their website) prior to and during the submission process, as it can lead to productive exchanges, as well as earlier and greater citation of published work.

Privacy Statement

The names and email addresses entered into the International Journal of Computing site will be used exclusively for the stated purposes of this journal and will not be made available for any other purpose or to any other party.

TENTATIVE CALL FOR PAPERS

IDAACS'2015

The 8th IEEE International Conference on
Intelligent Data Acquisition and Advanced Computing Systems: Technology and Applications

September 24-26, 2015
WARSAW, POLAND

Organized by
Research Institute for Intelligent Computer Systems, Ternopil National Economic University and V.M. Glushkov Institute of Cybernetics, National Academy of Sciences of Ukraine
in cooperation with

Faculty of Electronics and Information Technologies, Faculty of Mathematics and Information Science, Warsaw University of Technology
Warsaw, Poland
www.idaacs.net

Conference Co-Chairmen
Anatoly Sachenko, Ukraine
Wiesław Winiecki, Poland
International Programme Committee Co-Chairmen
Robert E. Hiromoto, USA
Linas Svilainis, Lithuania
IDAACS International Advisory Board
Dominique Dallet, France
Richard Duro, Spain
Domenico Grimaldi, Italy
Vladimir Haasz, Czech Republic
Robert Hiromoto, USA
Theodore Laopoulos, Greece
George Markowsky, USA, Chair
Vladimir Oleshchuk, Norway
Fernando Lopez Pena, Spain
Peter Reusch, Germany
Anatoly Sachenko, Ukraine
Wiesław Winiecki, Poland

Important dates
Abstract submission: 1 February 2015
Notification of Acceptance: 31 March 2015
Camera ready paper: 15 May 2015
Early registration: 31 March – 15 June 2015

Correspondence
The correspondence should be directed to IDAACS Organizing Committee:
IDAACS Organizing Committee
Research Institute for Intelligent Computer Systems
Ternopil National Economic University
3 Peremoga Square
Ternopil 46020 Ukraine
Phone: +380352-475050 ext.: 12234
Fax: +380352-475053 (24 hours)
E-mail: orgcom@idaacs.net

Tentative Streams and Topics

The conference scope includes, but it's not limited to:

1. Special Stream in Wireless Systems
2. Special Stream in Project Management
3. Special Stream in Cyber Security
4. Special Stream in High Performance Computing
5. Special Stream in eLearning Management
6. Special Stream in Advanced Information Technologies in Ecology
7. Special Stream in Intelligent Robotics and Components
8. Advanced Instrumentation and Data Acquisition Systems
9. Advanced Mathematical Methods for Data Acquisition and Computing Systems
10. Artificial Intelligence and Neural Networks for Advanced Data Acquisition and Computing Systems
11. Bio-Informatics
12. Software Tools and Environments
13. Data Analysis and Modeling
14. Embedded Systems
15. Information Computing Systems for Education and Commercial Applications
16. Intelligent Distributed Systems and Remote Control
17. Intelligent Information Systems, Data Mining and Ontology
18. Intelligent Testing and Diagnostics of Computing Systems
19. Internet of Things
20. Pattern Recognition and Digital Image and Signal Processing
21. Virtual Instrumentation Systems

It's our pleasure to invite the interested scientists to organize own Streams.




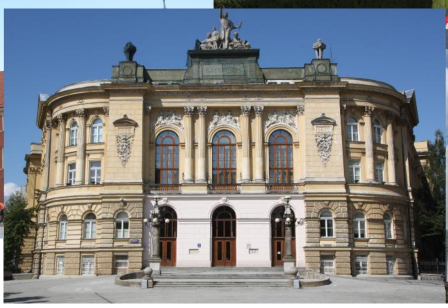
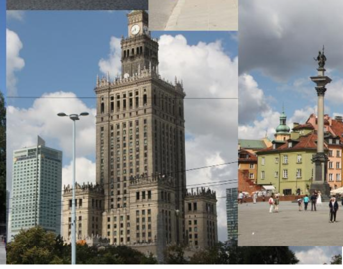
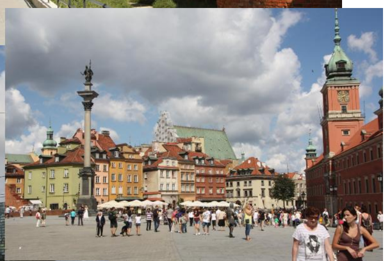

Підписано до друку 27. 03. 2014 р.
Формат 60x84 $^{1}/_{8}$. Гарнітура Times.
Папір офсетний. Друк на дублікаторі.
Умов. друк. арк. 11,5. Облік.-вид. арк. 13,1.
Зам. № 003-14П. Наклад 300 прим.

Тернопільський національний економічний університет
вул. Львівська, 11, м. Тернопіль, 46004

Свідоцтво про внесення суб'єкта видавничої справи
до Державного реєстру видавців ДК № 3467 від 23.04.2009 р.

Віддруковано у Видавничо-поліграфічному центрі «Економічна думка ТНЕУ»
46004 м. Тернопіль, вул. Львівська, 11
тел. (0352) 47-58-72
E-mail: edition@tneu.edu.ua